

# A guided intermediate resampling particle filter for inference on high dimensional systems

Joonha Park

Boston University, Boston, USA

Edward L. Ionides

University of Michigan, Ann Arbor, USA

## Abstract

Particle filter methods are a basic tool for inference on nonlinear partially observed Markov process (POMP) models. However, the performance of standard particle filter algorithms quickly deteriorates as the model dimension increases. We introduce guided intermediate resampling filter (GIRF) methodology to address this issue. GIRF methodology requires that the latent Markov process has a continuous time representation, allowing particles to be assessed at times intermediate to the observation times. We obtain theoretical results showing improved scaling of a GIRF algorithm, relative to widely used particle filters, as the model dimension increases. We present numerical comparisons with alternative methods on toy examples, including a stochastic version of the Lorenz 96 atmospheric circulation model. As predicted by the theoretical results, we find empirically that our GIRF algorithm greatly out-performs an auxiliary particle filter and an ensemble Kalman filter on nonlinear systems of moderately high dimension. Our GIRF algorithm is applicable to a broad range of models thanks to its plug-and-play property of not requiring the evaluation of the transition density of the process. We demonstrate the scientific applicability of GIRF methodology by solving a scientific challenge, carrying out likelihood based inference on epidemic coupling between forty cities from spatiotemporal infectious disease case reports.

**Keywords:** sequential Monte Carlo; particle filter; curse of dimensionality; spatiotemporal inference; plug-and-play property

## 1 Introduction

Partially observed Markov process (POMP) models offer a framework for statistical inference on dynamic systems. A POMP model, otherwise known as a state space model or a hidden Markov model, consists of a latent Markov process representing the time evolution of the system

---

*Address for correspondence:* Joonha Park, Department of Mathematics and Statistics, Boston University, 111 Cummington Mall, MA 02215, USA.

Email: joonhap@bu.edu

and a measurement process that provides partial or noisy information about the latent process. Sequential Monte Carlo (SMC) methods are recursive algorithms that enable estimation of the likelihood and the conditional distribution of the latent process given data from a POMP model (Doucet et al., 2001; Cappé et al., 2007; Doucet and Johansen, 2011). In the context of POMP models, SMC algorithms are known as particle filters, and the simulated random variables used by SMC to represent conditional latent processes are called particles.

Inference on some dynamic systems require fitting models with high dimensional latent processes to high dimensional data. For example, dynamic processes involving many spatial locations appear in the study of ecological, epidemiological and geophysical systems. For these spatiotemporal models, both the latent process and measurement dimension tend to scale linearly with the number of spatial locations. Ensemble Kalman filter (EnKF) methods have been used to predict atmospheric dynamics for weather forecasts due to their good scalability to high dimensions (Houtekamer and Mitchell, 2001; Evensen, 1994). However, these methods can be ineffective for highly nonlinear and non-Gaussian systems, because they rely on locally linear and Gaussian approximations (Ades and Van Leeuwen, 2015; Lei et al., 2010; Miller et al., 1999). In systems biology, models for networks of reactions may add stochasticity to collections of deterministic differential equations (Kitano, 2002). The model dimension typically increases with the number of system components, but even the state-of-the-art inference methods are not suitable for application beyond small systems (Owen et al., 2015).

Particle filter methods suffer from rapid deterioration in performance as the model dimension increases. This phenomenon occurs due to the weight degeneracy among particles. When highly unbalanced weights are given to the particles, resampling results in loss of particle diversity and poor approximation to the latent process distribution. Theoretical results demonstrating this phenomenon were established by Bengtsson et al. (2008) and Snyder et al. (2008). These authors found out that the number of particles required for filtering increases exponentially in the variance of the log density of the observation given the latent process, which is closely tied to the space dimension. Heuristically, these results indicate that the curse of dimensionality (COD) is related to high dimensional measurement density, implying that particle depletion happens because each observation carries too much information. In this sense, the COD in particle filtering may be understood as a curse of too much information.

Our approach, which we refer to as guided intermediate resampling filter (GIRF) methodology, uses the continuous time nature of the latent Markov process to avoid the curse of too much information by controlling the rate at which the filtering algorithm introduces new information. Specifically, GIRF methodology divides each time interval between observations into intermediate sub-intervals, with the number of sub-intervals growing together with the latent process dimension of the POMP model. Particles are resampled at each sub-interval with weights reflecting the assessment by a guide function. Particles are then propagated forward to the next sub-interval following the transition kernel of the latent process. GIRF methodology can therefore share with basic SMC the *plug-and-play* property that the algorithm requires a simulator of the latent dynamic process but does not require an evaluator of its transition density (Bretó et al., 2009; He et al., 2009). The GIRF algorithms we consider in this paper all enjoy this plug-and-play property, and we demonstrate that this facilitates applicability to complex mechanistic models defined by nonlinear stochastic differential equations and coupled over-dispersed Markov counting processes.

GIRF methodology gradually guides the particles toward plausible values of the latent process that are consistent with the next observations. Previous methods have used similar ideas of guiding particles using the available information, but have not directly addressed the COD. The auxiliary particle filter (APF) proposed by Pitt and Shephard (1999) assesses each particle based

on the compatibility with the next observation using a forward projection. Many particle filter methods attempt to target the conditional distribution of the latent process given its current value and the next observation, known as the “optimal” proposal distribution when only the next observation is available (Doucet et al., 2000). The implicit particle filter (Chorin and Tu, 2009; Chorin et al., 2013) approximates the optimal proposal by directly sampling particles at the vicinity of the maximum of the optimal importance density. The equivalent-weights particle filter (Van Leeuwen, 2010; Ades and Van Leeuwen, 2015) nudges particles toward the next observation over intermediate time steps; it was developed for applications in geosciences and is based on local Gaussianity of the transition density and the Gaussian measurement density. Papadakis et al. (2010) proposed using the ensemble Kalman filter updates as proposals within a particle filter. Bunch and Godsill (2016) proposed an algorithm that moves particles according to a Gaussian flow to target the optimal importance density. However, Snyder et al. (2015) demonstrated, using the case of linear Gaussian processes, that targeting the optimal proposal alone does not solve the COD. The aforementioned methods, except for APF, assume that the transition density is either known or locally Gaussian.

Our GIRF algorithm is the first plug-and-play particle filter with proven favorable scaling properties as the dimension of the latent process increases. Specifically, we show that the Monte Carlo error in our GIRF can be decomposed into components that grow polynomially with dimension and components that, under suitable circumstances, grow at a slow exponential rate. The intermediate resampling plays a key role in the polynomial scaling of the first component, which otherwise scales exponentially with the dimension. The guide function allows promising particles to be selected and therefore slows down the scaling rate of the second component.

The remainder of the paper is organized as follows. Section 2 reviews several ideas in the literature that are related to high dimensional filtering. Section 3 introduces and explains our GIRF algorithm. Section 4 reports some of its theoretical properties, including the main result (Theorem 2) that establishes a finite sample error bound for the estimates obtained by our GIRF. This result, obtained via a novel theoretical approach, helps explain why our GIRF scales better to high dimensions than standard methods. Section 5 discusses the choice of the guide function and gives a simulation-based construction applicable to a general class of models. Section 6 describes how one can estimate model parameters by combining GIRF methodology with the iterated filtering scheme of Ionides et al. (2015). Implementations of our algorithm in Section 7 empirically show the favorable scaling of GIRF methodology and its capability of facilitating spatiotemporal inference that has previously been considered inaccessible due to computational limitations. Section 8 is a concluding discussion.

## 2 Previous approaches to high dimensional filtering

Several theoretically motivated algorithms for high dimensional particle filtering have been proposed in the past few years. Rebeschini and Van Handel (2015) considered a filtering method that builds upon the assumption that the interaction between the spatial locations is local. Their algorithm partitions the latent variables into blocks and approximates the one step transitions of the latent process as being independent between the blocks. A theoretical bound for the filtering error was derived, which only depends on the size of the largest block but not on the entire space dimension. Despite this very desirable scaling property, this approach has some practical limitations, because it is not applicable to highly interdependent spatial models and the filter estimates are not reliable near the boundaries of the blocks, which may constitute a substantial fraction of

the total number of spatial locations.

Beskos et al. (2014a,b) applied the annealed importance sampling proposed by Neal (2001) to high dimensional filtering and investigated its theoretical properties. The annealed importance sampling method introduces a series of bridging distributions between observations. These bridging densities are set proportional to a fractional power of the desired target density. Between two adjacent importance resampling, the particles are transformed according to a transition kernel whose stationary distribution equals the target bridging distribution. These transition kernels provide mixing that helps maintain the stability of the particle approximations. The authors gave stability results for the case where the original high dimensional latent process is composed of many copies of independent and identically distributed (IID) one dimensional processes. In particular, Beskos et al. (2014a) showed that the importance weights are non-degenerate as the dimension goes to infinity even with fixed particle size. Beskos et al. (2014b) showed that both the  $L^2$  error of the filter estimates and the variance of the likelihood estimates are bounded uniformly in the space dimension. However, a major drawback of this approach is the absence of the plug-and-play property. Annealed importance sampling requires evaluable analytic expression of the density of the one-step transition in order to build artificial transition kernels between bridging distributions.

Beskos et al. (2017) studied the case where the spatial structure of the model can be hierarchically factorized and investigated the possibility of overcoming the COD. Specifically, they assumed that the one step transition density is given, or can be well approximated, by a product of functions of increasing collections of latent variables. The theoretical results they obtained by considering a few simple IID cases show that filtering can be stable when the number of particles increases linearly with the space dimension. These promising results provide insights into what might be achieved in more general cases.

Del Moral and Murray (2015) proposed a particle filtering algorithm for highly informative observations that is almost identical to our method at its core, though our motivation and theoretical analysis differ. The authors were motivated by the study of perfectly observed diffusion processes, which share with high dimensional POMP the difficulty that highly informative observations make computations challenging. In the present paper, we demonstrate the utility of this approach in high dimensions, both theoretically and empirically. We show that GIRF methodology can yield accurate estimates of the conditional latent process distributions given the data in high dimensions. In order to further avoid weight degeneracy, our method uses more than one future observations for particle assessment. This aspect of our algorithm was not relevant for the precisely measured low-dimensional processes considered by Del Moral and Murray (2015).

### 3 The guided intermediate resampling filter (GIRF)

We consider a latent Markov process defined in continuous time, denoted by  $\{X_t; t \geq t_0\}$ , where each random variable  $X_t$  takes value in a measurable space  $(\mathbb{X}, \mathcal{X})$ . We write  $n:m$  to represent  $\{n, n+1, \dots, m\}$  for integers  $n \leq m$ . The measurement process is defined at discrete time points  $t_n > t_0$ ,  $n \in 1:N$  and yields an observation  $Y_n \in \mathbb{Y}$  that is a noisy or incomplete measurement of  $X_{t_n}$ . The measurement  $Y_n$  is independent of other observations  $Y_m$ ,  $m \neq n$ , and of the latent process  $\{X_t\}$ , given the current state  $X_{t_n}$ . We will assume that the latent process space and the measurement space are  $d$ -dimensional,  $\mathbb{X} = \prod_{i=1}^d \mathbb{X}^{[i]}$ ,  $\mathbb{Y} = \prod_{i=1}^d \mathbb{Y}^{[i]}$ , and we study the scaling property of inference algorithms with respect to  $d$ . The observations  $Y_n = y_n$  for  $n \in 1:N$  are assumed to be fixed data. The latent process evolves over time according to Markov transition kernels  $K_{t,t'}$ , where  $t_0 \leq t \leq t'$ . That is, the probability distribution of the random state  $X_{t'}$

---

**Algorithm 1:** A guided intermediate resampling filter (GIRF)

---

**Input :** Data,  $y_{1:N}$   
 Observation times,  $t_{1:N}$ , and initialization time  $t_0$   
 Intermediate times,  $t_{n,s}$  for  $n \in 0:N-1$  and  $s \in 1:S-1$   
 Simulator for  $P_{t_0}(dx)$   
 Simulator for  $K_{t_{n,s-1},t_{n,s}}(dx; x_{t_{n,s}})$  for  $n \in 0:N-1$  and  $s \in 1:S$   
 Evaluator for the measurement density,  $g_n(y_n | x_{t_n})$  for  $n \in 1:N$   
 Evaluator for the guide function,  $u_{t_{n,s}}(x_{t_{n,s}})$  for  $n \in 0:N-1$  and  $s \in 1:S$   
 Number of particles,  $J$

**Output:** Filtered particle swarm,  $\{X_{t_N}^{F,j}; j \in 1:J\}$   
 Likelihood estimate,  $\hat{\ell}$

**Initialize:**  $\hat{\ell} \leftarrow 1$ ,  $X_{t_0}^{F,j} \sim P_{t_0}(dx)$  for  $j \in 1:J$   
**for**  $n \leftarrow 0:N-1$  **do**  
   **for**  $s \leftarrow 1:S$  **do**  
    $X_{t_{n,s}}^{P,j} \sim K_{t_{n,s-1},t_{n,s}}(dx; X_{t_{n,s-1}}^{F,j})$  for  $j \in 1:J$   
    $w^j \leftarrow w_{t_{n,s}}(X_{t_{n,s}}^{P,j}, X_{t_{n,s-1}}^{F,j})$  given by equation (1) for  $j \in 1:J$   
    $\hat{\ell} \leftarrow \hat{\ell} \times \left( \sum_{j=1}^J w^j \right) / J$   
   Draw  $a^j$  with  $\mathbb{P}(a^j = i) = w^i / \sum_{i'=1}^J w^{i'}$  for  $j \in 1:J$   
   Set  $X_{t_{n,s}}^{F,j} = X_{t_{n,s}}^{P,a^j}$   
   **end**  
   Set  $X_{t_{n+1},0}^{F,j} = X_{t_{n,S}}^{F,j}$  for  $j \in 1:J$   
**end**

---

conditioned on  $X_t = x_t$  is given by

$$X_{t'} \mid (X_t = x_t) \sim K_{t,t'}(dx; x_t).$$

The Markov property allows us to decompose the transition kernel as

$$K_{t,t'} = K_{t,\tau_1} K_{\tau_1,\tau_2} \cdots K_{\tau_{n-1},\tau_n} K_{\tau_n,t'}$$

for any number of intermediate time points  $t \leq \tau_1 \leq \cdots \leq \tau_n \leq t'$ . In what follows, we assume that the transition kernel of the latent process can be simulated, but we do not require its density to be evaluated. We denote the initial latent process distribution at time  $t_0$  by  $P_{t_0}$ . We will occasionally express the distributions of random variables in terms of their densities. For example, the density of  $X_{t_n}$  given  $X_{t_m} = x_{t_m}$  ( $m < n$ ) will be denoted by  $p_{X_{t_n} | X_{t_m}}(\cdot | x_{t_m})$  with respect to a reference measure on  $\mathbb{X}$  written as  $dx$ . The measurement process for  $Y_n$  conditioned on  $X_{t_n} = x_{t_n}$  is assumed to have density  $g_n(\cdot | x_{t_n})$ .

Pseudocode for our GIRF is given in Algorithm 1. This algorithm has the basic structure of all particle filters, with the characteristic features of GIRF methodology being the use of intermediate resampling between observation times and the specific way in which the particles are guided. The intermediate time points between  $t_n$  and  $t_{n+1}$  will be denoted by  $t_{n,s}$ ,  $s \in 1:S-1$ , and we write  $t_{n,0} = t_n$  and  $t_{n,S} = t_{n+1}$ . The set of all intermediate time points, including the initial and observation time points, will be denoted by  $\mathbb{I} := \{t_{n,s}; n \in 0:N-1, s \in 0:S\}$ . The collection of *filter particles*,  $\{X_{t_{n,s}}^{F,j}, j \in 1:J\}$ , provide a Monte Carlo representation of a *guided filter distribution* which is in turn related to the *filter density*,  $p_{X_{t_n} | Y_{1:n}}(\cdot | y_{1:n})$ . The filter particles are moved

according to the law of the latent process to construct the *propagated particles*,  $\{X_{t_{n,s+1}}^{P,j}, j \in 1:J\}$ . The collection of propagated particles is resampled recursively to obtain the next generation of filter particles. The weighting of the propagated particles is based on how likely the particles are to generate the future observations  $y_{n+1:n+B}$  for some  $B \geq 1$ . The function that approximates this forecast likelihood is called the guide function and denoted by  $u_{t_{n,s}}: \mathbb{X} \rightarrow \mathbb{R}^+$ , where  $\mathbb{R}^+$  denotes the set of positive real numbers. At the initial time point we require that  $u_{t_0}(x) = 1$  and at the last time point  $u_{t_N}(x) = g_N(y_N | x)$  for all  $x \in \mathbb{X}$ . The assigned importance weight for the  $j$ -th particle at time  $t_{n,s}$  is a function of both  $X_{t_{n,s}}^{P,j}$  and  $X_{t_{n,s-1}}^{F,j}$ :

$$w^j \leftarrow w_{t_{n,s}}(X_{t_{n,s}}^{P,j}, X_{t_{n,s-1}}^{F,j}) := \begin{cases} \frac{u_{t_{n,s}}(X_{t_{n,s}}^{P,j})}{u_{t_{n,s-1}}(X_{t_{n,s-1}}^{F,j})} & \text{if } t_{n,s-1} \notin t_{1:N} \\ \frac{u_{t_{n,s}}(X_{t_{n,s}}^{P,j})}{u_{t_{n,s-1}}(X_{t_{n,s-1}}^{F,j})} \cdot g_n(y_n | X_{t_{n,s-1}}^{F,j}) & \text{if } t_{n,s-1} \in t_{1:N}. \end{cases} \quad (1)$$

If  $t_{n,s-1} \in t_{1:N}$ , that is if  $s = 1$  and  $n \geq 1$ , the denominator  $u_{t_{n,s-1}}(X_{t_{n,s-1}}^{F,j})$  in (1) is effectively divided by  $g_n(y_n | X_{t_n}^{F,j})$ , because at time  $t_{n,1} > t_n$ , the past observation  $y_n$  should no longer be considered in assessing the fitness of the particle. The weights at observation times  $t_n$  are taken as  $w_{t_{n-1,S}}(X_{t_{n-1,S}}^{P,j}, X_{t_{n-1,S-1}}^{F,j})$ . Particles are resampled with probability proportional to these weights. We used systematic resampling for our numerical implementation (Douc et al., 2005).

The likelihood of data, an important quantity for inference on unknown parameters, is defined as

$$\ell_{1:N}(y_{1:N}) = \mathbb{E} \left[ \prod_{n=1}^N g_n(y_n | X_{t_n}) \right],$$

where the expectation is taken with respect to the law of  $\{X_t; t \geq t_0\}$ . In common with standard particle filters, Algorithm 1 computes a likelihood estimate denoted by  $\hat{\ell}$ .

The particle swarm  $\{X_{t_{n,s}}^{F,j}; j \in 1:J\}$  at time  $t_{n,s} \in \mathbb{I}$  targets, as  $J$  tends to infinity, a distribution  $P_{t_{n,s}}^G$  which we call the guided filter distribution. For  $s \in 1:S$ , the density of  $P_{t_{n,s}}^G$  is given by

$$\frac{dP_{t_{n,s}}^G}{dx} \propto u_{t_{n,s}}(x) \cdot p_{X_{t_{n,s}} | Y_{1:n}}(x | y_{1:n}). \quad (2)$$

We understand  $p_{X_{t_{n,s}} | Y_{1:n}}(x | y_{1:n}) = p_{X_{t_0,s}}(x)$  for  $n=0$ . If  $u_{t_{n,s}}(x_{t_{n,s}})$  approximates the forecast likelihood of  $y_{n+1:n+B}$  given  $X_{t_{n,s}} = x_{t_{n,s}}$ , the guided filter distribution  $P_{t_{n,s}}^G$  approximates the conditional distribution of  $X_{t_{n,s}} = x_{t_{n,s}}$  given  $y_{1:n+B}$ . The latent process distribution conditioned on observations up to  $B$  future time points is called the fixed lag ( $B$ ) smoothing distribution. Its use for stable filtering has been studied in the literature, for example, in Clapp and Godsill (1999), Chen et al. (2000), Doucet et al. (2006), and Johansen (2015). Fixed lag smoothing distributions tend to be less affected by outliers in the observed data than filtering distributions (Lin et al., 2013). Our contribution is to use this approach and intermediate resampling in a novel way to develop a plug-and-play algorithm with good scaling properties as the latent space dimension increases.

The weight term (1) can be justified formally as follows. If  $t = t_{n,s} \in \mathbb{I} \setminus \{t_0\}$ , we will write  $t^- := t_{n,s-1}$ , understanding that if  $s = 0$ ,  $t^- = t_{n-1,S-1}$ . If  $t = t_m$  for some  $m \in 1:N$ , we will

write  $\mathbf{n}(t) = m$ . For other values of  $t \in \mathbb{I}$ , we define  $\mathbf{n}(t)$  to be an arbitrary value in  $1:N$ . For  $n \in 0:N-1$ ,  $s \in 1:S$ , we consider the extended guided filter distribution with density

$$\pi_{n,s}^G(x_{t_0:t_{n,s}}) \propto p_{X_{t_0:t_{n,s}}|Y_{1:n}}(x_{t_0:t_{n,s}} | y_{1:n}) \cdot u_{t_{n,s}}(x_{t_{n,s}})$$

where

$$p_{X_{t_0:t_{n,s}}|Y_{1:n}}(x_{t_0:t_{n,s}} | y_{1:n}) \propto p_{X_{t_0}}(x_{t_0}) \cdot \prod_{\substack{t_0 < t \leq t_{n,s} \\ t \in \mathbb{I}}} p_{X_t|X_{t^-}}(x_t | x_{t^-}) \cdot g_{\mathbf{n}(t^-)}^{\mathbf{1}[t^- \in t_{1:N}]}(y_{\mathbf{n}(t^-)} | X_{t^-})$$

is the density of  $X_{t_0:t_{n,s}} = \{X_{t_0}, X_{t_{0,1}}, \dots, X_{t_{n,s}}\}$  given the observations  $y_{1:n}$ . The power  $\mathbf{1}[t^- \in t_{1:N}]$  is an indicator function of whether  $t^-$  is an observation time. Since particles are propagated according to  $p_{X_{t_{n,s}}|X_{t_{n,s-1}}}$  in Algorithm 1, the proper weight should be given by

$$w_{t_{n,s}}(x_{t_0:t_{n,s}}) = \frac{\pi_{n,s}^G(x_{t_0:t_{n,s}})}{\pi_{n,s-1}^G(x_{t_0:t_{n,s-1}}) \cdot p_{X_{t_{n,s}}|X_{t_{n,s-1}}}(x_{t_{n,s}} | x_{t_{n,s-1}})} = \frac{u_{t_{n,s}}(x_{t_{n,s}})}{u_{t_{n,s-1}}(x_{t_{n,s-1}})} g_n^{\mathbf{1}[t_{n,s-1} \in t_{1:N}]}(y_n | x_{t_n}),$$

which is the same as (1).

The most basic particle filter is the bootstrap filter of Gordon et al. (1993). GIRF (Algorithm 1) is equivalent to the bootstrap particle filter if we take  $S = 1$  and  $u_{t_n}(x_{t_n}) = g_n(y_n | x_{t_n})$ . A successful variant of the particle filter is the auxiliary particle filter (APF) of Pitt and Shephard (1999). GIRF (Algorithm 1) becomes an instance of APF in the special case where  $S = 1$  and  $u_{t_n}(x_{t_n}) = g_n(y_n | x_{t_n}) \cdot g_{n+1}\{y_{n+1} | \mu_{t_{n+1}}(x_{t_n})\}$ , where  $\mu_{t_{n+1}}(x_{t_n})$  denotes a deterministic or stochastic forecast of  $X_{t_{n+1}}$  given  $X_{t_n} = x_{t_n}$ . Since APF does not include intermediate resampling, we will find that it does not have the favorable scaling properties that GIRF methodology can enjoy when  $S \approx d$ .

The computational cost of Algorithm 1 typically scales as  $O(JSd)$ . The storage cost is  $O(Jd)$  since only the current latent process and guide function values need to be saved for each particle during the filtering and propagation recursions. Our implementation of Algorithm 1 is available at <https://github.com/joonhap/GIRF.git>. A critical scaling question is the rate at which  $J$  has to grow with  $d$  in order to obtain satisfactory Monte Carlo performance. If we take  $S = d$  and we have a guide function that provides a reasonable approximation to the forecast likelihood of future observations, Theorem 2 of Section 4 shows that we can let  $J$  increase slowly with  $d$ . Section 7 carries the burden of showing that the theoretical results correspond to useful practical performance.

## 4 Theoretical results

We first show that the standard results for SMC apply to GIRF (Algorithm 1). GIRF methodology can be cast into the standard framework of particle filters by extending the latent space to  $\mathbb{X}^2$  where the new latent variable is the pair  $(X_{t_{n,s}}, X_{t_{n,s-1}})$ . This extension is necessary because the resampling weights (1) depend on both  $X_{t_{n,s}}^{P,j}$  and  $X_{t_{n,s-1}}^{F,j}$ . Likelihood estimates obtained from the standard particle filter are unbiased (Del Moral and Jacod, 2001). It follows that the likelihood estimates from GIRF (Algorithm 1) are also unbiased. The consistency and the asymptotic normality of the filter estimates from GIRF (Algorithm 1) also follow naturally from the standard particle filter theory (Chopin, 2004; Del Moral, 2004).

**Theorem 1.** *The likelihood estimate  $\hat{\ell}$  of Algorithm 1 is unbiased for  $\ell_{1:N}(y_{1:N})$ .*

*Proof.* See Appendix A. □

We now study the scaling properties of GIRF (Algorithm 1) with respect to increasing dimension. GIRF methodology converts a filtering problem with highly informative observations into one that deals with a slower rate of incoming information, at the expense of operating on a refined time scale. There are many results in the literature which concern the stability of particle filters, see for example Del Moral and Guionnet (2001); Del Moral (2004); Le Gland and Oudjane (2004); Whiteley (2013); Giraud and Del Moral (2017). However, these results do not directly address the scaling with respect to increasing dimension. Another major issue in applying these results to the “infill” scenario we study in which the number of intermediate time steps  $S$  is increasing is that the number of time steps needed for the mixing of the latent process conditional on data increases proportionally with  $S$ . We provide a novel theoretical analysis of the scaling rate when the number of intermediate time steps grow linearly with the amount of information each observation carries, which in turn increases with the model dimension. In particular, we provide a finite sample bound on the filtering error (Theorem 2) and asymptotic bounds on the variance of the likelihood estimate (Theorem 3) and filter estimates (Theorem 4) for GIRF (Algorithm 1). These bounds show how intermediate resampling and the guide function can remedy the otherwise problematic dimensional scaling properties of particle filters.

We will introduce some notation. For a bounded measurable function  $f \in \mathcal{B}_b(\mathbb{X})$ , we denote its integral with respect to a measure  $\mu$  by  $\mu f$ , and the integral with respect to a Markov kernel  $K$  conditional on the starting state  $x$  by  $Kf(x)$ . The propagation of measure  $\mu$  by a kernel  $K$  is defined as  $(\mu K)f := \mu(Kf)$ . For any  $t, t'$  such that  $t_0 \leq t \leq t' \leq t_N$ , we define

$$Q_{t,t'}(f)(x) := \mathbb{E} \left[ f(X_{t'}) \prod_{t \leq t_n < t'} g_n(y_n | X_{t_n}) \middle| X_t = x \right], \quad (3)$$

for any bounded measurable function  $f$ . The collection  $\{Q_{t,t'}; t \leq t'\}$  forms a semigroup, in the sense that  $Q_{t,\tau}Q_{\tau,t'}(f) = Q_{t,t'}(f)$  for  $t \leq \tau \leq t'$  (Del Moral, 2004). Note that, if no observation was made in  $[t, t']$ , we have

$$Q_{t,t'}(f) = K_{t,t'}f, \quad (4)$$

and if a single observation  $y_n$  was made in this interval,

$$Q_{t,t'}(f) = K_{t,t_n} \{ (K_{t_n,t'}f) \cdot g_n(y_n | \cdot) \}. \quad (5)$$

We note that the term  $Q_{t,t_n}(g_n)(x)$ , for  $t \leq t_n$ , represents the forecast likelihood of observations in the interval  $[t, t_n]$  given the current state  $X_t = x$ . Here, we implicitly assumed that  $g_n$  is a function of  $X_{t_n}$ , such that  $g_n(X_{t_n}) := g_n(y_n | X_{t_n})$ . We also note that

$$Q_{t,t_n}(g_n) \equiv Q_{t,t_{n+1}}(1).$$

The guided filter distribution  $P_{t_n,s}^G$  defined in (2) can be expressed as

$$P_{t_n,s}^G f = \frac{P_{t_0} Q_{t_0,t_n,s}(u_{t_n,s} \cdot f)}{P_{t_0} Q_{t_0,t_n,s}(u_{t_n,s})} \quad (6)$$

for all bounded measurable function  $f$ .



Given the observations  $y_{1:N}$ , we are interested in knowing how accurate the quantity  $\frac{1}{J} \sum_{j=1}^J f(X_{t_N}^{F,j})$  is as an approximation to  $\mathbb{E}[f(X_{t_N})|Y_{1:N} = y_{1:N}]$ . We will establish a novel finite sample bound on the error in this approximation under a set of assumptions. This result will show how the number of intermediate time points and the construction of the guide function can affect the performance of GIRF methodology. In deriving our main result, we assume that multinomial resampling is used. Under multinomial resampling, the indices  $a^j$  in Algorithm 1 are drawn independently of each other, given  $\{w^j; j \in 1:J\}$ .

**Theorem 2.** *Suppose multinomial resampling is used in Algorithm 1. Also suppose that Assumptions 1 and 2 below, which define constants  $C_1$ ,  $C_2$ , and  $\rho$ , hold. If  $f$  is a measurable function such that  $\|f\|_\infty \leq 1$  and  $a > 1$  is an arbitrary constant, then we have*

$$\left| \frac{1}{J} \sum_{j=1}^J f(X_{t_N}^{F,j}) - \mathbb{E}[f(X_{t_N})|Y_{1:N} = y_{1:N}] \right| \leq \frac{4aC_2(C_1 + 1)}{\rho\sqrt{J}}(NS + 1) \quad (7)$$

with probability at least  $1 - \frac{(2NS+1)(NS+1)}{a^2}$ , given that  $\sqrt{J} \geq 8\rho^{-2}aC_2(C_1 + 1)NS$ .

*Proof.* See Appendix B for an outline of the proof. A full version is given in Supplementary section S1.  $\square$

Theorem 2 states that for a given POMP model, the size of the error in the estimated filtering distribution will be bounded by a number that increases polynomially in  $S$  with high probability, provided that the number of particles is large enough. If we are to keep the probability  $\frac{(2NS+1)(NS+1)}{a^2}$  with which the bound is violated at a fixed level, the number  $a$  needs to increase proportionally to  $S$ , and thus the error bound increases at a rate of at most  $O(S^2)$ . An error bound that does not increase exponentially with the number of time steps that are needed for mixing conditional on data is crucial to justify an algorithm with sub-divided time intervals. We note that the constant  $C_1$  also depends on  $S$ :  $C_1$  can stay at  $O(1)$  in  $d$  if  $S = d$ , whereas it will typically increase exponentially in  $d$  if  $S = 1$ . We will discuss more on this after introducing Assumption 1.

The constants  $C_1$  and  $C_2$  will determine the scaling rate of the error bound with respect to the space dimension  $d$ . These two constants are defined by Assumptions 1 and 2, which we now describe. As our first assumption, we will suppose that the forecast likelihood of future observations experiences a bounded change between two consecutive intermediate points.

**Assumption 1.** *There exists  $C_1 \geq 1$  such that for all  $t \leq t'$  in  $\mathbb{I} \setminus \{t_0\}$  and for all  $x \in \mathbb{X}$ ,*

$$\frac{K_{t-,t} \{Q_{t,t'}(u_{t'})\}^2}{[K_{t-,t} Q_{t,t'}(u_{t'})]^2}(x) \leq C_1^2.$$

This assumption says that over one intermediate time step,  $Q_{t,t'}(u_{t'})(X_t)$  has bounded variance relative to its squared mean, conditional on  $X_{t-}$ , since  $K_{t-,t} Q_{t,t'}(u_{t'})(X_{t-}) = \mathbb{E}[Q_{t,t'}(u_{t'})(X_t)|X_{t-}]$  and

$$\frac{K_{t-,t} \{Q_{t,t'}(u_{t'})\}^2}{[K_{t-,t} Q_{t,t'}(u_{t'})]^2}(X_{t-}) = \frac{\text{Var} \{Q_{t,t'}(u_{t'})(X_t)|X_{t-}\}}{\mathbb{E} \{Q_{t,t'}(u_{t'})(X_t)|X_{t-}\}^2} + 1.$$

We will later take  $u_{t'}$  to approximate the forecast likelihood of some number of future observations after  $t'$  (i.e.,  $u_{t'} \approx Q_{t',t'+B}(1)$  for some  $B \geq 1$ ), in which case  $Q_{t,t'}(u_{t'})(X_t) \approx Q_{t,t'+B}(1)(X_t)$  becomes an approximation to the forecast likelihood of the observations in  $[t, t' + B)$  given  $X_t$ .

Assumption 1 explains how GIRF methodology can achieve improved high-dimensional scaling by operating on a refined time scale. If the time interval was not divided, the constant  $C_1$  would typically increase exponentially as the space dimension  $d$  increases. To see this, we can consider a POMP consisting of  $d$  independent one-dimensional latent and measurement processes. For independent processes one can obviously run SMC on each dimension separately, but the case is considered by way of illustration because it simplifies equations but poses similar computational difficulties with the general, dependent cases as far as the filtering on high dimensions is concerned. Under independence, if we assume the guide function is given by  $u_t(X_t) = \prod_{i=1}^d u_t^{[i]}(X_t^{[i]})$  and  $Q_{t,t'}^{[i]}$  denotes a definition analogous to (3) for the  $i$ -th latent and measurement processes, the term  $Q_{t,t'}(u_{t'})(X_t)$  can be expressed as a product of  $d$  independent random variables  $Q_{t,t'}^{[i]}(u_{t'}^{[i]})(X_t^{[i]})$ ,  $i \in 1:d$ . Thus both its mean and variance will be exponential in  $d$ , making  $C_1$  scale exponentially if  $S$  is fixed as  $d$  increases.

In GIRF (Algorithm 1), if we divide the time interval into  $d$  sub-intervals (i.e.,  $S = d$ ), the constant  $C_1$  can be of constant order as  $d$  increases. Define  $\lambda_\tau := \log K_{t^-, \tau}(K_{\tau, t} Q_{t, \tau} u_\tau)^2$  for  $\tau \in [t^-, t]$ . Then Assumption 1 is equivalent to saying that  $\lambda_t - \lambda_{t^-} \leq 2 \log C_1$ . Thus, if  $\frac{d}{d\tau} \lambda_\tau \leq 2\xi$  for all  $\tau \in [t^-, t]$  for some  $\xi > 0$ , then Assumption 1 holds with  $C_1 = e^{\xi \cdot (t - t^-)}$ . Consider again a POMP model consisting of  $d$  independent one dimensional latent and measurement processes. Then we have

$$\frac{d\lambda_\tau}{d\tau} = \frac{d}{d\tau} \log \prod_{i=1}^d K_{t^-, \tau}^{[i]} \left( K_{\tau, t}^{[i]} Q_{t, \tau}^{[i]} u_\tau^{[i]} \right)^2 = \frac{d}{d\tau} \sum_{i=1}^d \log K_{t^-, \tau}^{[i]} \left( K_{\tau, t}^{[i]} Q_{t, \tau}^{[i]} u_\tau^{[i]} \right)^2 =: \frac{d}{d\tau} \sum_{i=1}^d \lambda_\tau^{[i]}. \quad (8)$$

Therefore, provided that  $\frac{d}{d\tau} \lambda_\tau^{[i]} \leq 2\xi^{[i]}$  for all  $\tau \in [t^-, t]$  and for some  $\xi^{[i]} > 0$ ,  $i \in 1:d$ , such that  $\sum_{i=1}^d \xi^{[i]} = O(d)$ , and given that  $t - t^- = O(\frac{1}{S}) = O(\frac{1}{d})$ , we have

$$C_1 = e^{(\sum_{i=1}^d \xi^{[i]}) \cdot (t - t^-)} = O(1) \text{ in } d. \quad (9)$$

In supplementary section S2, we derive a more explicit result for  $C_1$  for certain diffusion processes. Further, we demonstrate that the independence assumption is not crucial by showing that  $C_1$  is uniformly bounded over  $d$  when  $\{X_t\}$  is a Brownian motion with arbitrary correlation between components.

Assumption 1 takes explicit advantage of the requirement for GIRF methodology that the latent process operates in continuous time. The latent process transition kernel that is non-deterministic over intermediate time intervals provides the randomness necessary for gradually guiding the particles to the next guided filter distribution. As a counterexample, consider a case where the transition kernels  $K_{t_n, s-1, t_n, s}$  are deterministic for  $s \in 1:S-1$  and only the last kernel  $K_{t_n, S-1, t_{n+1}}$  is non-singular. Then necessarily  $K_{t_n, S-1, t_{n+1}} = K_{t_n, t_{n+1}}$ . For  $t = t_{n, s}$ ,  $s \in 1:S-1$ , we have  $\frac{K_{t^-, t} \{Q_{t, t'}(u_{t'})\}^2}{[K_{t^-, t} Q_{t, t'}(u_{t'})]^2} \equiv 1$ . However for  $t = t_{n+1}$ , we have

$$\frac{K_{t^-, t} \{Q_{t, t'}(u_{t'})\}^2}{[K_{t^-, t} Q_{t, t'}(u_{t'})]^2} = \frac{K_{t_{n-1}, t_n} \{Q_{t_n, t'}(u_{t'})\}^2}{[K_{t_{n-1}, t_n} Q_{t_n, t'}(u_{t'})]^2} = \prod_{i=1}^d \frac{K_{t_{n-1}, t_n}^{[i]} \{Q_{t_n, t'}^{[i]}(u_{t'}^{[i]})\}^2}{[K_{t_{n-1}, t_n}^{[i]} Q_{t_n, t'}^{[i]}(u_{t'}^{[i]})]^2},$$

for a POMP model consisting of  $d$  independent one dimensional processes. As argued earlier, the upper bound  $C_1^2$  increases exponentially in  $d$  in this case. We see that the continuously random property of the latent process transition kernels is necessary for GIRF methodology to be able to disperse the curse of too much information.

The second assumption concerns how closely the guide function  $u_t$  approximates the forecast likelihood of future observations.

**Assumption 2.** *There exist constants  $C_2 \geq 1$ ,  $\rho \in (0, 1)$ , and a sequence of regions  $\{\mathcal{C}_t \in \mathcal{X}; t \in \mathbb{I}\}$  such that the following hold:*

(i) *For all  $t \in \mathbb{I}$ ,  $P_t^G(\mathcal{C}_t) > \rho$ .*

(ii) *For all  $t \leq t' \in \mathbb{I}$ ,*

$$C_2 \cdot \inf_{x \in \mathcal{C}_t} \frac{Q_{t,t'}(u_{t'})}{u_t}(x) \geq \sup_{x \in \mathbb{X}} \frac{Q_{t,t'}(u_{t'})}{u_t}(x).$$

The value of  $C_2$  indicates how much the ratio  $\frac{Q_{t,t'}(u_{t'})}{u_t}$  varies. Thus a value of  $C_2$  that is close to the unity will indicate that the guide function  $u_t$  at time  $t$  approximates the forecast likelihood of future observations with good accuracy. If the guide functions were exactly taken to be the forecast likelihood of all future observations, namely  $u_t \equiv Q_{t,t_N}(g_N)$ , we would have  $Q_{t,t'}(u_{t'}) = Q_{t,t'}Q_{t',t_N}(g_N) = Q_{t,t_N}(g_N) = u_t$  due to the semi-group property of  $\{Q_{t,t'}\}$ . In this case, the constant  $C_2$  would be equal to the unity for any choice of the region  $\mathcal{C}_t$ . Since Theorem 2 says the error bound increases with  $C_2$ , the choice  $u_t := Q_{t,t_N}(g_N)$  is ideal. Of course, this choice is not available in most practical applications, and an appropriate approximation to the forecast likelihood will need to be taken as the guide function. The more accurate approximation to the forecast likelihood we can make, the smaller  $C_2$  will become.

The fact that the infimum of  $\frac{Q_{t,t'}(u_{t'})}{u_t}$  over  $\mathcal{C}_t$  is compared with the global supremum indicates that the guide function  $u_t$  can overestimate the forecast likelihood outside  $\mathcal{C}_t$ . This suggests that making conservative estimates of the forecast likelihood outside  $\mathcal{C}_t$  is allowed. For instance, if we consider the case where the region  $\mathcal{C}_t$  is defined via a relation  $\mathcal{C}_t := \{x \in \mathbb{X}; u_t > c\}$  for some value  $c > 0$ , then Assumption 2 (ii) might be interpreted as that  $u_t$  has thicker tails than the approximate forecast likelihood  $Q_{t,t'}(u_{t'})$ . The guide function  $u_t$ , however, should not overestimate the forecast likelihood by a large margin inside the central region  $\mathcal{C}_t$ . This central region also has to carry a probability mass greater than  $\rho$  with respect to  $P_t^G$  (condition (i)).

For  $B \geq 1$ , we will say that the latent process mixes well over the interval  $[t_{n,s}, t_{n+B+1}]$  conditional on data if the conditional expectation  $\mathbb{E}[f(X_{t_{n+B+1}}) | Y_{n+1:n+B} = y_{n+1:n+B}, X_{t_{n,s}} = x]$  does not vary greatly across the space as a function of  $x$ . Loosely speaking, this condition implies that the state  $X_{t_{n,s}}$  does not influence the future state  $X_{t_{n+B+1}}$  much, given the observations in between. The conditional expectation is given by

$$\begin{aligned} \mathbb{E}[f(X_{t_{n+B+1}}) | Y_{n+1:n+B} = y_{n+1:n+B}, X_{t_{n,s}} = x] &= \frac{\mathbb{E}\left[f(X_{t_{n+B+1}}) \prod_{m=n+1}^{n+B} g_m(y_m | X_{t_m}) \middle| X_{t_{n,s}} = x\right]}{\mathbb{E}\left[\prod_{m=n+1}^{n+B} g_m(y_m | X_{t_m}) \middle| X_{t_{n,s}} = x\right]} \\ &= \frac{Q_{t_{n,s}, t_{n+B+1}}(f)}{Q_{t_{n,s}, t_{n+B+1}}(1)}(x). \end{aligned} \quad (10)$$

We point out that the mixing of the latent process conditional on data over the interval  $[t_{n,s}, t_{n+B+1}]$  makes it easier to satisfy the condition (ii) of Assumption 2 for  $t = t_{n,s}$  and  $t' \geq t_{n+B+1}$ , as illustrated by the following proposition.

**Proposition 1.** Suppose  $t' \geq t_{n+B+1}$  and that the following two conditions hold for some constants  $\tilde{C}_2^{(a)}, \tilde{C}_2^{(b)} \geq 1$ :

$$(a) \quad \tilde{C}_2^{(a)} \inf_{x \in \mathcal{C}_{t_{n,s}}} \frac{Q_{t_{n,s},t'}(u_{t'})}{Q_{t_{n,s},t_{n+B+1}}(1)}(x) \geq \sup_{x \in \mathbb{X}} \frac{Q_{t_{n,s},t'}(u_{t'})}{Q_{t_{n,s},t_{n+B+1}}(1)}(x), \text{ and}$$

$$(b) \quad \tilde{C}_2^{(b)} \inf_{x \in \mathcal{C}_{t_{n,s}}} \frac{Q_{t_{n,s},t_{n+B+1}}(1)}{u_{t_{n,s}}}(x) \geq \sup_{x \in \mathbb{X}} \frac{Q_{t_{n,s},t_{n+B+1}}(1)}{u_{t_{n,s}}}(x).$$

Then Assumption 2 is satisfied with  $C_2 = \tilde{C}_2^{(a)} \tilde{C}_2^{(b)}$ .

*Proof.*

$$\begin{aligned} \tilde{C}_2^{(a)} \tilde{C}_2^{(b)} \inf_{\mathcal{C}_{t_{n,s}}} \frac{Q_{t_{n,s},t'}(u_{t'})}{u_{t_{n,s}}} &\geq \tilde{C}_2^{(a)} \inf_{\mathcal{C}_{t_{n,s}}} \frac{Q_{t_{n,s},t'}(u_{t'})}{Q_{t_{n,s},t_{n+B+1}}(1)} \cdot \tilde{C}_2^{(b)} \inf_{\mathcal{C}_{t_{n,s}}} \frac{Q_{t_{n,s},t_{n+B+1}}(1)}{u_{t_{n,s}}} \\ &\geq \sup_{\mathbb{X}} \frac{Q_{t_{n,s},t'}(u_{t'})}{Q_{t_{n,s},t_{n+B+1}}(1)} \cdot \sup_{\mathbb{X}} \frac{Q_{t_{n,s},t_{n+B+1}}(1)}{u_{t_{n,s}}} \geq \sup_{\mathbb{X}} \frac{Q_{t_{n,s},t'}(u_{t'})}{u_{t_{n,s}}}. \end{aligned}$$

□

Condition (a) above holds if the latent process mixes well conditional on data over the interval  $[t_{n,s}, t_{n+B+1}]$ . This can be seen by letting  $f = Q_{t_{n+B+1},t'}(u_{t'})$  in (10) and noting that  $Q_{t_{n,s},t'}(u_{t'}) \equiv Q_{t_{n,s},t_{n+B+1}}(f)$ . Condition (b) states that the guide function  $u_{t_{n,s}}$  approximates the forecast likelihood of  $B$  future observations  $y_{n+1:n+B}$  given the current state  $X_{t_{n,s}}$ . Thus Proposition 1 implies that an approximation  $u_{t_{n,s}}(x) \approx Q_{t_{n,s},t_{n+B+1}}(1)(x) = p_{Y_{n+1:n+B} | X_{t_{n,s}}}(y_{n+1:n+B} | x)$  is a sensible choice for  $s \in 1:S$ , provided that the latent process mixes well conditional on data.

As for the scaling with increasing dimensions, we note that the constant  $C_2$  will generally increase exponentially in  $d$ . For  $d$  independent one dimensional processes, for example, the ratio between the guide function  $u_t(x) := \prod_{i=1}^d u_t^{[i]}(x^{[i]})$  and  $Q_{t,t'}(u_{t'}) = \prod_{i=1}^d Q_{t,t'}^{[i]}(u_{t'}^{[i]})$  will scale exponentially. If the guide function approximates the forecast likelihood well and consequently if the ratio  $\frac{Q_{t,t'}^{[i]}(u_{t'}^{[i]})}{u_t^{[i]}}$  fluctuates by small amount across the space  $\mathbb{X}^{[i]}$  in each dimension, GIRF methodology can substantially slow down the rate of increase in  $C_2$  and reduce the filtering error. We call an algorithm *moderately scalable* if its cost has a slow rate of exponential growth as the latent dimension  $d$  increases. Moderately scalable algorithms are expected to be applicable to models of dimension substantially exceeding non-scalable algorithms. However, the exponential scaling limits applicability beyond some point. The standard particle filter corresponds to taking the guide function to be  $u_{t_n}(x) = g_n(y_n | x)$ ; in that case the ratio  $\frac{Q_{t,t'}^{[i]}(u_{t'}^{[i]})}{u_t^{[i]}}$  can vary greatly across the space in each dimension. In this case,  $C_1$  grows at a quick exponential rate with  $d$ .

The implications of Theorem 2 may be summarized as follows. Assumption 1 concerns the source of filtering error coming from Monte Carlo randomness in propagation steps. This source of error can be controlled by dividing observation time intervals in number that grows with the space dimension and thereby reducing  $C_1$ . By contrast, both theory and practice indicate that the auxiliary particle filter (equivalent to the GIRF in Algorithm 1 with  $S=1$ ) scales poorly even when equipped with a good guide function. Assumption 2 bounds the source of filtering error that originates from targeting the guided filter distribution  $P_t^G$  instead of the distribution of  $X_t$  conditioned on data  $y_{1:N}$ . Thus the filtering error decreases as the guide function accurately approximate the forecast likelihood, reducing  $C_2$ . In practice, fast mixing of the latent process

conditional on data may make it sufficient to approximate the forecast likelihood of only a few number of future observations.

We now present two results (Theorems 3 and 4) on the asymptotic normality of the Monte Carlo error for estimates from GIRF (Algorithm 1) of the filtered latent states and the likelihood. Under Assumptions 1 and 2, we derive upper bounds on the asymptotic variances of these quantities. The previous remarks on the scaling properties of these bounds when  $S = d$  also apply here. The connection with Assumptions 1 and 2 is the novel contribution of these results, since asymptotic normality itself follows directly from existing results in the literature (e.g., Section 9 in Del Moral (2004)) when we view GIRF (Algorithm 1) as a standard bootstrap particle filter on the discrete time latent process on the extended space,  $\{(X_t, X_{t-}); t \in \mathbb{I} \setminus \{t_0\}\}$ . The proof of the following theorems are given in Supplementary section S3.

**Theorem 3.** *In the limit where the particle size  $J$  tends to infinity, the likelihood estimate  $\hat{\ell}$  from GIRF (Algorithm 1) converges in distribution to a normal distribution:*

$$\sqrt{J} \left( \frac{\hat{\ell}}{\ell_{1:N}(y_{1:N})} - 1 \right) \Rightarrow \mathcal{N}(0, \mathcal{V}).$$

*Under Assumptions 1 and 2, the asymptotic variance is bounded above by*

$$\mathcal{V} < NS \left( \frac{C_1^2 C_2^2}{\rho^2} - 1 \right).$$

*An application of the delta method leads to the asymptotic normality of the log likelihood estimate:*

$$\sqrt{J} \left( \log \hat{\ell} - \log \ell_{1:N}(y_{1:N}) \right) \Rightarrow \mathcal{N}(0, \mathcal{V}).$$

**Theorem 4.** *In the limit where the particle size  $J$  tends to infinity, the following asymptotic normality holds for every measurable function  $f : \mathbb{X} \rightarrow \mathbb{R}$  such that  $\|f\|_\infty \leq 1$ :*

$$\sqrt{J} \left( \frac{1}{J} \sum_{j=1}^J f(X_{t_N}^{F,j}) - \mathbb{E}[f | Y_{1:N} = y_{1:N}] \right) \Rightarrow \mathcal{N}(0, \mathcal{W}(f)).$$

*Under Assumptions 1 and 2, the asymptotic variance is bounded above by*

$$\mathcal{W}(f) < 1 + 4NS \frac{C_1^2 C_2^2}{\rho^2}.$$

## 5 Constructing a guide function

Algorithm 1 is a properly weighted filter for any guide function  $u_{t_{n,s}} : \mathbb{X} \rightarrow \mathbb{R}^+$ . However, the choice of the guide function affects its numerical efficiency. This dependence was theoretically studied in Theorem 2. The current section develops a general approach to the construction of the guide function. This construction is used for the examples of Sections 7.2 and 7.3. Motivated by Theorem 2, we seek a guide function  $u_{t_{n,s}}(x)$  approximating the forecast likelihood of future observations given  $X_{t_{n,s}} = x$ . Looking ahead  $B \geq 1$  observations, we get

$$u_{t_{n,s}}(x) \approx p_{Y_{n+1:m} | X_{t_{n,s}}} (y_{n+1:m} | x), \quad (11)$$

where  $m = \min(n+B, N)$ . At observation time  $t_n$ , we set  $u_{t_n} = u_{t_{n-1}, S}$  in (11) so the guide function approximates the forecast likelihood of observations  $y_{n:n+B-1}$ . When  $B > 1$ , it is numerically convenient to first construct an approximation for the forecast likelihood of a single observation,

$$u_{t_{n,s}, t_{n+b}}(x) \approx p_{Y_{n+b} | X_{t_{n,s}}}(y_{n+b} | x)$$

for  $b \in 1:B$ , and then to specify the guide function by a product

$$u_{t_{n,s}}(x) = \prod_{b=1}^{\min(B, N-n)} u_{t_{n,s}, t_{n+b}}^{\eta_{t_{n,s}, t_{n+b}}}(x), \quad (12)$$

where  $0 \leq \eta_{t_{n,s}, t_{n+b}} \leq 1$  denote fractional powers that are non-decreasing as  $t_{n,s}$  increases. For observation times  $t_n$ , we interpret (12) as  $u_{t_{n-1}, S}$ . If  $s=S$  and  $b=1$ , we set  $u_{t_{n,S}, t_{n+1}}(x_{t_{n,S}}) := g_{n+1}(y_{n+1} | x_{t_{n,S}})$  and  $\eta_{t_{n,S}, t_{n+1}} = 1$ , because we can evaluate the measurement density at  $t_{n,S} = t_{n+1}$ . The fact that the powers  $\eta_{t_{n,s}, t_{n+b}}$  are non-decreasing as  $t_{n,s}$  increases may reflect the algorithm user's increasing confidence in the accuracy of the approximated forecast likelihood as the forecast interval becomes shorter. A possible choice for the powers is

$$\eta_{t_{n,s}, t_{n+b}} := 1 - \frac{t_{n+b} - t_{n,s}}{t_{n+b} - t_{\max(n+b-B, 0)}}, \quad (13)$$

such that  $1 - \eta_{t_{n,s}, t_{n+b}}$  is proportional to the forecast interval length. This choice gradually introduces the information provided by  $y_{n+B}$  to the filtering algorithm over the time interval  $[t_{n,1}, t_{n+B}]$ . If we set  $\eta_{t_{n,s}, t_{n+b}} = 1$  for all  $t_{n,s} \leq t_{n+b}$ , the effective sample sizes at  $s=1$  can be noticeably smaller than at other intermediate time points because a new term  $u_{t_{n,1}, t_{n+B}}$  is suddenly multiplied to the resampling weights at  $t_{n,1}$ .

We propose one way of obtaining an approximate forecast likelihood  $u_{t_{n,s}, t_{n+b}}$  in the absence of a closed-form transition density for the latent process. We will assume that the measurement density  $g_{n+b}(\cdot | X_{t_{n+b}})$  belongs to a family of densities  $\{\check{g}(\cdot | \mu, \Sigma); \mu, \Sigma\}$  that are parameterized by the mean  $\mu$  and the variance  $\Sigma$ . We make a forecast from the current state  $X_{t_{n,s}} = x$  to time  $t_{n+b}$  using a deterministic skeleton of  $\{X_t\}$ . A deterministic skeleton is a deterministic process that approximates the conditional mean of the latent process  $\{X_t; t \geq t_{n,s}\}$  given  $X_{t_{n,s}} = x$ . This deterministic forecast will be denoted by  $\mu_{t_{n+b}}(x)$ . We next approximate the forecast variance of  $X_{t_{n+b}}$  given  $X_{t_{n,s}} = x$ . The forecast variance may be estimated by computing the sample variance of a collection of random forecast simulations for  $X_{t_{n+b}}$  from  $X_{t_{n,s}} = x$ . We denote this forecast variability by  $\Xi_{n+b}(x)$  and let  $\Sigma_{n+b}(x)$  be the sum of  $\Xi_{n+b}(x)$  and the variance of the measurement process for  $Y_{n+b}$  given  $X_{t_{n+b}} = \mu_{t_{n+b}}(x)$ . We then approximate the forecast likelihood of  $Y_{n+b} = y_{n+b}$  given  $X_{t_{n,s}} = x$  by letting

$$u_{t_{n,s}, t_{n+b}}(x) = \check{g}(y_{n+b} | \mu_{t_{n+b}}(x), \Sigma_{n+b}(x)). \quad (14)$$

One may use (14) for measurement processes without well-defined first and second moments, if the measurement noise is additive and the measurement process belongs to a family that is closed under independent sums, such as the Cauchy distributions. We view the parameters  $\mu$  and  $\Sigma$  of the family  $\{\check{g}(\cdot | \mu, \Sigma)\}$  as representing the center and the variability of the distributions respectively. For two independent random variables  $X_1$  and  $X_2$  with densities  $\check{g}(\cdot | \mu, \Sigma_1)$  and  $\check{g}(\cdot | 0, \Sigma_2)$  respectively, we suppose that  $X_1 + X_2$  has density  $\check{g}(\cdot | \mu, \Sigma_1 + \Sigma_2)$ . The forecast variability  $\Xi_{n+b}(x)$  may be approximated by, for example, a value for which the distribution with

density  $\check{g}(\cdot | \mu_{t_{n+b}}(x), \Xi_{n+b}(x))$  has the same inter-quantile distance as the sample inter-quantile distance of the random forecasts.

Often times, the measurement process of a spatiotemporal POMP model is local, in the sense that the measurement in the  $i$ -th spatial unit depends only on the state of the same unit. In such cases, the measurement density can be expressed as

$$g_n(y_n | x_{t_n}) = \prod_{i=1}^d g_n^{[i]}(y_n^{[i]} | x_{t_n}^{[i]}).$$

If each one-dimensional process  $g_n^{[i]}$  belongs to a family  $\{\check{g}^{[i]}(\cdot | \mu, \Sigma)\}$ , we may take

$$u_{t_{n,s}, t_{n+b}}(x) := \prod_{i=1}^d \check{g}^{[i]} \left[ y_{n+b}^{[i]} \mid \mu_{t_{n+b}}(x)^{[i]}, \Sigma_{n+b}^{[i]}(x) \right], \quad (15)$$

where  $\mu_{t_{n+b}}(x)^{[i]}$  is the  $i$ -th component of the deterministic forecast  $\mu_{t_{n+b}}(x)$  and  $\Sigma_{n+b}^{[i]}(x)$  is the estimated variability of  $Y_{n+b}^{[i]}$  given  $X_{t_{n,s}} = x$ . We note that  $\mu_{t_{n+b}}(x)$  is obtained by simulating the deterministic skeleton jointly for all dimensions, and also  $\Sigma_{n+b}(x)$  by simulating the joint random latent process. Thus  $u_{t_{n,s}, t_{n+b}}(x)$  constructed by (15) makes some allowance for the correlation of the latent process between dimensions.

We finally note that one can save computational effort by using locally linear approximations for the forecast variability. Suppose that for  $t \in (t_{n,s}, t_{n+b})$  the ancestor of a particle  $X_t^j$  is  $X_{t_{n,s}}^{j'}$ . Suppose also that the variability of forecast from  $t_{n,s}$  to  $t_{n+b}$  was estimated to be  $\Xi_{n+b}(X_{t_{n,s}}^{j'})$ . One may approximate the forecast variability from  $t$  to  $t_{n+b}$  for particle  $X_t^j$  as

$$\Xi_{n+b}(X_t^j) \approx \Xi_{n+b}(X_{t_{n,s}}^{j'}) \cdot \frac{t_{n+b} - t}{t_{n+b} - t_{n,s}}. \quad (16)$$

The forecast variability can be re-estimated using new random forecasts at each  $t_{n,1}$ ,  $n \in 1:N-1$ , or more often if the locally linear approximation becomes unreliable.

## 6 Parameter inference using GIRF methodology

Being a Monte Carlo algorithm that yields unbiased estimates of the likelihood of data, GIRF (Algorithm 1) can be easily combined with existing parameter inference methods that build upon the particle filter. These parameter estimation methods include particle Markov chain Monte Carlo (PMCMC) (Andrieu et al., 2010), SMC<sup>2</sup> (Chopin et al., 2013), and iterated filtering (Ionides et al., 2015). For high dimensional POMP models, likelihood estimates often have large amount of Monte Carlo error, for any feasible amount of Monte Carlo effort, even when filtering is successful. This prevents the use of PMCMC, which requires a standard deviation order of 1 log unit (Doucet et al., 2015). In this paper, we will focus on parameter estimation carried out by iterated filtering. We will show that iterated filtering, together with Monte Carlo adjusted profile methodology (Ionides et al., 2017), is able to operate successfully in the presence of relatively high levels of Monte Carlo error.

The iterated filtering approach of Ionides et al. (2015) is a plug-and-play parameter estimation algorithm that finds the maximum likelihood estimate (MLE) of multi-dimensional parameters via an SMC approximation to an iterated, perturbed Bayes map. This algorithm, when implemented

---

**Algorithm 2:** An iterated guided intermediate resampling filter (iGIRF)

---

**Input :** Data,  $y_{1:N}$   
 Simulator for  $P_{t_0}(dx; \theta)$   
 Simulator for  $K_{t_{n,s-1}, t_{n,s}}(dx; x_{t_{n,s}}, \theta)$  for  $n \in 0:N-1$  and  $s \in 1:S$   
 Evaluator for  $g_n(y_n | x_{t_n}, \theta)$  for  $n \in 1:N$   
 Evaluator for  $u_{t_{n,s}}(x_{t_{n,s}}, \theta)$  for  $n \in 0:N-1$  and  $s \in 1:S$   
 Number of particles,  $J$   
 Initial parameter swarm,  $\{\Theta^{0,j}; j \in 1:J\}$   
 Perturbation kernel for initial value parameter,  $\kappa_0(d\theta; \phi, \sigma)$   
 Perturbation kernel,  $\kappa_{n,s}(d\theta; \phi, \sigma)$  for  $n \in 0:N-1$  and  $s \in 1:S$   
 Number of iterations,  $M$   
 Sequence of perturbation sizes,  $\sigma_{1:M}$   
  
**Output:** Final parameter swarm  $\{\Theta^{M,j}; j \in 1:J\}$   
**for**  $m \leftarrow 1:M$  **do**  
     Run Algorithm 1 on the extended latent space  $(X_{t_{n,s}}, \Theta_{t_{n,s}}^m)$  with initial draws from  
     (17) and subsequent draws from (18)  
     Set  $\Theta^{m,j} = \Theta_{t_N}^{F,m,j}$  for  $j \in 1:J$   
**end**

---

via a plug-and-play SMC filtering approach, provides plug-and-play inference on unknown model parameters. Iterated filtering runs a sequence of particle filter on the augmented space comprising the latent variable and the parameter, where the parameters are subject to random perturbations at each time point. The size of perturbations decrease over iterations to induce convergence. In the limit where the perturbation size approaches zero, Ionides et al. (2015) showed that the distribution of filtered parameters approaches a point mass at the MLE under regularity conditions.

Algorithm 2 presents an iterated guided intermediate resampling filter (iGIRF). The algorithm starts with an initial set of parameters  $\{\Theta^{0,j}; j \in 1:J\}$ . At the beginning of the  $m$ -th iteration, the parameter component of each particle is perturbed from its current position  $\Theta^{m-1,j}$  with kernel  $\kappa_0$  independently for each  $j \in 1:J$ . A pre-set decreasing sequence  $(\sigma_m)_{m=1:M}$  determines the size of perturbation. The initial latent variables  $X_{t_0}^{F,j}$  are drawn from the parameterized initial latent distribution, as follows:

$$\Theta_{t_0}^{F,m,j} \sim \kappa_0(d\theta; \Theta^{m-1,j}, \sigma_m), \quad X_{t_0}^{F,j} \sim P_{t_0}(dx; \Theta_{t_0}^{F,m,j}). \quad (17)$$

Parameters are perturbed at each intermediate time  $t_{n,s}$  with kernel  $\kappa_{n,s}$ , and the states are then drawn from the parameterized transition kernel:

$$\Theta_{t_{n,s}}^{P,m,j} \sim \kappa_{n,s}(d\theta; \Theta_{t_{n,s-1}}^{F,m,j}, \sigma_m), \quad X_{t_{n,s}}^{P,j} \sim K_{t_{n,s-1}, t_{n,s}}(dx; X_{t_{n,s-1}}^{F,j}, \Theta_{t_{n,s}}^{P,m,j}). \quad (18)$$

These perturbations define an extended POMP model, and the weighting and resampling steps are carried out on this extended model following GIRF (Algorithm 1). At the end of filtering, the parameter swarm  $\Theta_{t_N}^{F,m,j}$  are set as  $\Theta^{m,j}$ . After  $M$  iterations, the final parameter swarm  $\Theta^{M,j}$  is considered to be a collection of numerical approximations of the MLE.

Our implementation of iGIRF uses Gaussian parameter perturbations. For parameters with interval constraints, we apply certain transformations beforehand such as taking the logarithm for non-negative parameters to ensure that Gaussian perturbations do not violate the constraints. Our examples require us to consider two forms for the kernel  $\kappa_{n,s}$ . *Initial value parameters* (IVPs)



are perturbed only by  $\kappa_0$ , and all other  $\kappa_{n,s}$  have a point mass at the identity for the IVPs. IVPs are parameters which encode the value of  $X_{t_0}$  but play no subsequent role in the dynamics of the system. For our examples of iGIRF, all parameters other than IVPs use a non-singular kernel which does not depend on  $n$  and  $s$ , and we call these *regular parameters*. Intuitively, treating parameters as regular is appropriate in iGIRF if information about the parameters arrives at a steady rate through the time series.

## 7 Examples

In this section, we apply GIRF methodology to three examples. We investigate the empirical scaling properties of an implementation of GIRF (Algorithm 1) compared to alternative methods and demonstrate the practical utility of iGIRF (Algorithm 2) for inference on moderately high dimensional POMP models. In all our examples, the number of intermediate sub-intervals  $S$  is set equal to the space dimension  $d$ .

### 7.1 Correlated Brownian motion

We first applied our algorithm to a multi-dimensional correlated Brownian motion. Each component of the Brownian motion was identically distributed with increments per unit time having mean zero and unit variance. The correlation coefficient matrix  $A$  for the increments was chosen such that its all off-diagonal entries equaled  $\alpha$ . The initial latent distribution at time  $t_0 = 0$  was given by the point mass at the origin of  $\mathbb{R}^d$ . Measurements were made at positive integer time points  $t_{1:50} = 1:50$ , with independent Gaussian noises of mean zero and unit variance. The POMP model can be expressed as follows, where  $I$  denotes the  $d$  dimensional identity matrix:

$$X_{t+\delta} = X_t + \mathcal{N}(0, \delta A), \quad Y_n = X_{t_n} + \mathcal{N}(0, I).$$

The guide function  $u_{t_{n,s}}$  was defined as in (12), where all  $\eta_{t_{n,s}, t_{n+b}}$  were taken to equal the unity. Since the process had zero drift, the forward state projection by the deterministic mean process was given by  $\mu_{t_{n+b}}(x_{t_{n,s}}) = x_{t_{n,s}}$ . The variance of  $X_{t_{n+b}}$  conditioned on  $X_{t_{n,s}} = x_{t_{n,s}}$  was equal to  $(t_{n+b} - t_{n,s}) \cdot A$ , so the guide function was defined as

$$u_{t_{n,s}}(x_{t_{n,s}}) = \prod_{b=1}^B \phi_d[y_{t_{n+b}}; x_{t_{n,s}}, (t_{n+b} - t_{n,s}) \cdot A + I], \quad (19)$$

where  $\phi_d(\cdot; \mu, \Sigma)$  denotes the density of the  $d$ -dimensional Gaussian distribution with mean  $\mu$  and variance  $\Sigma$ . Evaluating (19) typically requires procedures such as the Cholesky decomposition and takes  $O(d^3)$  computations. Since this could be demanding for large  $d$ , we also used an approximation of (19) obtained by ignoring the off-diagonal elements of  $A$ ,

$$u_{t_{n,s}}(x_{t_{n,s}}) = \prod_{b=1}^B \phi_d[y_{t_{n+b}}; x_{t_{n,s}}, \{(t_{n+b} - t_{n,s}) + 1\} I]. \quad (20)$$

We first graphically illustrate the role of intermediate resampling and the guide function using a twenty dimensional model. The guide function was set to the exact forecast likelihood with  $B = 1$ . In this case the guided filter distribution at  $t_{0,s}$  equals the conditional distribution of  $X_{t_{0,s}}$  given  $Y_1 = y_1$ . Figure 1 shows the first two coordinates of the filtered particles  $X_{t_{0,s}}^{F,j}$  at three

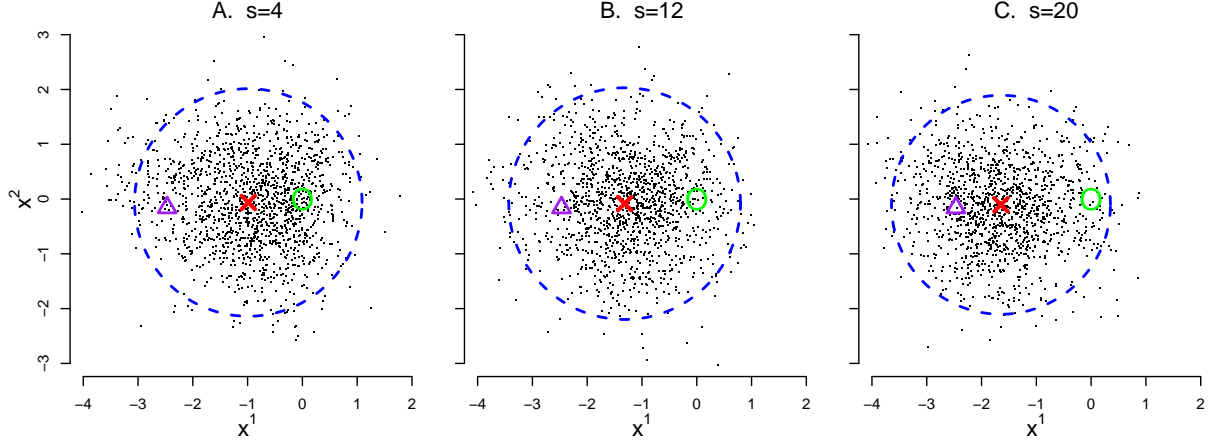


Figure 1: The first two coordinates of the filtered particles  $X_{t_{0,s}}^{F,j}$  from GIRF run at three intermediate time steps (A,  $s=4$ ; B,  $s=12$ ; C,  $s=20$ ) for twenty dimensional linear Gaussian model.

	Total no. of particles	$S$	$B$	CPU time (sec)			
				$d = 5$	$d = 10$	$d = 50$	$d = 200$
APF	$2,000 \times d$	1	1	1	3	63	1084
GIRF	2,000	$d$	2	1	3	57	835

(a) Computational costs

	$d = 5$		$d = 10$		$d = 50$		$d = 200$	
	APF	GIRF	APF	GIRF	APF	GIRF	APF	GIRF
$\log \ell$	-485.6		-949.8		-4790		-18908	
$\log \hat{\ell}$	-487.1	-485.5	-953.5	-951.2	-6757	-4798	-54946	-19036
MSE	0.0004	0.0009	0.01	0.002	2.2	0.013	9.3	0.068

(b) Estimated log likelihood and the average squared error of the estimated filter means

Table 1: Comparison between the auxiliary particle filter and GIRF for the correlated Brownian motion model.

intermediate time points. The mean of the initial distribution is marked by a green ‘O’, and the observation  $y_1$  by a purple triangle. The mean of the guided filter distribution at  $t_{0,s}$  is marked by a red ‘X’, and the 95% coverage region by a blue dashed circle. As time progresses, the red ‘X’ shifts from the origin toward  $y_1$ , and the coverage region changes in size. The filtered particles almost exactly follow the guided filter distributions at intermediate steps.

In following experiments, we let the guide function to approximate  $B = 2$  future observations. We first compared the filtering performance of the auxiliary particle filter (APF) and GIRF for varying dimensions  $d = 5, 10, 50$ , and 200. The total number of particles for APF was  $d$  times larger than that for GIRF to allow similar computation time to both algorithms. For  $d = 50$  and 200, we divided the particles into  $d/10$  islands by applying the island particle method of Vergé et al. (2015) in order to avoid memory deficiency. The computational resources used and the numerical results are shown in Table 1. The true likelihood of the data and the true filtering distributions were exactly computed by the Kalman filter for comparison. We compared the log likelihood estimates and the squared error of the estimated filter means at the terminal time ( $t = 50$ ) averaged over all  $d$  components. The performance of APF decayed rapidly with dimension

beyond  $d = 10$ . In contrast, GIRF produced relatively accurate estimates of the likelihoods and the filter means up to  $d = 200$ .

Next we investigated varying the dimension  $d$  and correlation coefficient  $\alpha$ . We parallelized Algorithm 1 using the method of Vergé et al. (2015) in a straightforward way. Sixty particle islands with one thousand particles in each island were used in all following experiments. Snyder et al. (2008) reported that at least  $10^{11}$  particles were required for the same filtering problem in two hundred dimension using the standard bootstrap particle filter. We varied the space dimension from twenty to fifty, one hundred, and two hundred while fixing the correlation coefficient at zero. Each filtering on average took 15 seconds, 81 seconds, 5 minutes, and 20 minutes respectively. Figure 2 shows the mean squared error of the estimated filter mean at the terminal time averaged over all dimensions. The results were obtained from forty independent filtering repetitions for each case. The estimated squared biases, shown in triangles, were roughly  $\frac{1}{40}$  times the MSE, implying that the estimator was effectively unbiased. The MSE increased as the dimension grew, but the MSE at dimension two hundred was still less than 0.01, which was much smaller than the variance of the exact filtering distribution at the terminal time, which was 0.62.

The estimated log likelihoods are shown in Table 2. The estimated standard errors of the log likelihoods are shown in parentheses. In dimensions twenty and fifty, the true likelihood was well within one standard error of the likelihood estimates. In dimensions one hundred and two hundred, the likelihood estimates are more than one standard error below the true likelihood. Since the likelihood estimator is guaranteed to be unbiased, this shows that the Monte Carlo likelihood estimate is above the true value with small probability, while the likelihood estimate is below the true value with high probability. This phenomenon reflects that filtering becomes less accurate as the dimension increases.

In the second set of experiments, the dimension was fixed at either twenty or fifty, and the correlation coefficient varied from 0 to 0.5 with intervals of 0.1. Figure 3 shows the MSE of the estimates of the filtering mean at the terminal time. The error bars indicate the sizes of the standard errors of the MSE. When the guide function used the exact covariance as in (19), the MSEs were almost constant or increasing very slowly as the correlation  $\alpha$  increased. When we used the diagonal approximation as in (20), the errors in the filter estimates increased much more rapidly as  $\alpha$  increased. However, the errors were still reasonably small. The MSEs were about 0.02 both in twenty and fifty dimensions at  $\alpha = 0.5$ , where the variance of the filtering distribution was 0.52 and 0.51 respectively. The log likelihood estimates reported in Table 3 shows a similar pattern in the filtering accuracy. These results illustrate that the performance of GIRF methodology depends on how well the guide functions approximate the forecast likelihoods of future observations, agreeing with our theoretical investigation.

## 7.2 Stochastic Lorenz 96 model

The Lorenz 96 model is a nonlinear chaotic system which provides a simplified representation of global atmospheric circulation (Lorenz, 1996). Stochastic versions of this model have been used to support the increased use of non-deterministic models for atmospheric science (Wilks, 2005; Palmer, 2012). We considered a stochastic Lorenz 96 model with added Gaussian process noise, defined as follows:

$$dX_t^{[i]} = \{(X_t^{[i+1]} - X_t^{[i-2]}) \cdot X_t^{[i-1]} - X_t^{[i]} + F\}dt + \sigma_p dB_t^{[i]}, \quad i \in 1:d. \quad (21)$$

In the equation above, we understand that  $X^{[0]} = X^{[d]}$ ,  $X^{[-1]} = X^{[d-1]}$ , and  $X^{[d+1]} = X^{[1]}$ . The terms  $\{B_t^{[i]}; i \in 1:d\}$  denote  $d$  independent standard Brownian motions, and  $\sigma_p$  the process

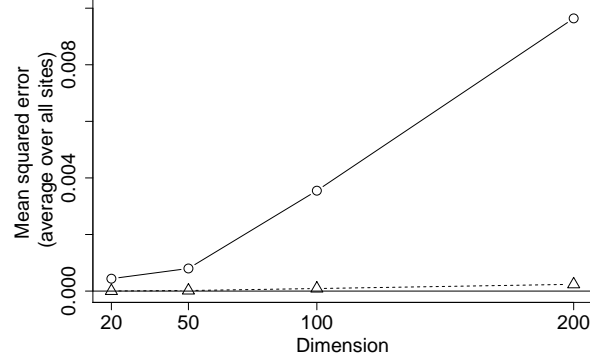


Figure 2: The MSE of the estimates of the filtering mean:  $\circ$ , MSE;  $\triangle$ , bias squared

$d$	20	50	100	200
$\log \ell$	-1916.30	-4703.83	-9499.10	-18908.62
$\log \hat{\ell}$	-1916.28 (0.06)	-4703.72 (0.17)	-9501.20 (0.36)	-18932.69 (0.87)

Table 2: Log likelihood estimates under varying dimensions

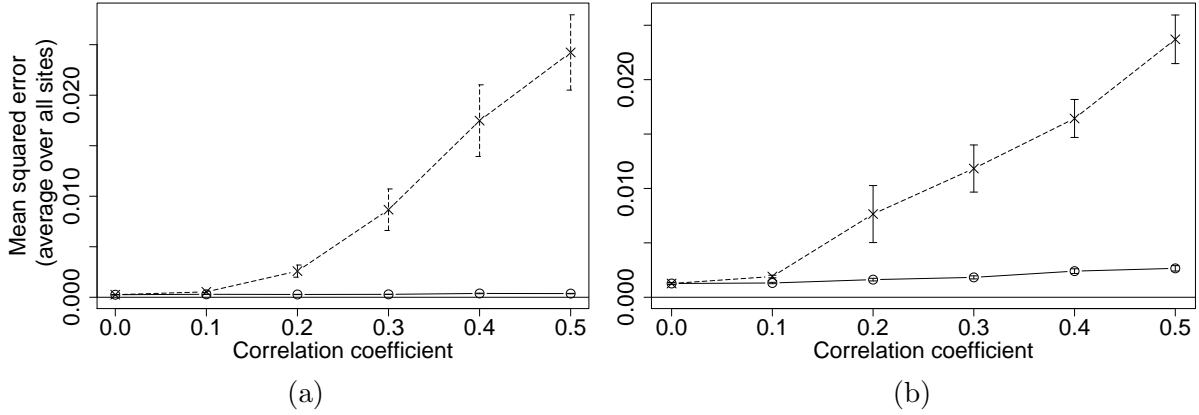


Figure 3: The MSE of the estimates of the filtering mean under varying degrees of correlation, (a)  $d = 20$ , (b)  $d = 50$ :  $\circ$ , exact covariance used;  $\times$ , diagonal covariance used

Correlation coefficient	0.0	0.1	0.2	0.3	0.4	0.5
$\log \ell$	-1904.04	-1897.75	-1884.24	-1866.33	-1844.90	-1820.02
$\log \hat{\ell}$	-1903.92	-1897.71	-1884.25	-1866.31	-1844.90	-1820.05
[exact covariance]	(0.05)	(0.05)	(0.06)	(0.05)	(0.06)	(0.06)
$\log \hat{\ell}$	-1903.92	-1897.79	-1884.91	-1868.35	-1852.62	-1831.77
[diagonal covariance]	(0.05)	(0.09)	(0.20)	(0.59)	(0.44)	(0.71)
$\log \ell$	-4790.18	-4750.63	-4701.90	-4644.46	-4579.29	-4505.73
$\log \hat{\ell}$	-4790.49	-4750.35	-4702.02	-4644.88	-4579.82	-4505.96
[exact covariance]	(0.19)	(0.24)	(0.29)	(0.27)	(0.38)	(0.62)
$\log \hat{\ell}$	-4790.49	-4754.44	-4722.03	-4685.83	-4649.51	-4609.30
[diagonal covariance]	(0.19)	(0.43)	(0.57)	(0.68)	(0.89)	(0.83)

Table 3: Log likelihood estimates under varying degrees of correlation, top,  $d = 20$ ; bottom,  $d = 50$

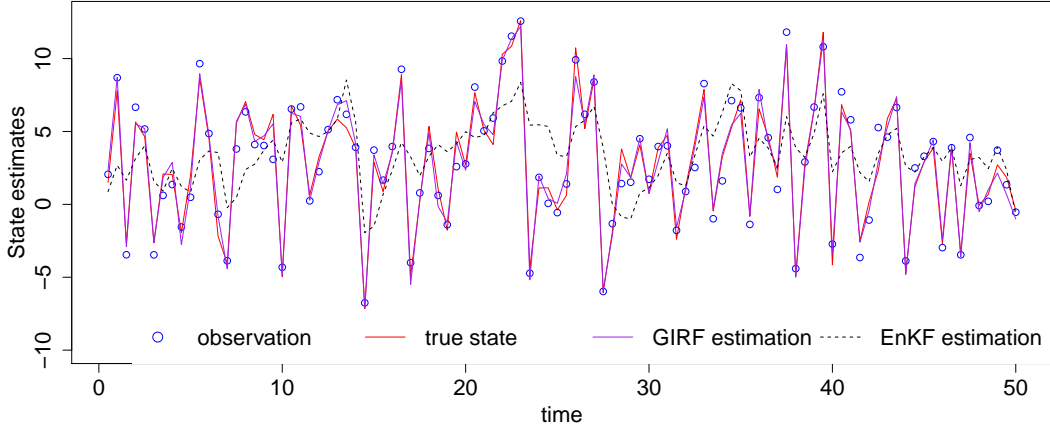


Figure 4: The estimated filter means for the first coordinate for fifty dimensional stochastic Lorenz 96 model.

noise magnitude.  $F$  is a forcing constant, with  $F=8$  considered by Lorenz (1996) to induce chaotic behavior. The system is started at the initial state  $X_0^{[i]} = 0$  for  $i \in 1:d-1$  and  $X_0^{[d]} = 0.01$ . Observations are independently made for each dimension at  $t_n = 0.5n$  for  $n \in 1:200$  with Gaussian measurement noise of mean zero and standard deviation  $\sigma_m$ . We generated data for varying dimensions with  $F=8$  and  $\sigma_p = \sigma_m = 1$ , using the Euler-Maruyama method for numerical approximation of the sample paths of  $X_t$  with time increments of 0.01.

We compared our implementation of GIRF with an ensemble Kalman filter (EnKF) for the generated data. The likelihood of data was estimated from EnKF runs using the Gaussian approximation to the empirical distribution of the particle swarm using the sample mean and the sample variance. Our GIRF implementation used the guide function constructed according to (12)–(16) with  $B = 2$ . The log likelihood of the data for the fifty dimensional model was estimated to be  $-2.0 \times 10^4$  by GIRF and  $-1.0 \times 10^5$  by EnKF. The estimated filter means for the same data are plotted for the first coordinate (i.e.,  $X_{t_n}^{[1]}$ ) for the first one hundred observation time points in Figure 4. The GIRF used 2,000 particles and EnKF used 16,000 particles. Both algorithms took 78 minutes to run. The estimated filter means by GIRF closely matched the observations and the true states, whereas the estimates by the EnKF deviated a lot from the truth. The difference of  $8.0 \times 10^4$  log units in the likelihood estimates and the inaccurately estimated filter means imply that EnKF is not suitable for this model. We remark that EnKF failed due to the nonlinearity of the model rather than due to the dimensionality—EnKF also failed to produce reasonable filter estimates in dimension  $d = 4$ . When the observations were obtained at intervals of 0.1 instead, EnKF produced good results in  $d = 200$  (Figure S-7 and Table S-5 in the supplementary text). This is due to the fact that our stochastic Lorenz 96 model behaves almost like a linear Gaussian model in time interval of 0.1.

In order to test the parameter estimation capability of iGIRF, we made inference on  $F$  with or without the knowledge of  $\sigma_p$  and  $\sigma_m$  from the data for the fifty dimensional Lorenz model (Figure 5). The likelihoods of data were estimated at values of  $F$  between 6.0 and 10.0 with intervals of 0.5. The likelihoods estimated at  $\sigma_p = \sigma_m = 1$  were used to estimate the slice likelihood curve. We also estimated the MLEs for  $\sigma_p$  and  $\sigma_m$  using iGIRF (Algorithm 2) and estimated the likelihoods at the obtained Monte Carlo MLE using Algorithm 1 to approximate the profile likelihood curve. The Monte Carlo MLE was taken to be the mean value of the parameter swarm at the end of the twentieth iteration in Algorithm 2 (i.e.,  $M = 20$ ). The estimation at each value of  $F$  was repeated

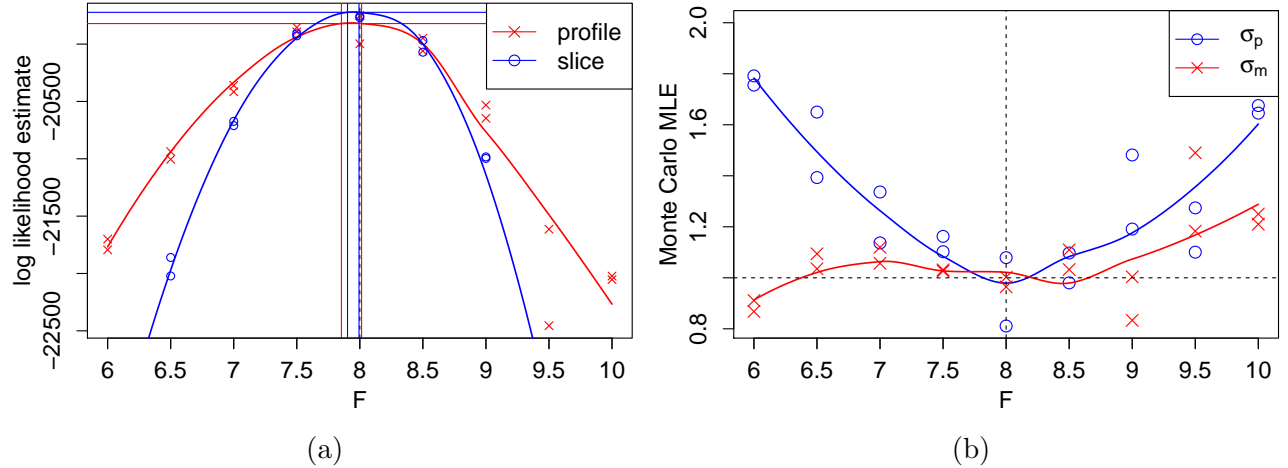


Figure 5: Inference on the fifty dimensional stochastic Lorenz 96 model. (a) Estimated slice and profile likelihood curves and Monte Carlo confidence intervals for  $F$ . (b) Monte Carlo MLE for  $\sigma_p$  and  $\sigma_m$ .

twice independently. Five particle islands with two thousand particles each were used to estimate the slice and the profile likelihood estimates. Smooth fits through the estimated likelihoods were obtained using the non-parametric local regression procedure `loess` (Cleveland et al., 1992, implemented in R-3.4.1). We constructed approximate 95% confidence intervals for  $F$  based on locally quadratic fits through the likelihood estimates around the maximum of the smoothed fits, following the procedure proposed in Ionides et al. (2017), which further developed methods of parameter inference proposed by Diggle and Gratton (1984) from models that are implicitly defined by simulation algorithms. We provide more details on this procedure in supplementary section S4. The estimated Monte Carlo adjusted confidence intervals from the slice and the profile likelihood estimates, indicated by two blue and red vertical lines in Figure 5a, were given by (7.90, 7.99) and (7.85, 8.01) respectively. The upper ends of both confidence intervals were located near the true value of  $F=8$ . We remark that the log likelihood estimates with known  $\sigma_p$  and  $\sigma_m$  dropped rapidly to around  $-4.7 \times 10^4$  at  $F=10$  (Figure S-8 in supplementary text), and for this reason the log likelihood estimates at this value of  $F$  was excluded from fitting a locally quadratic slice likelihood curve to compute the Monte Carlo adjusted confidence interval. In contrast, the profile likelihood estimates at  $F=10$  did not drop suddenly, thanks to the inflated Monte Carlo MLE for the process noise  $\sigma_p$  (Figure 5b). Inaccurate values of the forcing constant  $F$  were compensated by the process noise estimates larger than the truth. The Monte Carlo MLE for the process noise tended to increase as the value of  $F$  deviated from the truth.

### 7.3 Coupled spatiotemporal measles epidemics model

Spatiotemporal inference for epidemiological and ecological systems is arguably the last remaining open problem from the six challenges in time series analysis of nonlinear systems posed by Bjørnstad and Grenfell (2001). Plug-and-play SMC techniques have been central to solving the other five challenges of Bjørnstad and Grenfell (2001), all of which can be represented in the framework of inference for low-dimensional nonlinear non-Gaussian POMP models. Population dynamics of ecological and epidemiological systems can exhibit highly nonlinear stochastic behavior, leading to computational challenges even in low dimensions. Likelihood maximization via iterated filtering has emerged as a practical inference tool for such systems (e.g., Blackwood et al.,

2013; Blake et al., 2014; Bakker et al., 2016; Becker et al., 2016; Ranjeva et al., 2017; Pons-Salort and Grassly, 2018).

We demonstrate that GIRF methodology can enable likelihood based inference on a spatiotemporal mechanistic model addressing a scientific application. We studied the epidemic dynamics of measles, which is well understood compared to other infectious diseases and is characterized by patterns that are closely replicable using a mechanistic model. The study of measles has motivated previous statistical methodology for spatiotemporal population dynamics based on a log-linearization (Xia et al., 2004) and other approximations (Eggo et al., 2010) but full likelihood-based fitting using spatially coupled versions of city-level measles transmission models has not previously been carried out. We built on the model of He et al. (2009), adding spatial interaction between multiple cities. We implemented our algorithms with the parameter estimation approach described in Section 6 to make inference on the spatial coupling parameter. We used the data collated and studied by Dalziel et al. (2016). The data consisted of biweekly reported case counts in the prevaccination era from year 1949 to 1964 for forty largest cities in England and Wales. Likelihood-based inference for the nonlinear coupled stochastic dynamics of infectious disease in forty cities has not previously been demonstrated and opens the possibility of various scientific investigations in epidemiological systems and beyond.

The model compartmentalized the population of each city into susceptible ( $S$ ), exposed ( $E$ ), infectious ( $I$ ), and recovered/removed ( $R$ ) categories. Their sizes for the  $k$ -city were denoted by  $S_k$ ,  $E_k$ ,  $I_k$ , and  $R_k$ . The population dynamics was described by the following set of stochastic differential equations:

$$\begin{aligned} dS_k(t) &= r_k(t)dt - dN_{SE,k}(t) - \mu S_k(t)dt \\ dE_k(t) &= dN_{SE,k}(t) - dN_{EI,k}(t) - \mu E_k(t)dt \\ dI_k(t) &= dN_{EI,k}(t) - dN_{IR,k}(t) - \mu I_k(t)dt \end{aligned} \quad k \in 1:d.$$

Here,  $N_{SE,k}(t)$ ,  $N_{EI,k}(t)$ , and  $N_{IR,k}(t)$  denote the cumulative number of transitions between the corresponding compartments up to time  $t$  in city  $k$ ,  $\mu$  denotes per-capita mortality rate, and  $r_k$  the recruitment rate of susceptible population. The cumulative transitions were modelled as counting processes with overdispersion relative to Poisson processes, following the construction of Bretó et al. (2009). The term  $N_{SE,k}(t)$ , representing the cumulative number of infections in the  $k$ -th city, has the expected increment of

$$\mathbb{E}[N_{SE,k}(t+dt) - N_{SE,k}(t)] = \beta(t) \cdot S_k(t) \cdot \left[ \left( \frac{I_k}{P_k} \right)^\alpha + \sum_{l \neq k} \frac{v_{kl}}{P_k} \left\{ \left( \frac{I_l}{P_l} \right)^\alpha - \left( \frac{I_k}{P_k} \right)^\alpha \right\} \right] dt + o(dt), \quad (22)$$

where  $\beta(t)$  denotes the seasonal transmission coefficient and  $\alpha$  the mixing exponent (He et al., 2009). The population of city  $k$  was denoted by  $P_k$ , and the number of travelers from city  $k$  to  $l$  by  $v_{kl}$ . We used the gravity model of Xia et al. (2004) that describes the number of travelers by

$$v_{kl} = G \cdot \frac{\bar{d}}{\bar{P}^2} \cdot \frac{P_k \cdot P_l}{d_{kl}}, \quad (23)$$

where  $d_{kl}$  denotes the distance between city  $k$  and city  $l$ . The gravitation constant  $G$  in (23) was scaled with respect to the average population of all forty cities  $\bar{P}$  and their average distance  $\bar{d}$ . The data consisted of the biweekly reported case numbers in each city. The model assumed that a certain fraction  $\rho_k$ , called the reporting probability, of the transitions from the infectious

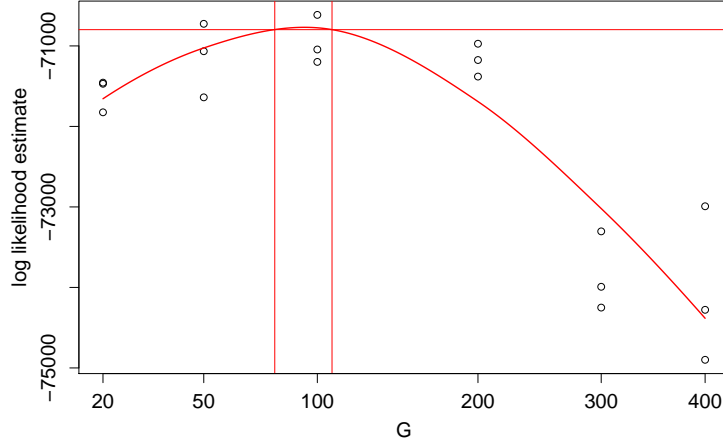


Figure 6: Estimated profile likelihood points for various values of  $G$  in our spatiotemporal measles dynamics model and the estimated approximate 95% confidence interval (between red vertical lines).

compartment to the recovered compartment were, on average, counted as reported cases. The measurement model was chosen to allow for overdispersion relative to the binomial distribution with success probability  $\rho_k$ . More details on the model and the inference procedure are given in the supplementary text S5.

We made inference on the gravitation constant  $G$ , based on an estimated profile likelihood curve. Ability to infer about the spatial coupling parameter  $G$  implies that the filter can recover the full joint distribution for all spatial locations. We fixed  $G$  at various levels and estimated other parameters using Algorithm 2. The reporting probabilities  $\rho_k$  were estimated by dividing the total case reports by the total births for the corresponding periods in each city, due to the modelling assumption that individuals who once contracted to measles attain lifelong immunity. The estimated  $\rho_k$  closely matched the values estimated in He et al. (2009) separately for each city using a mechanistic model. We evaluated the guide function  $u_t$  using the approach described in equations (12)–(16) in Section 5 to approximate the forecast likelihood of  $B = 3$  future data points. The forecast variability was estimated by making forty random forecasts at every first intermediate time point after observation time (i.e.,  $t_{n,1}$ ).

All parameters except  $G$  and  $\rho_k$  were estimated using the iterated filtering method (Algorithm 2). The IVPs and the regular parameters were estimated alternately. For IVP estimation we only used the first three data points, because the information about the initial states was concentrated on the early data points. We iterated fifty times the filtering over the three data points using fifty particle islands comprising sixty particles each. Since the IVPs were only perturbed at the start of each filtering, the particle swarm tended to quickly collapse to a single point. Using many particle islands helped maintain diversity among particles. The regular parameters were estimated by filtering through the whole data once starting from the estimated IVP values. Five islands of six hundred particles each were used for regular parameter estimation. The estimation of IVPs and regular parameters in total took about thirty hours on average using 5 cores. We iterated the alternating estimation ten times. The parameter perturbation size decreased at a geometric factor of 0.92 for each subsequent iteration. The mean of the final swarm of regular parameters was taken as the Monte Carlo MLE. We estimated the IVP corresponding to the Monte Carlo MLE and estimated the likelihood of data using Algorithm 1 with ten islands of one thousand particles each. The obtained likelihood estimate was considered a Monte Carlo profile likelihood for the specified  $G$  value. We independently repeated the estimation of profile likelihood six times



for each value of  $G$ .

We constructed an approximate 95% confidence interval based on the obtained profile likelihood estimates. We used three points of highest profile likelihood estimates among six points for each value of  $G$ . Figure 6 shows the estimates of profile log likelihoods and the approximate 95% confidence interval for  $G$ . The procedure for obtaining the Monte Carlo adjusted confidence interval was carried out on a transformed scale of  $\sqrt{G}$  for a better quadratic fit. The approximate confidence interval was found to be (79, 108), indicated by two vertical lines, using a Monte Carlo adjusted profile cut-off of 35.1 log units. All experiments in Section 7.2 and 7.3 were conducted on the Olympus cluster at the Pittsburgh Supercomputing Center.

## 8 Discussion

Sharp deterioration of standard particle filters in high dimensions has been an obstacle to making inference from spatiotemporal data using complex dynamic models. GIRF methodology offers an advance in analyzing coupled highly nonlinear dynamic systems of moderately large dimensions. The approach is applicable to complex mechanistic models for which the latent process does not have analytically tractable transition density. We have shown that GIRF methodology can have good scaling properties with growing dimensions using a novel theoretical approach. Empirically, we have demonstrated that GIRF can scale up to dimensions substantially larger than the capabilities of alternative algorithms such as APF, and that GIRF can be successfully applied to highly nonlinear models for which the ensemble Kalman filter fails. We also showed that GIRF methodology enables inference on a scientifically challenging spatiotemporal epidemiological model. Further potential applications may be found in areas such as ecology, behavioral sciences, or epidemiology, when the data are collected at linked spatial locations or structured into many categories.

GIRF methodology proceeds on a time scale finer than the observation time scale. Each of the increased number of resampling steps therefore deals with a reduced amount of information and consequently suffers less from the weight degeneracy. Theoretical investigation revealed that GIRF can produce accurate filtering estimates in moderately high dimensions under certain assumptions on the POMP model and the guide function. These conditions offer a perspective on the abundance of information causing the COD for SMC, and how GIRF methodology can partially resolve the problem.

Some analyses of high dimensional dynamic systems rely on information reduction techniques. Approximate Bayesian computation, for example, approximates the posterior probability of parameters given data using the distance between carefully chosen summary statistics of the observed data and those of the simulated data under various parameter values. This simplified approach in principle enables analyses of data for any model that can be simulated. However, information reduction methods can fail to capture full complexities in the model or result in inaccurate parameter estimates (Fasiolo et al., 2016). Also, different conclusions might be drawn depending on the summary statistics and the distance measures being used. There is a risk of subconscious bias when the scientist’s expert knowledge is used to select these fitting criteria. By contrast, GIRF methodology enables likelihood-based inference on relatively high-dimensional nonlinear dynamic models. Likelihood-based inference can add to the reliability of scientific conclusions, because the likelihood of data is uniquely defined by a model and provides a common measure of fit. In addition, the statistical efficiency of likelihood-based inference leads to inferences that might be unobtainable for methods requiring information reduction. Many scientific and statistical challenges remain involving analysis of partially observed, highly nonlinear, coupled stochastic

systems, and we have shown that GIRF methodology provides a framework for progress in this enterprise.

**Acknowledgement** The authors thank Aaron King for the discussions motivating this research and for insightful feedback. Comments on the manuscript by Kidus Asfaw have led to improvements. This work was supported by National Science Foundation grants DMS-1308919, DMS-1761603, and DMS-1513040, and National Institutes of Health grants 1-U54-GM111274 and 1-U01-GM110712.

## A Proof of Theorem 1

We augment the latent space in order to make the weight function  $w_{t_{n,s}}$  defined in (1) depend only on the current latent variable at time  $t_{n,s}$ . Let  $\{Z_{t_{n,s}}; n \in 0:N-1, s \in 1:S\}$  be a process defined on discrete time points  $\mathbb{I}$  such that  $Z_{t_{n,s}} := (X_{t_{n,s}}, X_{t_{n,s-1}})$  for  $t_{n,s} > t_0$  and  $Z_{t_0} := (X_{t_0}, x^*)$  where  $x^*$  is an arbitrary point in  $\mathbb{X}$ . The transition kernel of the discrete time process  $\{Z_{t_{n,s}}; t_{n,s} \in \mathbb{I}\}$ , denoted by  $\tilde{K}_{t_{n,s-1}, t_{n,s}}: \mathcal{X}^2 \times \mathbb{X}^2 \rightarrow [0, 1]$ , satisfies

$$\tilde{K}_{t_{n,s-1}, t_{n,s}}(A_1 \times A_2; (x_{t_{n,s-1}}, x_{t_{n,s-2}})) = K_{t_{n,s-1}, t_{n,s}}(A_1; x_{t_{n,s-1}}) \cdot \delta_{x_{t_{n,s-1}}}(A_2), \quad n \in 0:N-1, s \in 1:S$$

for  $A_1, A_2 \in \mathcal{X}$ . Then the bootstrap particle filter with the initial particle draws given by  $\{Z_{t_0}^{F,j}; j \in 1:J\} = \{(X_{t_0}^{F,j}, x^*); j \in 1:J\}$ , subsequent draws made according to  $Z_{t_{n,s}}^{P,j} \sim \tilde{K}_{t_{n,s-1}, t_{n,s}}(\cdot; Z_{t_{n,s-1}}^{F,j})$ , and resampling weights proportional to  $w_{t_{n,s}}(Z_{t_{n,s}}^{P,j})$  from (1) is algorithmically equivalent to GIRF (Algorithm 1) when we equate  $Z_{t_{n,s}}^{P,j}$  with the pair  $(X_{t_{n,s}}^{P,j}, X_{t_{n,s-1}}^{F,j})$  in Algorithm 1. Moreover, the likelihood estimate from this particle filter is given by  $\prod_{n=0}^{N-1} \prod_{s=1}^S \left[ \sum_{j=1}^J w_{t_{n,s}}(Z_{t_{n,s}}^{P,j}) \right]$ , which is exactly the same as  $\hat{\ell}$  in Algorithm 1. The likelihood estimate obtained from this particle filter is unbiased for

$$\mathbb{E} \left[ \prod_{n=0}^{N-1} \prod_{s=1}^S w_{t_{n,s}}(Z_{t_{n,s}}) \right] = \mathbb{E} \left[ \prod_{n=1}^N g_N(y_N | X_{t_n}) \right], \quad (24)$$

due to the unbiasedness property for standard particle filters (Del Moral and Jacod, 2001). The equality in the above equation comes from (1) and the fact that  $u_{t_0} \equiv 1$  and  $u_{t_N} \equiv g_N(y_N | \cdot)$ . We conclude that  $\hat{\ell}$  is an unbiased estimate for  $\ell_{1:N}(y_{1:N})$ .

## B An outline for the proof of Theorem 2

We start by defining the necessary notation to describe the key steps in the proof of Theorem 2 in Section S1. At  $t_{n,s} \in \mathbb{I}$ , we denote the empirical distributions of the propagated and the filtered particles by  $\hat{P}_{t_{n,s}}^{P,J} = \frac{1}{J} \sum_{j=1}^J \delta_{X_{t_{n,s}}^{P,j}}$  and  $\hat{P}_{t_{n,s}}^{F,J} = \frac{1}{J} \sum_{j=1}^J \delta_{X_{t_{n,s}}^{F,j}}$ , respectively. The empirical distribution of the  $J$  matching pairs  $(X_{t_{n,s}}^{P,j}, X_{t_{n,s-1}}^{F,j})$  on the product space  $\mathbb{X}^2$  is denoted by  $M_{t_{n,s}}^J$ . The  $\sigma$ -algebra generated by the propagated and the filtered particles up to time  $t_{n,s}$  will be denoted by  $\mathcal{B}_{t_{n,s}}^{F,J}$ . The  $\sigma$ -algebra generated by the propagated particles up to time  $t_{n,s}$  and the filtered particles up to time  $t_{n,s-1}$  will be denoted by  $\mathcal{B}_{t_{n,s}}^{P,J}$ . Let  $f$  be a measurable function such that  $\|f\|_\infty \leq 1$ . For  $t \leq t' \in \mathbb{I}$ , we define

$$b_{t,t'}^J(f) := \int \frac{Q_{t,t'}(u_{t'} \cdot f)}{u_t} d\hat{P}_t^{F,J}. \quad (25)$$

The ratio  $b_{t,t_N}^J(f) / b_{t,t_N}^J(1)$  represents the expected value of  $f(X_{t_N})$  given the observations after  $t$  under the approximation of  $P_t^G$  by  $\hat{P}_t^{F,J}$ . We now specify some Monte Carlo outcomes on which the filtering and prediction errors are controlled. For  $t, t' \in \mathbb{I}$  with  $t \leq t'$  we define the events

$$\mathcal{E}_{t,t'}^{f,a,F,J} := \left\{ \left| b_{t,t'}^J(f) - \mathbb{E} \left[ b_{t,t'}^J(f) | \mathcal{B}_t^{P,J} \right] \right| \leq \frac{a}{\sqrt{J}} \sup \left[ \frac{Q_{t,t'}(u_{t'})}{u_t} \right] \right\}, \quad (26)$$

$$\mathcal{E}_{t,t'}^{f,a,P,J} := \left\{ \left| \int \frac{Q_{t,t'}(u_{t'} \cdot f)}{u_t} \cdot w_t dM_t^J - b_{t,t'}^J(f) \right| \leq \frac{aC_1}{\sqrt{J}} \sup \left[ \frac{Q_{t,t'}(u_{t'})}{u_{t-}} \right] \right\}. \quad (27)$$

In the following lemma, we show that these events can be guaranteed to have high probability.

**Lemma 1.** Let  $\mathbb{P}^{MC}$  denote the probability measure describing the law of all Monte Carlo draws in Algorithm 1. For any constant  $a > 1$ , particle size  $J \geq 1$ , and measurable function  $\|f\|_\infty \leq 1$ , we have

$$\mathbb{P}^{MC}(\mathcal{E}_{t,t'}^{f,a,F,J}) \geq 1 - \frac{1}{a^2} \quad (28)$$

for  $t \leq t' \in \mathbb{I}$ , provided that multinomial resampling is used in Algorithm 1. Also for  $t \leq t' \in \mathbb{I} \setminus \{t_0\}$  and under Assumption 1,

$$\mathbb{P}^{MC}(\mathcal{E}_{t,t'}^{f,a,P,J}) \geq 1 - \frac{1}{a^2}. \quad (29)$$

The proof of Lemma 1 in Section S1 involves applications of Markov's inequality. Non-asymptotic probabilistic bounds of the form (28) or (29) have not been previously used to investigate particle filters, so far as we are aware. Lemma 1 provides a useful contribution to the theory of high-dimensional particle filtering because the constant  $C_1$  can hold uniformly as model dimension increases as long as the number of intermediate time steps also grows, as discussed following the statement of Assumption 1. We proceed to bound the filtering error at time  $t_N$  by a sum of propagated Monte Carlo errors arising from all the intermediate steps in GIRF (Algorithm 1). Specifically, we develop the following proposition.

**Lemma 2.** Suppose  $f$  is a measurable function such that  $\|f\|_\infty \leq 1$ . Let  $a > 1$  and  $C_1$  be arbitrary constants used to construct  $\mathcal{E}_{t,t'}^{f,a,F,J}$  and  $\mathcal{E}_{t,t'}^{f,a,P,J}$  in equations (26) and (27). Then under Assumption 2 and provided that  $\sqrt{J} \geq 8\rho^{-2}aC_2(C_1 + 1) \cdot (nS + s)$ , we have for any  $t_{n,s} \in \mathbb{I}$

$$\left| \int f d\hat{P}_{t_{n,s}}^{F,J} - \int f dP_{t_{n,s}}^G \right| \leq \frac{4aC_2(C_1 + 1)}{\rho\sqrt{J}}(nS + s + 1) \quad (30)$$

on the event set  $\bar{\mathcal{E}}_{t_{n,s}}^{f,a,J}$  defined in (S35) as an intersection over sets of the form  $\mathcal{E}_{t,t'}^{f,a,F,J}$  and  $\mathcal{E}_{t,t'}^{f,a,P,J}$ .

The proof of Lemma 2 in Section S1 involves using a telescoping sum and the triangle inequality to obtain

$$\begin{aligned} \left| \int f d\hat{P}_{t_{n,s}}^{F,J} - \int f dP_{t_{n,s}}^G \right| &\leq \left| \frac{b_{t_0,t_{n,s}}^J(f)}{b_{t_0,t_{n,s}}^J(1)} - \int f dP_{t_{n,s}}^G \right| \\ &+ \sum_{\substack{t_0 < t \leq t_{n,s} \\ t \in \mathbb{I}}} \left\{ \left| \frac{b_{t,t_{n,s}}^J(f)}{b_{t,t_{n,s}}^J(1)} - \frac{\mathbb{E} \left[ b_{t,t_{n,s}}^J(f) \middle| \mathcal{B}_t^{P,J} \right]}{\mathbb{E} \left[ b_{t,t_{n,s}}^J(1) \middle| \mathcal{B}_t^{P,J} \right]} \right| + \left| \frac{\mathbb{E} \left[ b_{t,t_{n,s}}^J(f) \middle| \mathcal{B}_t^{P,J} \right]}{\mathbb{E} \left[ b_{t,t_{n,s}}^J(1) \middle| \mathcal{B}_t^{P,J} \right]} - \frac{b_{t^-,t_{n,s}}^J(f)}{b_{t^-,t_{n,s}}^J(1)} \right| \right\}. \quad (31) \end{aligned}$$

Assumption 2 and the definition of  $\bar{\mathcal{E}}_{t_{n,s}}^{f,a,J}$  enable bounds for each term in (31). The full argument in Section S1 requires the development of several algebraic identities relating  $Q_{t,t'}$  and  $b_{t,t'}^J$  and their ratios and conditional expectations. The proof of Theorem 2 in Section S1 then follows by setting  $t_{n,s} = t_N$  in Lemma 2 and bounding the Monte Carlo probability of the set  $\bar{\mathcal{E}}_{t_N}^{f,a,J}$  using Lemma 1.

# Supplementary Information

## S1 Proof of Lemmas 1 and 2 and Theorem 2

To prepare for the proof of Theorem 2 we develop Lemma 1 and Lemma 2. We first set up some additional notation, then we state and prove each result.

Let  $(\Omega^{\text{MC}}, \mathcal{A}^{\text{MC}}, \mathbb{P}^{\text{MC}})$  be the probability space describing the law of all Monte Carlo draws in the algorithm. At the time step  $t_{n,s}$  in Algorithm 1, we denote the empirical distributions corresponding to the propagated particles and the filtered particles by  $\hat{P}_{t_{n,s}}^{P,J} = \frac{1}{J} \sum_{j=1}^J \delta_{X_{t_{n,s}}^{P,j}}$  and  $\hat{P}_{t_{n,s}}^{F,J} = \frac{1}{J} \sum_{j=1}^J \delta_{X_{t_{n,s}}^{F,j}}$  respectively. The empirical distribution of the  $J$  pairs  $\{(X_{t_{n,s}}^{P,j}, X_{t_{n,s-1}}^{F,j}), j \in 1:J\}$  on the product space  $\mathbb{X}^2$  will be denoted by  $M_{t_{n,s}}^J$ . The  $\sigma$ -algebra generated by the set of random draws  $D_{t_{n,s}}^{P,J} := \{X_{t_{n',s'}}^{F,j}; t_{n',s'} \leq t_{n,s-1}, j \in 1:J\} \cup \{X_{t_{n',s'}}^{P,j}; t_{n',s'} \leq t_{n,s}, j \in 1:J\}$  is denoted by  $\mathcal{B}_{t_{n,s}}^{P,J}$ , and the  $\sigma$ -algebra generated by  $D_{t_{n,s}}^{P,J} \cup \{X_{t_{n,s}}^{F,j}; j \in 1:J\}$  is denoted by  $\mathcal{B}_{t_{n,s}}^{F,J}$ .

Given that one has filtered particles  $\{X_t^{F,j}; j \in 1:J\}$  at time  $t \in \mathbb{I}$ , we define for  $t' \in \mathbb{I} \cap [t, t_N]$

$$b_{t,t'}^J(f) := \int \frac{Q_{t,t'}(u_{t'} \cdot f)}{u_t} d\hat{P}_t^{F,J} \quad (25)$$

for all bounded measurable functions  $f$  on  $\mathbb{X}$ . Note that this definition implies  $b_{t,t}^J(f) = \int f d\hat{P}_t^{F,J}$ . Since resampling weights at time  $t \in \mathbb{I} \setminus \{t_0\}$  are proportional to  $w_t(X_t^{P,j}, X_{t-}^{F,j})$ , we have

$$\mathbb{E} \left[ b_{t,t'}^J(f) \middle| \mathcal{B}_t^{P,J} \right] = \frac{\int \frac{Q_{t,t'}(u_{t'} \cdot f)}{u_t}(x_t) \cdot w_t(x_t, x_{t-}) dM_t^J(x_t, x_{t-})}{\int w_t(x_t, x_{t-}) dM_t^J(x_t, x_{t-})}. \quad (\text{S32})$$

If  $t = t_m$  for some  $m \in 0:N$ , we write  $\mathbf{n}(t) = m$ . The conditional expectation of the numerator in the right hand side of (S32) with respect to  $\mathcal{B}_{t-}^{F,J}$  equals

$$\begin{aligned} \mathbb{E} \left[ \int \frac{Q_{t,t'}(u_{t'} \cdot f)}{u_t} \cdot w_t dM_t^J \middle| \mathcal{B}_{t-}^{F,J} \right] &= \begin{cases} \int \frac{K_{t-,t} \{Q_{t,t'}(u_{t'} \cdot f)\}}{u_{t-}} d\hat{P}_{t-}^{F,J} & \text{if } t- \notin t_{1:N} \\ \int \frac{K_{t-,t} \{Q_{t,t'}(u_{t'} \cdot f)\}}{u_{t-}} \cdot g_{\mathbf{n}(t-)} d\hat{P}_{t-}^{F,J} & \text{if } t- \in t_{1:N} \end{cases} \\ &= \int \frac{Q_{t-,t'}(u_{t'} \cdot f)}{u_{t-}} d\hat{P}_{t-}^{F,J} = b_{t-,t}^J(f), \end{aligned} \quad (\text{S33})$$

by (1), (4), (5), and (25). Note that here we implicitly assumed that  $g_{\mathbf{n}(t-)}$  is a function of  $X_{t-}$ , such that  $g_{\mathbf{n}(t-)}(X_{t-}) := g_{\mathbf{n}(t-)}(y_{\mathbf{n}(t-)} | X_{t-})$ .

For  $t, t' \in \mathbb{I}$  such that  $t \leq t'$ , we define the event sets

$$\mathcal{E}_{t,t'}^{f,a,F,J} := \left\{ \omega \in \Omega^{\text{MC}}; \left| b_{t,t'}^J(f) - \mathbb{E} \left[ b_{t,t'}^J(f) \middle| \mathcal{B}_t^{P,J} \right] \right| \leq \frac{a}{\sqrt{J}} \sup \left[ \frac{Q_{t,t'}(u_{t'})}{u_t} \right] \right\},$$

and for  $t_0 < t \leq t'$ ,

$$\mathcal{E}_{t,t'}^{f,a,P,J} := \left\{ \omega \in \Omega^{\text{MC}}; \left| \int \frac{Q_{t,t'}(u_{t'} \cdot f)}{u_t}(x_t) \cdot w_t(x_t, x_{t-}) dM_t^J(x_t, x_{t-}) - b_{t-,t'}^J(f) \right| \leq \frac{aC_1}{\sqrt{J}} \sup \left[ \frac{Q_{t-,t'}(u_{t'})}{u_{t-}} \right] \right\}$$

for any measurable function  $\|f\|_\infty \leq 1$  and a constant  $a > 1$ . The superscript  $F$  signifies that the event sets are related to the Monte Carlo error associated with the resampling (filtering) operation at time  $t$ , and the superscript  $P$  the Monte Carlo error associated with the particle propagation from time  $t^-$  to  $t$ . We note that the set  $\mathcal{E}_{t_0,t'}^{f,a,F,J}$ , where the first subscript is  $t_0$ , is associated with the Monte Carlo error in the sampling at the initial time. In this case, we understand that  $\mathcal{B}_{t_0}^{P,J}$  is the trivial  $\sigma$ -algebra, that is,  $\mathcal{B}_{t_0}^{P,J} = \{\emptyset, \Omega^{\text{MC}}\}$ , and the conditional expectation  $\mathbb{E} \left[ b_{t_0,t'}^J(f) \middle| \mathcal{B}_{t_0}^{P,J} \right]$  becomes the unconditioned expectation  $\mathbb{E} b_{t_0,t'}^J(f)$ . Since we set  $u_{t_0} \equiv 1$  and assume that the initial particles  $\{X_{t_0}^{F,j}; j \in 1:J\}$  are drawn directly from  $P_{t_0}$ , we have  $\mathbb{E} b_{t_0,t'}^J(f) = P_{t_0} Q_{t_0,t'}(u_{t'} \cdot f)$ .

**Lemma 1.** *For any constant  $a > 1$ , particle size  $J \geq 1$ , and measurable function  $\|f\|_\infty \leq 1$ , we have*

$$\mathbb{P}^{\text{MC}}(\mathcal{E}_{t,t'}^{f,a,F,J}) \geq 1 - \frac{1}{a^2} \quad (28)$$

for  $t \leq t' \in \mathbb{I}$ , provided that multinomial resampling is used in Algorithm 1. Also, under Assumption 1,

$$\mathbb{P}^{\text{MC}}(\mathcal{E}_{t,t'}^{f,a,P,J}) \geq 1 - \frac{1}{a^2} \quad (29)$$

for  $t \leq t' \in \mathbb{I} \setminus \{t_0\}$ .

*Proof of Lemma 1.* First we prove (28). We observe that

$$\begin{aligned} \text{Var} \left( b_{t,t'}^J(f) \middle| \mathcal{B}_t^{P,J} \right) &= \text{Var} \left( \frac{1}{J} \sum_{j=1}^J \frac{Q_{t,t'}(u_{t'} \cdot f)}{u_t} (X_t^{F,j}) \middle| \mathcal{B}_t^{P,J} \right) \\ &= \frac{1}{J} \text{Var} \left( \frac{Q_{t,t'}(u_{t'} \cdot f)}{u_t} (X_t^{F,1}) \middle| \mathcal{B}_t^{P,J} \right) \\ &\leq \frac{1}{J} \mathbb{E} \left[ \left\{ \frac{Q_{t,t'}(u_{t'} \cdot f)}{u_t} (X_t^{F,1}) \right\}^2 \middle| \mathcal{B}_t^{P,J} \right] \\ &\leq \frac{1}{J} \sup \left\{ \frac{Q_{t,t'}(u_{t'})}{u_t} \right\}^2, \end{aligned}$$

because  $\|f\|_\infty \leq 1$ . This implies that, by Markov's inequality, for any  $a > 1$ ,

$$\left( b_{t,t'}^J(f) - \mathbb{E} \left[ b_{t,t'}^J(f) \middle| \mathcal{B}_t^{P,J} \right] \right)^2 \leq \frac{a^2}{J} \sup \left\{ \frac{Q_{t,t'}(u_{t'})}{u_t} \right\}^2 \quad (\text{S34})$$

with probability at least  $1 - \frac{1}{a^2}$ .

Next we show (29). From (S33), we know

$$\mathbb{E} \left[ \int \frac{Q_{t,t'}(u_{t'} \cdot f)}{u_t}(x_t) \cdot w_t(x_t, x_{t-}) dM_t^J(x_t, x_{t-}) \middle| \mathcal{B}_{t-}^{F,J} \right] = b_{t-,t'}^J(f).$$

Thus,

$$\begin{aligned}
& \mathbb{E} \left[ \left\{ \int \frac{Q_{t,t'}(u_{t'} \cdot f)}{u_t} \cdot w_t dM_t^J - b_{t^-,t'}^J(f) \right\}^2 \middle| \mathcal{B}_{t^-}^{F,J} \right] \\
&= \text{Var} \left( \int \frac{Q_{t,t'}(u_{t'} \cdot f)}{u_t} \cdot w_t dM_t^J \middle| \mathcal{B}_{t^-}^{F,J} \right) \\
&= \text{Var} \left( \frac{1}{J} \sum_j \frac{Q_{t,t'}(u_{t'} \cdot f) (X_t^{P,j})}{\left\{ u_{t^-} / g_{\mathbf{n}(t^-)}^{\mathbf{1}[t^- \in t_{1:N}]} \right\} (X_{t^-}^{F,j})} \middle| \mathcal{B}_{t^-}^{F,J} \right) \\
&= \frac{1}{J^2} \sum_j \frac{\text{Var} \left( Q_{t,t'}(u_{t'} \cdot f) (X_t^{P,j}) \middle| \mathcal{B}_{t^-}^{F,J} \right)}{\left\{ K_{t^-,t} Q_{t,t'}(u_{t'}) (X_{t^-}^{F,j}) \right\}^2} \cdot \frac{\left\{ K_{t^-,t} Q_{t,t'}(u_{t'}) (X_{t^-}^{F,j}) \right\}^2}{\left\{ u_{t^-} / g_{\mathbf{n}(t^-)}^{\mathbf{1}[t^- \in t_{1:N}]} (X_{t^-}^{F,j}) \right\}^2} \\
&\leq \frac{1}{J^2} \sum_j \frac{K_{t^-,t} \{Q_{t,t'}(u_{t'} \cdot |f|)\}^2}{\{K_{t^-,t} Q_{t,t'}(u_{t'})\}^2} (X_{t^-}^{F,j}) \cdot \left\{ \frac{Q_{t^-,t'}(u_{t'})}{u_{t^-}} (X_{t^-}^{F,j}) \right\}^2 \\
&\leq \frac{1}{J} C_1^2 \cdot \sup \left\{ \frac{Q_{t^-,t'}(u_{t'})}{u_{t^-}} \right\}^2,
\end{aligned}$$

where we have used the fact

$$Q_{t^-,t'}(u_{t'}) = g_{\mathbf{n}(t^-)}^{\mathbf{1}[t^- \in t_{1:N}]} K_{t^-,t} Q_{t,t'}(u_{t'}),$$

and the last inequality comes from Assumption 1. Hence by Markov's inequality, for any  $a > 1$ ,

$$\left\{ \int \frac{Q_{t,t'}(u_{t'} \cdot f)}{u_t} \cdot w_t dM_t^J - b_{t^-,t'}^J(f) \right\}^2 \leq \frac{a^2 C_1^2}{J} \sup \left\{ \frac{Q_{t^-,t'}(u_{t'})}{u_{t^-}} \right\}^2$$

with probability at least  $1 - \frac{1}{a^2}$ . This completes the proof of Lemma 1.  $\square$

We define for all  $t_{n,s} \in \mathbb{I}$  and for any measurable function  $\|f\|_\infty \leq 1$  the sets  $\bar{\mathcal{E}}_{t_{n,s}}^{f,a,J}$  recursively as follows:

$$\bar{\mathcal{E}}_{t_0}^{f,a,J} := \mathcal{E}_{t_0,t_0}^{f,a,F,J},$$

and for  $t_{n,s} > t_0$ ,

$$\begin{aligned}
\bar{\mathcal{E}}_{t_{n,s}}^{f,a,J} &:= \bar{\mathcal{E}}_{t_{n,s-1}}^{\mathbf{1}_{\mathcal{C}_{t_{n,s-1}}},a,J} \cap \left( \bigcap_{\substack{t_0 \leq t \leq t_{n,s} \\ t \in \mathbb{I}}} \mathcal{E}_{t,t_{n,s}}^{f,a,F,J} \right) \cap \left( \bigcap_{\substack{t_0 \leq t < t_{n,s} \\ t \in \mathbb{I}}} \mathcal{E}_{t,t_{n,s}}^{1,a,F,J} \right) \\
&\quad \cap \left( \bigcap_{\substack{t_0 < t \leq t_{n,s} \\ t \in \mathbb{I}}} \mathcal{E}_{t,t_{n,s}}^{f,a,P,J} \right) \cap \left( \bigcap_{\substack{t_0 < t \leq t_{n,s} \\ t \in \mathbb{I}}} \mathcal{E}_{t,t_{n,s}}^{1,a,P,J} \right), \quad (\text{S35})
\end{aligned}$$

where  $\mathbf{1}_{\mathcal{C}_t}$  denotes the indicator function corresponding to the set  $\mathcal{C}_t$  defined in Assumption 2. We now prove the following lemma.

**Lemma 2.** Suppose  $f$  is a measurable function such that  $\|f\|_\infty \leq 1$  and  $a > 1$  is an arbitrary constant. Then under Assumption 2 and provided that  $\sqrt{J} \geq 8\rho^{-2}aC_2(C_1 + 1) \cdot (nS + s)$ , we have for any  $t_{n,s} \in \mathbb{I}$

$$\left| \int f d\hat{P}_{t_{n,s}}^{F,J} - \int f dP_{t_{n,s}}^G \right| \leq \frac{4aC_2(C_1 + 1)}{\rho\sqrt{J}}(nS + s + 1) \quad (30)$$

on the event set  $\bar{\mathcal{E}}_{t_{n,s}}^{f,a,J}$ .

*Proof of Lemma 2.* We prove by induction on  $t_{n,s}$ . First, at  $t_0$ , on the set  $\bar{\mathcal{E}}_{t_0}^{f,a,J} = \mathcal{E}_{t_0,t_0}^{f,a,F,J}$ , we have

$$\left| \int f d\hat{P}_{t_0}^{F,J} - \int f dP_{t_0}^G \right| = \left| b_{t_0,t_0}^J(f) - \mathbb{E} \left[ b_{t_0,t_0}^J(f) \middle| \mathcal{B}_{t_0}^{P,J} \right] \right| \leq \frac{a}{\sqrt{J}} \leq \frac{4aC_2(C_1 + 1)}{\rho\sqrt{J}},$$

noting that  $P_{t_0}^G = P_{t_0}$ . Now, assume that the assertion of the lemma holds for  $t_{n,s-1}$  for some  $n \in 0:N-1$  and  $s \in 1:S$ . Now assume  $\sqrt{J} \geq 8\rho^{-2}aC_2(C_1 + 1) \cdot (nS + s)$  and  $\|f\|_\infty \leq 1$ . The left hand side of (30) is bounded above by

$$\begin{aligned} \left| \int f d\hat{P}_{t_{n,s}}^{F,J} - \int f dP_{t_{n,s}}^G \right| &\leq \left| b_{t_{n,s},t_{n,s}}^J(f) - \frac{b_{t_{n,s},t_{n,s}}^J(f)}{b_{t_{n,s},t_{n,s}}^J(1)} \right| + \left| \frac{b_{t_{n,s},t_{n,s}}^J(f)}{b_{t_{n,s},t_{n,s}}^J(1)} - \int f dP_{t_{n,s}}^G \right| \\ &\leq \sum_{\substack{t_0 < t \leq t_{n,s} \\ t \in \mathbb{I}}} \left| \frac{b_{t,t_{n,s}}^J(f)}{b_{t,t_{n,s}}^J(1)} - \frac{b_{t^-,t_{n,s}}^J(f)}{b_{t^-,t_{n,s}}^J(1)} \right| + \left| \frac{b_{t,t_{n,s}}^J(f)}{b_{t,t_{n,s}}^J(1)} - \int f dP_{t_{n,s}}^G \right|. \end{aligned} \quad (S36)$$

Here, we used the fact that  $b_{t_{n,s},t_{n,s}}^J(1) = \int 1 d\hat{P}_{t_{n,s}}^{F,J} = 1$ . Thus it suffices to show that each term in the right hand side of (S36) is bounded above by  $\frac{4aC_2(C_1+1)}{\rho\sqrt{J}}$  on the event set  $\bar{\mathcal{E}}_{t_{n,s}}^{f,a,J}$ . We decompose each difference in the sum into two terms

$$\left| \frac{b_{t,t_{n,s}}^J(f)}{b_{t,t_{n,s}}^J(1)} - \frac{b_{t^-,t_{n,s}}^J(f)}{b_{t^-,t_{n,s}}^J(1)} \right| \leq \left| \frac{b_{t,t_{n,s}}^J(f)}{b_{t,t_{n,s}}^J(1)} - \frac{\mathbb{E} \left[ b_{t,t_{n,s}}^J(f) \middle| \mathcal{B}_t^{P,J} \right]}{\mathbb{E} \left[ b_{t,t_{n,s}}^J(1) \middle| \mathcal{B}_t^{P,J} \right]} \right| + \left| \frac{\mathbb{E} \left[ b_{t,t_{n,s}}^J(f) \middle| \mathcal{B}_t^{P,J} \right]}{\mathbb{E} \left[ b_{t,t_{n,s}}^J(1) \middle| \mathcal{B}_t^{P,J} \right]} - \frac{b_{t^-,t_{n,s}}^J(f)}{b_{t^-,t_{n,s}}^J(1)} \right|. \quad (S37)$$

We will temporarily denote the first term on the right hand side of (S37) by

$$\left| \frac{b_{t,t_{n,s}}^J(f)}{b_{t,t_{n,s}}^J(1)} - \frac{\mathbb{E} \left[ b_{t,t_{n,s}}^J(f) \middle| \mathcal{B}_t^{P,J} \right]}{\mathbb{E} \left[ b_{t,t_{n,s}}^J(1) \middle| \mathcal{B}_t^{P,J} \right]} \right| = \left| \frac{A'}{A} - \frac{B'}{B} \right|,$$

where  $A, B > 0$ . The above expression is bounded above by

$$\left| \frac{A'}{A} - \frac{B'}{B} \right| = \left| \frac{A'B - B'B + B'B - AB'}{AB} \right| \leq \frac{|A' - B'|}{A} + \frac{|A - B|}{A} \cdot \frac{|B'|}{B} \leq \frac{|A - B| + |A' - B'|}{A}, \quad (S38)$$

because we have  $|B'| \leq B$  from  $\|f\|_\infty \leq 1$ . Since the set  $\bar{\mathcal{E}}_{t_{n,s}}^{f,a,J}$  is contained in  $\mathcal{E}_{t,t_{n,s}}^{f,a,F,J}$ , we have

$$|A' - B'| = \left| b_{t,t_{n,s}}^J(f) - \mathbb{E} \left[ b_{t,t_{n,s}}^J(f) \middle| \mathcal{B}_t^{P,J} \right] \right| \leq \frac{a}{\sqrt{J}} \sup \left[ \frac{Q_{t,t_{n,s}}(u_{t_{n,s}})}{u_t} \right]. \quad (S39)$$

Similarly, for  $t < t_{n,s}$ , since  $\bar{\mathcal{E}}_{t_{n,s}}^{f,a,J}$  is contained in  $\mathcal{E}_{t_{n,s}}^{1,a,F,J}$ , we have

$$|A - B| = \left| b_{t,t_{n,s}}^J(1) - \mathbb{E} \left[ b_{t,t_{n,s}}^J(1) \middle| \mathcal{B}_t^{P,J} \right] \right| \leq \frac{a}{\sqrt{J}} \sup \left[ \frac{Q_{t,t_{n,s}}(u_{t_{n,s}})}{u_t} \right]. \quad (\text{S40})$$

In the case of  $t = t_{n,s}$ , both  $A = b_{t_{n,s},t_{n,s}}^J(1)$  and  $B = \mathbb{E} \left[ b_{t_{n,s},t_{n,s}}^J(1) \middle| \mathcal{B}_{t_{n,s}}^{P,J} \right]$  equals unity, so the difference is zero. Now notice that

$$A = b_{t,t_{n,s}}^J(1) = \int \frac{Q_{t,t_{n,s}}(u_{t_{n,s}})}{u_t} d\hat{P}_t^{F,J} \geq \int_{\mathcal{C}_t} \frac{Q_{t,t_{n,s}}(u_{t_{n,s}})}{u_t} d\hat{P}_t^{F,J} \geq \inf_{x \in \mathcal{C}_t} \frac{Q_{t,t_{n,s}}(u_{t_{n,s}})}{u_t}(x) \cdot \hat{P}_t^{F,J}(\mathcal{C}_t).$$

By Assumption 2(ii), we have

$$\inf_{x \in \mathcal{C}_t} \frac{Q_{t,t_{n,s}}(u_{t_{n,s}})}{u_t}(x) \geq \frac{1}{C_2} \sup_{x \in \mathcal{X}} \frac{Q_{t,t_{n,s}}(u_{t_{n,s}})}{u_t}(x).$$

On the other hand, for  $t < t_{n,s}$  we have

$$\left| \int \mathbf{1}_{\mathcal{C}_t} d\hat{P}_t^{F,J} - \int \mathbf{1}_{\mathcal{C}_t} dP_t^G \right| \leq \frac{4aC_2(C_1 + 1)}{\rho\sqrt{J}}(nS + s) \leq \frac{\rho}{2}$$

by the induction hypothesis and the required lower bound on  $J$ , because the event set  $\bar{\mathcal{E}}_{t_{n,s}}^{f,a,J}$  is contained in the set  $\bar{\mathcal{E}}_t^{1,c_t,a,J}$  for  $t < t_{n,s}$  due to the definition (S35). Since  $P_t^G(\mathcal{C}_t) > \rho$  by Assumption 2(i), we have  $\hat{P}_t^{F,J}(\mathcal{C}_t) > \frac{\rho}{2}$ . It follows that for  $t < t_{n,s}$ ,

$$A \geq \frac{\rho}{2C_2} \sup \left[ \frac{Q_{t,t_{n,s}}(u_{t_{n,s}})}{u_t} \right]. \quad (\text{S41})$$

For  $t = t_{n,s}$ ,

$$A = 1 \geq \frac{\rho}{2C_2} = \frac{\rho}{2C_2} \cdot \sup \left[ \frac{Q_{t_{n,s},t_{n,s}}(u_{t_{n,s}})}{u_{t_{n,s}}} \right].$$

Thus from (S38), (S39), (S40), and (S41), we have

$$\left| \frac{b_{t,t_{n,s}}^J(f)}{b_{t,t_{n,s}}^J(1)} - \frac{\mathbb{E} \left[ b_{t,t_{n,s}}^J(f) \middle| \mathcal{B}_t^{P,J} \right]}{\mathbb{E} \left[ b_{t,t_{n,s}}^J(1) \middle| \mathcal{B}_t^{P,J} \right]} \right| \leq \frac{4aC_2}{\rho\sqrt{J}}. \quad (\text{S42})$$

Noting that

$$\int f dP_{t_{n,s}}^G = \frac{P_{t_0} Q_{t_0,t_{n,s}}(u_{t_{n,s}} \cdot f)}{P_{t_0} Q_{t_0,t_{n,s}}(u_{t_{n,s}})} = \frac{\mathbb{E} \left[ b_{t_0,t_{n,s}}^J(f) \middle| \mathcal{B}_{t_0}^{P,J} \right]}{\mathbb{E} \left[ b_{t_0,t_{n,s}}^J(1) \middle| \mathcal{B}_{t_0}^{P,J} \right]}$$

where we understand that  $\mathcal{B}_{t_0}^{P,J}$  is the trivial  $\sigma$ -algebra on  $\Omega^{\text{MC}}$ , we see that the above argument also shows that

$$\left| \frac{b_{t_0,t_{n,s}}^J(f)}{b_{t_0,t_{n,s}}^J(1)} - \int f dP_{t_{n,s}}^G \right| \leq \frac{4aC_2}{\rho\sqrt{J}}. \quad (\text{S43})$$



This bounds the last term on the right hand side of (S36). Next, we consider the second term on the right hand side of (S37). Due to (S32), we have

$$\frac{\mathbb{E} \left[ b_{t,t_n,s}^J(f) \middle| \mathcal{B}_t^{P,J} \right]}{\mathbb{E} \left[ b_{t,t_n,s}^J(1) \middle| \mathcal{B}_t^{P,J} \right]} = \frac{\int \frac{Q_{t,t_n,s}(u_{t_n,s} \cdot f)}{u_t} \cdot w_t dM_t^J}{\int \frac{Q_{t,t_n,s}(u_{t_n,s})}{u_t} \cdot w_t dM_t^J}.$$

Now, on the set  $\bar{\mathcal{E}}_{t_n,s}^{f,a,J} \subset \mathcal{E}_{t,t_n,s}^{f,a,P,J} \cap \mathcal{E}_{t,t_n,s}^{1,a,P,J}$ ,

$$\left| \int \frac{Q_{t,t_n,s}(u_{t_n,s} \cdot f)}{u_t} \cdot w_t dM_t^J - b_{t^-,t_n,s}^J(f) \right| \leq \frac{aC_1}{\sqrt{J}} \sup \left[ \frac{Q_{t^-,t_n,s}(u_{t_n,s})}{u_{t^-}} \right],$$

and

$$\left| \int \frac{Q_{t,t_n,s}(u_{t_n,s})}{u_t} \cdot w_t dM_t^J - b_{t^-,t_n,s}^J(1) \right| \leq \frac{aC_1}{\sqrt{J}} \sup \left[ \frac{Q_{t^-,t_n,s}(u_{t_n,s})}{u_{t^-}} \right].$$

We have already seen above that

$$b_{t^-,t_n,s}^J(1) \geq \frac{\rho}{2C_2} \sup \left[ \frac{Q_{t^-,t_n,s}(u_{t_n,s})}{u_{t^-}} \right].$$

Therefore, invoking (S38) again, we have

$$\left| \frac{\mathbb{E} \left[ b_{t,t_n,s}^J(f) \middle| \mathcal{B}_t^{P,J} \right]}{\mathbb{E} \left[ b_{t,t_n,s}^J(1) \middle| \mathcal{B}_t^{P,J} \right]} - \frac{b_{t^-,t_n,s}^J(f)}{b_{t^-,t_n,s}^J(1)} \right| \leq \frac{4aC_2C_1}{\rho\sqrt{J}}. \quad (\text{S44})$$

Thus, summing (S42) and (S44), we obtain

$$\left| \frac{b_{t,t_n,s}^J(f)}{b_{t,t_n,s}^J(1)} - \frac{b_{t^-,t_n,s}^J(f)}{b_{t^-,t_n,s}^J(1)} \right| \leq \frac{4aC_2(C_1+1)}{\rho\sqrt{J}} \quad (\text{S45})$$

on the set  $\bar{\mathcal{E}}_{t_n,s}^{f,a,J}$ . From (S36), (S43), and (S45), we have

$$\left| \int f d\hat{P}_{t_n,s}^{F,J} - \int f dP_{t_n,s}^G \right| \leq \frac{4aC_2(C_1+1)}{\rho\sqrt{J}}(nS + s + 1)$$

on the event set  $\bar{\mathcal{E}}_{t_n,s}^{f,a,J}$ , completing the induction step for  $t_{n,s}$ .  $\square$

As a direct consequence of Lemma 1 and Lemma 2, we obtain the proof of Theorem 2.

**Theorem 2.** *Suppose multinomial resampling is used in Algorithm 1. Also suppose that Assumptions 1 and 2, which define constants  $\rho$ ,  $C_1$ , and  $C_2$ , hold. If  $f$  is a measurable function such that  $\|f\|_\infty \leq 1$  and  $a > 1$  is an arbitrary constant, then we have*

$$\left| \frac{1}{J} \sum_{j=1}^J f(X_{t_N}^{F,j}) - \mathbb{E}[f(X_{t_N}) | Y_{1:N} = y_{1:N}] \right| \leq \frac{4aC_2(C_1+1)}{\rho\sqrt{J}}(NS + 1) \quad (7)$$

with probability at least  $1 - \frac{(2NS+1)(NS+1)}{a^2}$ , given that  $\sqrt{J} \geq 8\rho^{-2}aC_2(C_1+1)NS$ .

*Proof of Theorem 2.* From Lemma 2, we have

$$\left| \int f d\hat{P}_{t_N}^{F,J} - \int f dP_{t_N}^G \right| \leq \frac{4aC_2(C_1+1)}{\rho\sqrt{J}}(NS+1)$$

on the event set  $\bar{\mathcal{E}}_{t_N}^{f,a,J}$ . We recall the definition

$$\bar{\mathcal{E}}_{t_{n,s}}^{f,a,J} := \bar{\mathcal{E}}_{t_{n,s-1}}^{1_{c_{t_{n,s-1}}},a,J} \cap \left( \bigcap_{\substack{t_0 \leq t \leq t_{n,s} \\ t \in \mathbb{I}}} \mathcal{E}_{t,t_{n,s}}^{f,a,F,J} \right) \cap \left( \bigcap_{\substack{t_0 \leq t < t_{n,s} \\ t \in \mathbb{I}}} \mathcal{E}_{t,t_{n,s}}^{1,a,F,J} \right) \cap \left( \bigcap_{\substack{t_0 < t \leq t_{n,s} \\ t \in \mathbb{I}}} \mathcal{E}_{t,t_{n,s}}^{f,a,P,J} \right) \cap \left( \bigcap_{\substack{t_0 < t < t_{n,s} \\ t \in \mathbb{I}}} \mathcal{E}_{t,t_{n,s}}^{1,a,P,J} \right). \quad (\text{S47})$$

Thus

$$\begin{aligned} \left( \bar{\mathcal{E}}_{t_{n,s}}^{1_{c_{t_{n,s}}},a,J} \right)^c &= \left( \bar{\mathcal{E}}_{t_{n,s-1}}^{1_{c_{t_{n,s-1}}},a,J} \right)^c \cup \left( \bigcup_{\substack{t_0 \leq t \leq t_{n,s} \\ t \in \mathbb{I}}} \left( \mathcal{E}_{t,t_{n,s}}^{1_{c_{t_{n,s}}},a,F,J} \right)^c \right) \cup \left( \bigcup_{\substack{t_0 \leq t < t_{n,s} \\ t \in \mathbb{I}}} \left( \mathcal{E}_{t,t_{n,s}}^{1,a,F,J} \right)^c \right) \\ &\quad \cup \left( \bigcup_{\substack{t_0 < t \leq t_{n,s} \\ t \in \mathbb{I}}} \left( \mathcal{E}_{t,t_{n,s}}^{1_{c_{t_{n,s}}},a,P,J} \right)^c \right) \cup \left( \bigcup_{\substack{t_0 < t < t_{n,s} \\ t \in \mathbb{I}}} \left( \mathcal{E}_{t,t_{n,s}}^{1,a,P,J} \right)^c \right). \end{aligned}$$

By Lemma 1, we have

$$\begin{aligned} \mathbb{P}^{\text{MC}} \left[ \left( \mathcal{E}_{t,t_{n,s}}^{1_{c_{t_{n,s}}},a,F,J} \right)^c \right] &\leq \frac{1}{a^2}, & \mathbb{P}^{\text{MC}} \left[ \left( \mathcal{E}_{t,t_{n,s}}^{1,a,F,J} \right)^c \right] &\leq \frac{1}{a^2}, \\ \mathbb{P}^{\text{MC}} \left[ \left( \mathcal{E}_{t,t_{n,s}}^{1_{c_{t_{n,s}}},a,P,J} \right)^c \right] &\leq \frac{1}{a^2}, & \mathbb{P}^{\text{MC}} \left[ \left( \mathcal{E}_{t,t_{n,s}}^{1,a,P,J} \right)^c \right] &\leq \frac{1}{a^2}, \end{aligned}$$

so we obtain

$$\mathbb{P}^{\text{MC}} \left[ \left( \bar{\mathcal{E}}_{t_{n,s}}^{1_{c_{t_{n,s}}},a,J} \right)^c \right] \leq \mathbb{P}^{\text{MC}} \left[ \left( \bar{\mathcal{E}}_{t_{n,s-1}}^{1_{c_{t_{n,s-1}}},a,J} \right)^c \right] + \frac{1}{a^2} \{4(nS+s)+1\}.$$

Since

$$\mathbb{P}^{\text{MC}} \left[ \left( \bar{\mathcal{E}}_{t_0}^{1_{c_{t_0}},a,J} \right) \right] \leq \frac{1}{a^2},$$

we reach through a recursion the conclusion that

$$\mathbb{P}^{\text{MC}} \left[ \left( \bar{\mathcal{E}}_{t_{N-1,S-1}}^{1_{c_{t_{N-1,S-1}}},a,J} \right)^c \right] \leq \frac{1}{a^2} \sum_{nS+s=0}^{NS-1} \{4(nS+s)+1\} = \frac{1}{a^2} NS(2NS-1).$$

Thus by (S47) and using a similar argument we obtain

$$\mathbb{P}^{\text{MC}} \left[ \left( \bar{\mathcal{E}}_{t_N}^{f,a,J} \right)^c \right] \leq \frac{1}{a^2} \{NS(2NS-1) + 4NS + 1\} = \frac{1}{a^2} (2NS+1)(NS+1).$$

We finish the proof by noting that

$$\int f dP_{t_N}^G = \frac{P_{t_0} Q_{t_0,t_N}(g_N \cdot f)}{P_{t_0} Q_{t_0,t_N}(g_N)} = \mathbb{E}[f(X_{t_N}) | Y_{1:N} = y_{1:N}].$$

□

## S2 Dimension scaling of constant $C_1$ in Assumption 1

In the main text, we argued that the constant  $C_1$  in Assumption 1 is bounded uniformly over  $d$  for POMP models consisting of a collection of  $d$  independent processes. In this supplementary section, we derive more explicit results on the constant  $C_1$  for time-homogeneous processes and diffusion processes. Based on these results, we demonstrate that  $C_1$  is uniformly bounded over  $d$  for latent Brownian motions with arbitrary correlation between components.

We first consider the case where the latent process  $\{X_t\}$  is time-homogeneous. The transition kernels may be written as  $K_{t,t'} = H_{t'-t}$  where the kernels  $\{H_t; t \geq 0\}$  are parameterized by the time duration. The infinitesimal generator of  $\{H_t\}$  is an operator  $\mathcal{L}$  such that  $\mathcal{L}f = \lim_{t \downarrow 0} \frac{1}{t}(H_t f - f)$  for measurable functions  $f$  for which the right hand side limit exists. We denote the associated carré-du-champ operator by  $\Gamma(f) := \frac{1}{2}\mathcal{L}f^2 - f \cdot \mathcal{L}f$  (Bakry et al., 2013). The next proposition derives an explicit bound for  $C_1$  for time-homogeneous latent processes. We assume that the generator  $\mathcal{L}$  is defined for both  $K_{\tau,t}Q_{t,t'}u_{t'}$  and its square.

**Proposition 2.** *Suppose the latent process is time-homogeneous with the associated carré-du-champ operator  $\Gamma$ . Assume that for  $t, t' \in \mathbb{I} \setminus \{t_0\}$  such that  $t \leq t'$ ,*

$$\frac{\Gamma(K_{\tau,t}Q_{t,t'}u_{t'})}{(K_{\tau,t}Q_{t,t'}u_{t'})^2} \leq \xi$$

*holds for  $\tau \in [t^-, t]$ . Then Assumption 1 holds with  $C_1 = e^{\xi \cdot (t-t^-)}$ .*

*Proof of Proposition 2.* Define  $\lambda_\tau := \log K_{t^-, \tau}(K_{\tau,t}Q_{t,t'}u_{t'})^2$  and  $h := Q_{t,t'}u_{t'}$ . Now observe that

$$\begin{aligned} \frac{d}{d\tau} \lambda_\tau &= \frac{K_{t^-, \tau} \mathcal{L}(K_{\tau,t}h)^2 + K_{t^-, \tau} \frac{d}{d\tau}(K_{\tau,t}h)^2}{K_{t^-, \tau}(K_{\tau,t}h)^2} \\ &= \frac{K_{t^-, \tau} [\mathcal{L}(K_{\tau,t}h)^2 - 2K_{\tau,t}h \cdot \mathcal{L}K_{\tau,t}h]}{K_{t^-, \tau}(K_{\tau,t}h)^2} \\ &= \frac{2K_{t^-, \tau} \Gamma(K_{\tau,t}h)}{K_{t^-, \tau}(K_{\tau,t}h)^2}. \end{aligned}$$

Recalling the relation  $h = Q_{t,t'}u_{t'}$ , we see that  $0 \leq \frac{d}{d\tau} \lambda_\tau \leq 2\xi$  for  $\tau \in [t^-, t]$  and thus  $\lambda_t - \lambda_{t^-} \leq 2\xi \cdot (t - t^-)$ . The desired conclusion follows by noting that  $C_1$  is an upper bound on  $e^{(\lambda_t - \lambda_{t^-})/2}$ .  $\square$

Next we show that the bound  $\xi$  in Proposition 2 scales linearly with  $d$  and thus  $C_1$  is uniformly bounded over  $d$  for independent time-homogeneous processes if  $S = d$ . Proposition 3 makes the argument (8) and (9) in the main text more concrete for time-homogeneous latent processes.

**Proposition 3.** *Consider a POMP model comprising  $d$  independent one-dimensional time-homogeneous latent processes and corresponding independent one-dimensional measurement processes. For this model we consider the guide function of the form  $u_t(x) = \prod_{i=1}^d u_t^{[i]}(x^{[i]})$ . Then we have*

$$\frac{\Gamma(K_{\tau,t}Q_{t,t'}u_{t'})}{(K_{\tau,t}Q_{t,t'}u_{t'})^2} = \sum_{i=1}^d \frac{\Gamma^{[i]}(K_{\tau,t}^{[i]}Q_{t,t'}^{[i]}u_{t'}^{[i]})}{(K_{\tau,t}^{[i]}Q_{t,t'}^{[i]}u_{t'}^{[i]})^2}. \quad (\text{S48})$$

Here,  $\Gamma^{[i]}$  denotes the carré-du-champ operator for the latent process corresponding to the  $i$ -th dimension. Suppose that the observation time interval length is given by  $\Delta$ , which is divided into  $d$  sub-intervals so that  $t - t^- = \frac{\Delta}{d}$ . Then in view of Proposition 2, Assumption 1 holds with  $C_1 = e^{\bar{\xi}\Delta}$ , which is bounded uniformly over  $d$ , provided that each term in the sum (S48) is bounded above by  $\bar{\xi}$ .

*Proof of Proposition 3.* For a bounded measurable  $f : \mathbb{X} \rightarrow \mathbb{R}^+$  that factorizes into functions of each dimension component as

$$f(x) = \prod_{i=1}^d f^{[i]}(x^{[i]}),$$

we may write  $H_t f = \prod_{i=1}^d H_t^{[i]} f^{[i]}$  where  $\{H_t^{[i]}; t \geq 0\}$  is a time-homogeneous transition kernel for the  $i$ -th component of the latent process,  $\{X_t^{[i]}\}$ . We have

$$\mathcal{L}f = \frac{d}{dt} \prod_{i=1}^d H_t^{[i]} f^{[i]} \Big|_{t=0} = \prod_{i=1}^d H_t^{[i]} f^{[i]} \cdot \sum_{i=1}^d \frac{\frac{d}{dt} H_t^{[i]} f^{[i]}}{H_t^{[i]} f^{[i]}} \Big|_{t=0} = f \cdot \sum_{i=1}^d \frac{\mathcal{L}^{[i]} f^{[i]}}{f^{[i]}}$$

It follows that

$$\frac{\Gamma(f)}{f^2} = \frac{\frac{1}{2} \mathcal{L}f^2 - f \cdot \mathcal{L}f}{f^2} = \sum_{i=1}^d \frac{\frac{1}{2} \mathcal{L}^{[i]} f^{[i]2} - f^{[i]} \cdot \mathcal{L}^{[i]} f^{[i]}}{f^{[i]2}} = \sum_{i=1}^d \frac{\Gamma^{[i]}(f^{[i]})}{f^{[i]2}}.$$

□

We can further develop the argument when the latent process  $\{X_t\}$  is a  $d$  dimensional Ito process defined by

$$dX_t = \mu(X_t)dt + R(X_t)dB_t, \quad (\text{S49})$$

where  $\mu(X_t) \in \mathbb{R}^d$  denotes the drift and  $R(X_t) \in \mathbb{R}^{d \times d}$  denotes the (matrix-valued) volatility of the process  $\{X_t\}$ . The term  $B_t = \{B_t^{[1]}, \dots, B_t^{[d]}\}$  denotes a  $d$  dimensional standard Brownian motion. We call  $\Sigma_p := RR^T$  the process noise covariance. Assume that  $f : \mathbb{R}^d \rightarrow \mathbb{R}$  is twice continuously differentiable. Then by Ito's formula

$$df(X_t) = Df(X_t)dX_t + \frac{1}{2} \text{Tr} \{D^2 f(X_t)d[X]_t\}$$

where  $[X]$  is the quadratic variation process of  $X$  (Rogers and Williams, 1994). In the context of (S49),  $d[X]_t$  is given by  $\Sigma_p(X_t)dt$ . The first order derivative  $Df(X_t)$  will be viewed as a  $d$  dimensional row vector and the second order derivative  $D^2 f(X_t)$  as a  $d \times d$  symmetric matrix. We have

$$df(X_t) = Df(X_t) \{ \mu(X_t)dt + R(X_t)dB_t \} + \frac{1}{2} \text{Tr} \{D^2 f(X_t) \cdot \Sigma_p(X_t)\} dt$$

and thus

$$\mathcal{L}f(x) = \lim_{t \downarrow 0} \frac{1}{t} [\mathbb{E}^x f(X_t) - f(x)] = Df(x) \cdot \mu(x) + \frac{1}{2} \text{Tr} [D^2 f(x) \cdot \Sigma_p(x)].$$

From the relations

$$Df^2 = 2fDf, \quad D^2 f^2 = 2(Df)^T Df + 2fD^2 f,$$

and the definition of the carré-du-champ operator  $\Gamma(f) = \frac{1}{2} \mathcal{L}f^2 - f \cdot \mathcal{L}f$ , we obtain

$$\Gamma(f) = \frac{1}{2} (Df) \Sigma_p (Df)^T.$$

Thus for  $f$  strictly positive, we may write

$$\frac{\Gamma(f)}{f^2} = \frac{1}{2} (D \log f) \Sigma_p (D \log f)^T. \quad (\text{S50})$$

Now we consider a concrete example of correlated Brownian motion.

**Example S1.** Suppose that  $\{X_t\}$  is a  $d$  dimensional correlated Brownian motion. This corresponds to the case where the drift  $\mu$  and the volatility  $\Sigma_p$  are constant in the Ito diffusion (S49). Without loss of generality for the following argument, we may and will assume  $\mu = 0$ . Suppose that the measurement of the process  $\{X_t\}$  is made at times  $t_{1:N}$  with Gaussian noise of mean zero and variance  $\Sigma_m \in \mathbb{R}^{d \times d}$ . We will show that Assumption 1 holds with  $C_1$  uniformly bounded over  $d$  for this POMP model, where the correlation between the components of the latent Brownian motion is arbitrary. For simplicity of argument, we assume that the guide function  $u_t$  is given by the forecast likelihood of  $B = 1$  future observation and consider the case where  $t' = t_{n+1}$  and  $t \in (t_n, t_{n+1}] \cap \mathbb{I}$ . The general case involves more complicated equations but follows the same logic. In the case we consider, we have  $u_{t_{n+1}} \equiv g_{n+1}(y_{n+1} | \cdot)$  and for  $\tau \in [t^-, t]$ ,

$$K_{\tau,t} Q_{t,t_{n+1}}(u_{t_{n+1}})(x) = p_{Y_{n+1}|X_\tau}(y_{n+1} | x) = \phi\{y_{n+1}; x, \Sigma_m + \Sigma_p \cdot (t_{n+1} - \tau)\},$$

where  $\phi(\cdot; \eta, \Xi)$  denotes the multivariate normal density with mean  $\eta$  and variance  $\Xi$ . Thus

$$\log K_{\tau,t} Q_{t,t_{n+1}}(u_{t_{n+1}})(x) = -\frac{1}{2}(y_{n+1} - x)^T \{\Sigma_m + \Sigma_p \cdot (t_{n+1} - \tau)\}^{-1} (y_{n+1} - x) + \text{const.}$$

In view of (S50), we have

$$\frac{\Gamma(f)}{f^2} = \frac{1}{2}(y_{n+1} - x)^T \{\Sigma_m + \Sigma_p \cdot (t_{n+1} - \tau)\}^{-1} \Sigma_p \{\Sigma_m + \Sigma_p \cdot (t_{n+1} - \tau)\}^{-1} (y_{n+1} - x) \quad (\text{S51})$$

where  $f = K_{\tau,t} Q_{t,t_{n+1}}(u_{t_{n+1}})$ . Our goal is to show that  $\frac{\Gamma(f)}{f^2}$  is  $O(d)$ , because then by Proposition 2  $C_1 = O(1)$ . Since

$$Y_{n+1} | (X_\tau = x) \sim \mathcal{N}[x, \Sigma_m + \Sigma_p \cdot (t_{n+1} - \tau)],$$

we have

$$\{\Sigma_m + \Sigma_p \cdot (t_{n+1} - \tau)\}^{-1/2} (Y_{n+1} - x) =: W \sim \mathcal{N}(0, I)$$

where  $I$  denotes the  $d$  dimensional identity matrix. Let  $v_1, \dots, v_d$  be the eigenvalues of

$$\Upsilon := \{\Sigma_m + \Sigma_p \cdot (t_{n+1} - \tau)\}^{-1/2} \Sigma_p \{\Sigma_m + \Sigma_p \cdot (t_{n+1} - \tau)\}^{-1/2}.$$

Then

$$W^T \Upsilon W \stackrel{d}{=} v_1 Z_1^2 + \dots + v_d Z_d^2 = O_p(v_1 + \dots + v_d) = O_p[\text{Tr}(\Upsilon)],$$

where  $Z_1, \dots, Z_d$  denote independent  $\mathcal{N}(0, 1)$  random variables. When considering a fixed  $y_{n+1}$ , it is therefore reasonable to assume that (S51) is  $O[\text{Tr}(\Upsilon)]$ . Our goal then simplifies to showing that  $\text{Tr}(\Upsilon) = O(d)$ .

We will assume that  $\Sigma_m$  is positive definite and  $\Sigma_p$  positive semi-definite. We will denote the maximal diagonal entry of  $\Sigma_p$  by  $\bar{\sigma}_p^2 := \max_{i \in 1:d} (\Sigma_p)_{ii}$  and the smallest eigenvalue of  $\Sigma_m$  by  $\underline{\lambda}_m > 0$ . We will suppose that both  $\bar{\sigma}_p^2$  and  $\underline{\lambda}_m^{-1}$  are  $O(1)$  in  $d$ . The assumption that  $\bar{\sigma}_p^2 = O(1)$  asserts that the marginal distribution of each component of the latent Brownian motion has increments of size not growing with  $d$ . The assumption that  $\underline{\lambda}_m^{-1} = O(1)$  can be satisfied if, for example, the measurement noise is given by the sum of a noise term that is independent in each spatial unit and a correlated noise term such that when we write  $\Sigma_m = \Sigma_m^{\text{ind}} + \Sigma_m^{\text{cor}}$ , the correlated noise covariance  $\Sigma_m^{\text{cor}}$  is positive semi-definite and the independent noise covariance  $\Sigma_m^{\text{ind}}$  is given by a diagonal matrix for which the smallest diagonal entry is greater than some positive constant that

is not decreasing as  $d$  increases. We will write  $A \preceq B$  if the matrix  $B - A$  is positive semi-definite. We then have

$$\underline{\lambda}_m I \preceq \Sigma_m \preceq \Sigma_m + \Sigma_p \cdot (t_{n+1} - \tau),$$

and so

$$\{\Sigma_m + \Sigma_p \cdot (t_{n+1} - \tau)\}^{-1} \preceq \underline{\lambda}_m^{-1} I.$$

Since it follows that

$$\Sigma_p^{1/2} [\underline{\lambda}_m^{-1} I - \{\Sigma_m + \Sigma_p \cdot (t_{n+1} - \tau)\}^{-1}] \Sigma_p^{1/2}$$

is positive semi-definite, we have

$$\text{Tr}([\underline{\lambda}_m^{-1} I - \{\Sigma_m + \Sigma_p \cdot (t_{n+1} - \tau)\}^{-1}] \Sigma_p) \geq 0. \quad (\text{S52})$$

Thus

$$\begin{aligned} \text{Tr}(\Upsilon) &= \text{Tr}[\{\Sigma_m + \Sigma_p \cdot (t_{n+1} - \tau)\}^{-1/2} \Sigma_p \{\Sigma_m + \Sigma_p \cdot (t_{n+1} - \tau)\}^{-1/2}] \\ &= \text{Tr}[\{\Sigma_m + \Sigma_p \cdot (t_{n+1} - \tau)\}^{-1} \Sigma_p] \\ &\leq \underline{\lambda}_m^{-1} \text{Tr}(\Sigma_p) \quad \text{due to (S52)} \\ &\leq \underline{\lambda}_m^{-1} \cdot d \bar{\sigma}_p^2 = O(d), \end{aligned}$$

due to our assumptions on  $\underline{\lambda}_m^{-1}$  and  $\bar{\sigma}_p^2$ . Therefore,  $\frac{\Gamma(f)}{f^2}$  in (S51) is  $O(d)$ , and by Proposition 2 we have that  $C_1$  is uniformly bounded over  $d$  for latent Brownian motions with arbitrary correlation.

### S3 Proof of Theorems 3 and 4

Theorems 3 and 4 establish the asymptotic normality of the likelihood estimate and that of the filtering error by GIRF (Algorithm 1) and develop their bounds under Assumptions 1 and 2.

**Theorem 3.** *In the limit where the particle size  $J$  tends to infinity, the likelihood estimate  $\hat{\ell}$  by GIRF (Algorithm 1) converges in distribution to a normal distribution:*

$$\sqrt{J} \left( \frac{\hat{\ell}}{\ell_{1:N}(y_{1:N})} - 1 \right) \Longrightarrow \mathcal{N}(0, \mathcal{V}).$$

*Under Assumptions 1 and 2, the asymptotic variance is bounded above by*

$$\mathcal{V} < NS \left( \frac{C_1^2 C_2^2}{\rho^2} - 1 \right).$$

*An application of the delta method leads to the asymptotic normality of the log likelihood estimate:*

$$\sqrt{J} \left( \log \hat{\ell} - \log \ell_{1:N}(y_{1:N}) \right) \Longrightarrow \mathcal{N}(0, \mathcal{V}).$$

**Theorem 4.** *In the limit where the particle size  $J$  tends to infinity, the following asymptotic normality holds for every measurable function  $f : \mathbb{X} \rightarrow \mathbb{R}$  such that  $\|f\|_\infty \leq 1$ :*

$$\sqrt{J} \left( \frac{1}{J} \sum_{j=1}^J f(X_{t_N}^{F,j}) - \mathbb{E}[f(X_{t_N}) | Y_{1:N} = y_{1:N}] \right) \Longrightarrow \mathcal{N}[0, \mathcal{W}(f)].$$

Under Assumptions 1 and 2, the asymptotic variance is bounded above by

$$\mathcal{W}(f) < 1 + 4NS \frac{C_1^2 C_2^2}{\rho^2}.$$

*Proof of Theorems 3 and 4.* We consider the discrete time POMP model constructed in Appendix A, which consists in the latent process  $\{Z_t := (X_t, X_{t-}); t \in \mathbb{I}\}$  and the weight function  $\{w_t; t \in \mathbb{I} \setminus \{t_0\}\}$ . We recall that the transition kernel of  $\{Z_t\}$  is given by

$$\tilde{K}_{t-,t}(A_1 \times A_2; (x_{t-}, x_{t--})) = K_{t-,t}(A_1; x_{t-}) \cdot \delta_{x_{t-}}(A_2)$$

for  $\forall A_1, A_2 \in \mathcal{X}$ . We note that GIRF (Algorithm 1) corresponds to the standard bootstrap particle filter with the transition kernel  $\tilde{K}_{t-,t}$  and the weight function  $w_t$ . In order to simplify application of existing results in the literature to our construction, we consider a time point  $t_{N,1}$  that is thought to be one intermediate time step after  $t_N$ . The transition kernel of the original latent process  $\{X_t\}$  for the interval  $[t_N, t_{N,1}]$  does not matter in the application, so we define it arbitrarily. Similar to the definition of  $Q_{t,t'}$  in (3), we define  $\tilde{Q}_{t,t'}$  on the extended space  $\mathbb{X}^2$  such that for any bounded measurable function  $\varphi : \mathbb{X}^2 \rightarrow \mathbb{R}$ ,

$$\tilde{Q}_{t,t'}(\varphi)(z) := \mathbb{E} \left[ \varphi(Z_{t'}) \prod_{\substack{t \leq \tau < t' \\ \tau \in \mathbb{I}}} w_\tau(Z_\tau) \middle| Z_t = z \right]. \quad (\text{S53})$$

We define a probability measure  $\tilde{P}_t$  on  $\mathbb{X}^2$  as the law of  $(X_t, X_{t-})$  where

$$X_{t-} \sim P_{t-}^G \quad \text{and} \quad X_t | (X_{t-} = x) \sim K_{t-,t}(\cdot; x).$$

One can check that for bounded measurable  $\varphi : \mathbb{X}^2 \rightarrow \mathbb{R}$ ,

$$\tilde{P}_t \varphi = \frac{\tilde{P}_{t_0,1} \tilde{Q}_{t_0,1,t} \varphi}{\tilde{P}_{t_0,1} \tilde{Q}_{t_0,1,t} 1}. \quad (\text{S54})$$

To see this, we first write  $\varphi_{t-,t}(x) := \mathbb{E}[\varphi(Z_t) | X_{t-} = x]$ ,  $\forall x \in \mathbb{X}$ , and observe that

$$\begin{aligned} \tilde{P}_{t_0,1} \tilde{Q}_{t_0,1,t} \varphi &= \mathbb{E} \mathbb{E} \left[ \varphi(Z_t) \prod_{\substack{t_0,1 \leq \tau < t \\ \tau \in \mathbb{I}}} w_\tau(Z_\tau) \middle| Z_{t_0,1} \right] \\ &= \mathbb{E} \mathbb{E} \left[ \varphi_{t-,t}(X_{t-}) \frac{u_{t-}(X_{t-})}{u_{t_0}(X_{t_0})} \prod_{n; t_n < t-} g_n(y_n | X_{t_n}) \middle| X_{t_0,1}, X_{t_0} \right] \\ &= \mathbb{E} Q_{t_0,1,t-}(\varphi_{t-,t} \cdot u_{t-})(X_{t_0,1}) \quad (\text{since } u_{t_0} \equiv 1) \\ &= P_{t_0} Q_{t_0,t-}(\varphi_{t-,t} \cdot u_{t-}), \end{aligned}$$

where all expectations are taken respect to the (unconditional) law of  $\{X_t\}$ . By (6), we see

$$\frac{\tilde{P}_{t_0,1} \tilde{Q}_{t_0,1,t} \varphi}{\tilde{P}_{t_0,1} \tilde{Q}_{t_0,1,t} 1} = \frac{P_{t_0} Q_{t_0,t-}(\varphi_{t-,t} \cdot u_{t-})}{P_{t_0} Q_{t_0,t-}(u_{t-})} = P_{t-}^G \varphi_{t-,t} = \tilde{P}_t \varphi,$$

confirming (S54). We now define

$$\bar{\tilde{Q}}_{t,t'}(\varphi) := \frac{\tilde{Q}_{t,t'}(\varphi)}{\tilde{P}_t \tilde{Q}_{t,t'}(1)}$$

and recall the definition of the empirical measure

$$M_t^J := \frac{1}{J} \sum_{j=1}^J \delta_{(X_t^{P,j}, X_{t-}^{F,j})} = \frac{1}{J} \sum_{j=1}^J \delta_{Z_t^{P,j}}$$

in Section S1. For every probability measure  $\eta$  on  $(\mathbb{X}^2, \mathcal{X}^2)$  and for every  $t \in \mathbb{I} \setminus \{t_0\}$ , we define a new probability measure  $\Phi_t(\eta)$  on  $(\mathbb{X}^2, \mathcal{X}^2)$  such that

$$\Phi_t(\eta)(\varphi) = \frac{\eta(w_t \cdot \varphi)}{\eta w_t}$$

holds for every bounded measurable  $\varphi : \mathbb{X}^2 \rightarrow \mathbb{R}$ . Corollary 9.3.1 in Del Moral (2004) states that there exists a sequence of independent, centered Gaussian random fields  $\{V_t; t \in \mathbb{I} \setminus \{t_0\}\}$  such that

$$\sqrt{J} [M_t^J(\varphi) - \Phi_t(M_{t-}^J)(\varphi)] \implies V_t \varphi$$

as  $J$  tends to infinity, where  $\implies$  implies the convergence in distribution and the variance of the random field  $V_t$  is given by

$$\text{Var}[V_t(\varphi)] = \tilde{P}_t \varphi^2 - (\tilde{P}_t \varphi)^2. \quad (\text{S55})$$

Applications of this result can lead to the asymptotic normality of the likelihood estimate and that of the filtering error. Bérard et al. (2014, Equation 1.23) gives a concise statement of the asymptotic normality of the likelihood estimate. We note that within our construction the likelihood of data can be expressed as

$$\ell_{1:N}(y_{1:N}) = \tilde{P}_{t_0,1} \tilde{Q}_{t_0,1,t_{N,1}}(1)$$

and the likelihood estimate  $\hat{\ell}$  from GIRF (Algorithm 1) can be expressed as

$$\hat{\ell} = \prod_{t \in \mathbb{I} \setminus \{t_0\}} M_t^J w_t.$$

Applying Equation (1.23) of Bérard et al. (2014) in our context gives

$$\sqrt{J} \left( \frac{\hat{\ell}}{\ell_{1:N}(y_{1:N})} - 1 \right) \implies \sum_{t \in \mathbb{I} \setminus \{t_0\}} V_t \left( \bar{\tilde{Q}}_{t,t_{N,1}}(1) \right).$$

Using (S55), we readily see that

$$\sqrt{J} \left( \frac{\hat{\ell}}{\ell_{1:N}(y_{1:N})} - 1 \right) \implies \mathcal{N} \left( 0, \sum_{t \in \mathbb{I} \setminus \{t_0\}} \left[ \frac{\tilde{P}_t \{\tilde{Q}_{t,t_{N,1}}(1)\}^2}{\{\tilde{P}_t \tilde{Q}_{t,t_{N,1}}(1)\}^2} - 1 \right] \right), \quad (\text{S56})$$

which means that the asymptotic variance is given by

$$\mathcal{V} = \sum_{t \in \mathbb{I} \setminus \{t_0\}} \left[ \frac{\tilde{P}_t \{\tilde{Q}_{t,t_{N,1}}(1)\}^2}{\{\tilde{P}_t \tilde{Q}_{t,t_{N,1}}(1)\}^2} - 1 \right]. \quad (\text{S57})$$



As for the asymptotic normality of the filtering error, application of Proposition 9.4.2 in Del Moral (2004) or Theorem 3 in Whiteley (2013) gives

$$\sqrt{J} \left( M_{t_{N,1}}^J \varphi - \tilde{P}_{t_{N,1}} \varphi \right) \Longrightarrow \sum_{t_{0,1} \leq t \leq t_{N,1}} V_t \left( \tilde{Q}_{t,t_{N,1}}(\varphi) - \tilde{Q}_{t,t_{N,1}}(1) \cdot \tilde{P}_{t_{N,1}} \varphi \right).$$

If we consider  $\varphi : \mathbb{X}^2 \rightarrow \mathbb{R}$  of the form  $\varphi(x_{t_{N,1}}, x_{t_N}) = f(x_{t_N})$ ,  $\forall (x_{t_{N,1}}, x_{t_N}) \in \mathbb{X}^2$ , for some bounded measurable  $f : \mathbb{X} \rightarrow \mathbb{R}$ , we have

$$M_{t_{N,1}}^J \varphi - \tilde{P}_{t_{N,1}} \varphi = \frac{1}{J} \sum_{j=1}^J f(X_{t_N}^{F,j}) - P_{t_N}^G f = \hat{P}_{t_N}^{F,J} f - \mathbb{E}[f(X_{t_N}) | Y_{1:N} = y_{1:N}].$$

Thus

$$\sqrt{J} \left( \hat{P}_{t_N}^{F,J} f - \mathbb{E}[f(X_{t_N}) | Y_{1:N} = y_{1:N}] \right) \Longrightarrow \mathcal{N}[0, \mathcal{W}(\varphi)],$$

where the asymptotic variance is given by

$$\mathcal{W}(\varphi) := \sum_{t_{0,1} \leq t \leq t_{N,1}} \frac{\tilde{P}_t \left\{ \tilde{Q}_{t,t_{N,1}}(\varphi) - \tilde{Q}_{t,t_{N,1}}(1) \cdot \tilde{P}_{t_{N,1}}(\varphi) \right\}^2}{\left\{ \tilde{P}_t \tilde{Q}_{t,t_{N,1}}(1) \right\}^2}. \quad (\text{S58})$$

In order to bound  $\mathcal{V}$  and  $\mathcal{W}(\varphi)$ , we first calculate that

$$\begin{aligned} \tilde{Q}_{t,t_{N,1}}(\varphi)(x_t, x_{t^-}) &= \mathbb{E} \left[ \varphi(Z_{t_{N,1}}) \prod_{\substack{t \leq \tau \leq t_N \\ \tau \in \mathbb{I}}} w_\tau(Z_\tau) \middle| Z_t = (x_t, x_{t^-}) \right] \\ &= \mathbb{E} \left[ \varphi_{t_N, t_{N,1}}(X_{t_N}) \frac{g_{\mathbf{n}(t^-)}^{\mathbf{1}[t^- \in t_{1:N}]}(y_{\mathbf{n}(t^-)} | X_{t^-})}{u_{t^-}(X_{t^-})} \prod_{n; t_n \geq t} g_n(y_n | X_{t_n}) \middle| X_t = x_t, X_{t^-} = x_{t^-} \right] \\ &= \frac{g_{\mathbf{n}(t^-)}^{\mathbf{1}[t^- \in t_{1:N}]}(y_{\mathbf{n}(t^-)} | x_{t^-})}{u_{t^-}(x_{t^-})} \cdot Q_{t,t_N}(\varphi_{t_N, t_{N,1}} \cdot g_N)(x_t), \end{aligned}$$

where we again used the notation  $\varphi_{t_N, t_{N,1}}(x) = \mathbb{E}[\varphi(Z_{t_{N,1}}) | X_{t_N} = x]$  and the fact that  $u_{t_N} \equiv g_N$ . From this and the definition of  $\tilde{P}_t$ , we see that

$$\tilde{P}_t \tilde{Q}_{t,t_{N,1}}(\varphi) = P_{t^-}^G \left( \frac{g_{\mathbf{n}(t^-)}^{\mathbf{1}[t^- \in t_{1:N}]}(y_{\mathbf{n}(t^-)} | \cdot)}{u_{t^-}} \cdot K_{t^-,t} Q_{t,t_N}(\varphi_{t_N, t_{N,1}} \cdot g_N) \right) = P_{t^-}^G \left( \frac{Q_{t^-,t_N}(\varphi_{t_N, t_{N,1}} \cdot g_N)}{u_{t^-}} \right),$$

and

$$\tilde{P}_t \{ \tilde{Q}_{t,t_{N,1}}(\varphi) \}^2 = P_{t^-}^G \left( \frac{\left\{ \frac{g_{\mathbf{n}(t^-)}^{\mathbf{1}[t^- \in t_{1:N}]}(y_{\mathbf{n}(t^-)} | \cdot)}{u_{t^-}} \right\}^2}{u_{t^-}^2} \cdot K_{t^-,t} \{ Q_{t,t_N}(\varphi_{t_N, t_{N,1}} \cdot g_N) \}^2 \right). \quad (\text{S59})$$

Now suppose that Assumption 1 holds, so that

$$\frac{K_{t^-,t} \{ Q_{t,t_N}(g_N) \}^2}{\{ K_{t^-,t} Q_{t,t_N}(g_N) \}^2} \leq C_1^2.$$

Also assume that  $\|\varphi\|_\infty \leq 1$ . Then from (S59) we see that

$$\begin{aligned}\tilde{P}_t\{\tilde{Q}_{t,t_{N,1}}(\varphi)\}^2 &\leq C_1^2 \cdot P_{t^-}^G \left( \frac{\left\{ g_{\mathbf{n}(t^-)}^{\mathbf{1}[t^- \in t_{1:N}]}(y_{\mathbf{n}(t^-)} \mid \cdot) \right\}^2}{u_{t^-}^2} \cdot \{K_{t^-,t}Q_{t,t_N}(g_N)\}^2 \right) \\ &= C_1^2 \cdot P_{t^-}^G \left( \frac{Q_{t^-,t_N}(g_N)^2}{u_{t^-}^2} \right).\end{aligned}$$

If we additionally suppose that Assumption 2 holds, we see that

$$\frac{\tilde{P}_t\{\tilde{Q}_{t,t_{N,1}}(\varphi)\}^2}{\{\tilde{P}_t\tilde{Q}_{t,t_{N,1}}(1)\}^2} \leq C_1^2 \cdot \frac{P_{t^-}^G \left( \frac{Q_{t^-,t_N}(g_N)}{u_{t^-}} \right)^2}{\left\{ P_{t^-}^G \left( \frac{Q_{t^-,t_N}(g_N)}{u_{t^-}} \right) \right\}^2} \leq C_1^2 \cdot \frac{\sup_{x \in \mathbb{X}} \left( \frac{Q_{t^-,t_N}(g_N)}{u_{t^-}} \right)^2}{(P_{t^-}^G \mathbf{1}_{\mathcal{C}_{t^-}})^2 \cdot \inf_{x \in \mathcal{C}_{t^-}} \left( \frac{Q_{t^-,t_N}(g_N)}{u_{t^-}} \right)^2} < \frac{C_1^2 C_2^2}{\rho^2}.$$

From (S57), we see that the asymptotic variance of the likelihood is bounded above by

$$\mathcal{V} < NS \left( \frac{C_1^2 C_2^2}{\rho^2} - 1 \right).$$

As for the asymptotic variance of the filtering error (S58), we note that

$$\left\{ \tilde{Q}_{t,t_{N,1}}(\varphi) - \tilde{Q}_{t,t_{N,1}}(1) \cdot \tilde{P}_{t_{N,1}}(\varphi) \right\}^2 \leq 2 \left[ \tilde{Q}_{t,t_{N,1}}(\varphi)^2 + \tilde{Q}_{t,t_{N,1}}(1)^2 \right],$$

and that the last term in (S58) is bounded above by unity:

$$\frac{\tilde{P}_{t_{N,1}} \left\{ \tilde{Q}_{t_{N,1},t_{N,1}}(\varphi) - \tilde{Q}_{t_{N,1},t_{N,1}}(1) \cdot \tilde{P}_{t_{N,1}}(\varphi) \right\}^2}{\left\{ \tilde{P}_{t_{N,1}} \tilde{Q}_{t_{N,1},t_{N,1}}(1) \right\}^2} = \tilde{P}_{t_{N,1}}(\varphi - \tilde{P}_{t_{N,1}}\varphi)^2 \leq 1.$$

Therefore, it follows that

$$\mathcal{W}(\varphi) < 1 + 4NS \frac{C_1^2 C_2^2}{\rho^2}.$$

□

## S4 Monte Carlo adjusted profile confidence intervals

When the likelihood of data from a one-parameter model can be exactly evaluated, the 95%-confidence interval for the maximum likelihood estimate of the parameter can be obtained by a cut-off on the likelihood curve at  $\frac{z_{0.975}^2}{2} = 1.92$ , where  $z_{0.975}$  is the 0.975 quantile of the standard normal distribution. In large and complex models where the likelihoods of data are estimated with Monte Carlo methods with non-negligible amount of error, the uncertainty in the likelihood estimates has to be taken into account in computing the cut-off. Ionides et al. (2017) developed a general procedure for constructing confidence intervals for a parameter of interest when the profile likelihoods with respect to that parameter can be estimated with some Monte Carlo errors. The

procedure for constructing the Monte Carlo adjusted profile (MCAP) confidence intervals are as follows.

We assume that the Monte Carlo profile points  $\check{\ell}_{1:K}^P$  are evaluated at  $\phi_{1:K}$ . We fit a smooth curve  $\check{\ell}^S(\phi)$  through the profile points using a local smoother, such as the R function `loess` (Cleveland et al., 1992). The MLE of the parameter  $\phi$  can be taken as the point  $\check{\phi}$  at which the maximum of the smoothed curve  $\check{\ell}^S$  is attained. In order to quantify the Monte Carlo error in the estimated maximum likelihood  $\check{\ell}^S(\check{\phi})$ , we make a local quadratic fit near the maximum, using the weights  $w_{1:K}$  that were used in evaluating the smoothed curve  $\check{\ell}^S$  at  $\check{\phi}$ . Write the fitted quadratic equation as  $-\check{a}\phi^2 + \check{b}\phi + \check{c}$ . The variance and covariance of the coefficients  $\check{\text{Var}}[\check{a}]$ ,  $\check{\text{Var}}[\check{b}]$ , and  $\check{\text{Cov}}[\check{a}, \check{b}]$  can be obtained as usual. Using the delta method, the standard error of the maximum  $\frac{\check{b}}{2\check{a}}$  can be estimated as

$$\text{SE}_{\text{mc}}^2 = \frac{1}{4\check{a}^2} \left( \check{\text{Var}}[\check{b}] - \frac{2\check{b}}{\check{a}} \check{\text{Cov}}[\check{a}, \check{b}] + \frac{\check{b}^2}{\check{a}^2} \check{\text{Var}}[\check{a}] \right).$$

On the other hand, the statistical error originating from the randomness in data can be estimated with the usual formula

$$\text{SE}_{\text{stat}} = \frac{1}{\sqrt{2\check{a}}}.$$

Assuming that the size of the Monte Carlo error is roughly the same across the possible realizations of the data, we can reasonably approximate the total standard error of the Monte Carlo maximum likelihood estimate as

$$\text{SE}_{\text{total}} = \sqrt{\text{SE}_{\text{stat}}^2 + \text{SE}_{\text{mc}}^2}.$$

It follows that the cut-off for an approximate  $(1 - \alpha)$  confidence interval can be obtained as

$$\delta = \check{a} \cdot \text{SE}_{\text{total}}^2 \cdot \chi_{\alpha} = \left( \check{a} \cdot \text{SE}_{\text{mc}}^2 + \frac{1}{2} \right) \cdot \chi_{\alpha},$$

where  $\chi_{\alpha}$  is the  $(1 - \alpha)$  quantile of the  $\chi$ -square distribution on one degree of freedom.

## S5 Details on the spatiotemporal measles transmission dynamics model and implementation of GIRF

The city-level measles transmission dynamics in our spatiotemporal model follow He et al. (2009). The model parameters are summarized in Table S-4. We assume the transmission coefficient  $\beta(t)$  in (22) depends on whether it is school term or holiday, because most measles infections happen via transmissions between children:

$$\beta(t) = \begin{cases} (1 + 2(1 - p)a)\bar{\beta} & \text{during school term} \\ (1 - 2pa)\bar{\beta} & \text{during school holiday.} \end{cases}$$

Here,  $p = 0.739$  is the proportion of the year taken up by the school term,  $a$  the amplitude of variation, and  $\bar{\beta}$  the annual average of the transmission rate. School holidays in the calendar day include: Christmas, 356–365 and 0–6; Easter, 100–115; summer, 199–252; autumn half-term, 300–308.

The susceptible recruitment rate  $r(t)$  is defined as follows. In the calendar year  $x$ , a certain fraction  $c$  of the annual births of the calendar year  $x - 4$  enters the susceptible compartment at

symbol	description
$R_0$	basic reproduction number
$a$	amplitude of seasonality
$\alpha$	mixing exponent
$\mu$	mortality rate
$\nu_{EI}^{-1}$	latent period
$\nu_{IR}^{-1}$	infectious period
$\sigma^2$	white-noise intensity
$\rho$	reporting probability
$\psi$	reporting overdispersion
$G$	gravitation constant
$c$	cohort entry fraction

Table S-4: Table of parameters for the spatiotemporal measles transmission dynamics model

the school admission date, which is the 251st day of a year. The remaining  $1 - c$  fraction enters the susceptible compartment continuously with a constant rate throughout the year.

The transition rates from the exposed to the infectious and from the infectious to the recovered compartments are defined as

$$\begin{aligned}\mathbb{E} \frac{dN_{EI}(t)}{dt} &= \nu_{EI} E(t), \\ \mathbb{E} \frac{dN_{IR}(t)}{dt} &= \nu_{IR} I(t),\end{aligned}\tag{S60}$$

where  $\nu_{EI}$  and  $\nu_{IR}$  are per capita progression rates between the respective compartments. We added randomness to the latent process dynamics as follows. For all cumulative transition processes  $\{N_{\cdot}(t)\}$ , we let the noise intensity equal to  $\sigma^2$  (Bretó et al., 2009; Karlin and Taylor, 1981), such that over a short time interval  $[t, t + \delta]$ , the infinitesimal increment  $N_{\cdot}(t + \delta) - N_{\cdot}(t)$  is Poisson distributed with the mean parameter given by the product of a gamma random variable  $\text{Gamma}(\delta/\sigma^2, \sigma^2)$  and the mean transition rate  $\mathbb{E} \frac{dN_{\cdot}}{dt}$ . In the limit as  $\delta$  approaches zero, this amounts to

$$N_{\cdot}(t + \delta) - N_{\cdot}(t) \sim \text{NegBin} \left( \frac{\delta}{\sigma^2}, \frac{\sigma^2 \cdot \mathbb{E} \frac{dN_{\cdot}(t)}{dt}}{\sigma^2 \cdot \mathbb{E} \frac{dN_{\cdot}(t)}{dt} + 1} \right),\tag{S61}$$

where the negative binomial random variable  $\text{NegBin}(r, p)$  has the probability mass function

$$\mathbb{P}[\text{NegBin}(r, p) = k] = \binom{k + r - 1}{k} \cdot (1 - p)^r p^k, \quad k = 0, 1, 2, \dots$$

with mean  $\frac{pr}{1-p}$  and variance  $\frac{pr}{(1-p)^2}$ . Bretó et al. (2009) explained a construction of such stochastic compartment models, which we adopt in our implementation. This construction defines a continuous-time Markov latent process which allows for overdispersion compared to Poisson processes (Bretó and Ionides, 2011).

As for the measurement model, the mean of biweekly case reports is given by the biweekly cumulative transitions from the infectious compartment to the recovered compartment multiplied by the city-specific reporting rate  $\rho_k$ . The number of biweekly case reports is assumed to follow a discrete normal distribution, which adds overdispersion parameterized by  $\psi$  to a binomial distribution with success parameter  $\rho_k$ . Specifically, we define the cumulative distribution  $F_k$  for the

number of biweekly case reports from the  $k$ -th city by

$$F_k(y; \rho_k, \psi, \Delta N_{IR,k}) := \Phi \left[ y + 0.5; \rho_k \Delta N_{IR,k}, \rho_k(1 - \rho_k) \Delta N_{IR,k} + \psi^2 \rho_k^2 \Delta N_{IR,k}^2 + 1 \right] \quad (\text{S62})$$

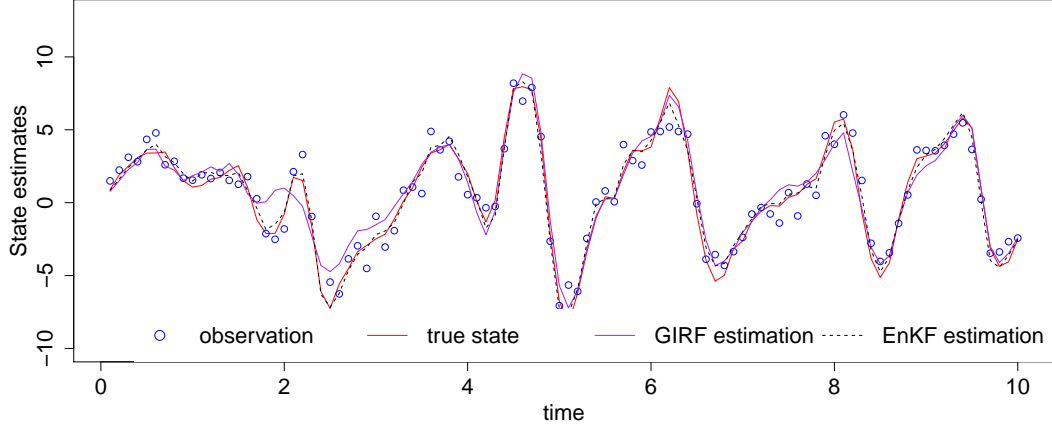
for  $y \in \{0, 1, 2, \dots\}$ , where  $\Delta N_{IR,k}$  denotes the biweekly transitions from the infectious to the recovered compartment for the  $k$ -th city and  $\Phi(\cdot; \mu, \sigma^2)$  denotes the cdf of the normal distribution with mean  $\mu$  and variance  $\sigma^2$ .

The latent process  $X(t)$  is composed of the components  $S_k(t)$ ,  $E_k(t)$ ,  $I_k(t)$ , and  $N_{IR,k}^{\text{biweek}}(t)$  for each city, where  $N_{IR,k}^{\text{biweek}}(t)$  denotes the number of transitions from the infectious to the recovered compartment up to time  $t$  since the beginning of the corresponding biweek, that is  $N_{IR,k}^{\text{biweek}}(t) = N_{IR,k}(t) - N_{IR,k}(t_n)$  where  $t_n$  is the start of the biweek that  $t$  is in. In the implementation of GIRF (Algorithms 1 and 2) on this model, we defined the guide function  $u_{t_n,s}$  using the formula (12)–(15) in Section 5 of the main text, with the number of lookaheads  $B = 3$ . The forecast variability was estimated at every first intermediate step (i.e.,  $s = 1$ ) using forty random forecasts. The forecast variability at other times was approximated using the local linear approximation (16). We calculated the distance between the first and the third quartiles of the sample obtained by multiplying the forecasts of  $N_{IR,k}^{\text{biweek}}(t)$  with the city-specific reporting probability  $\rho_k$ . In order to provide a conservative estimate of the forecast variability, a factor of  $1 + \frac{2}{\sqrt{N}}$  was multiplied to the sample inter-quartile distance, where  $N = 40$  denotes the number of forecast simulations. An estimate of the forecast variance for  $\rho_k \cdot N_{IR,k}^{\text{biweek}}(t)$  was obtained by multiplying 0.55 to the squared inter-quartile distance, because the ratio of the variance to the squared inter-quartile distance of a normal distribution is approximately 0.55 and the measurement model followed a discrete normal distribution.

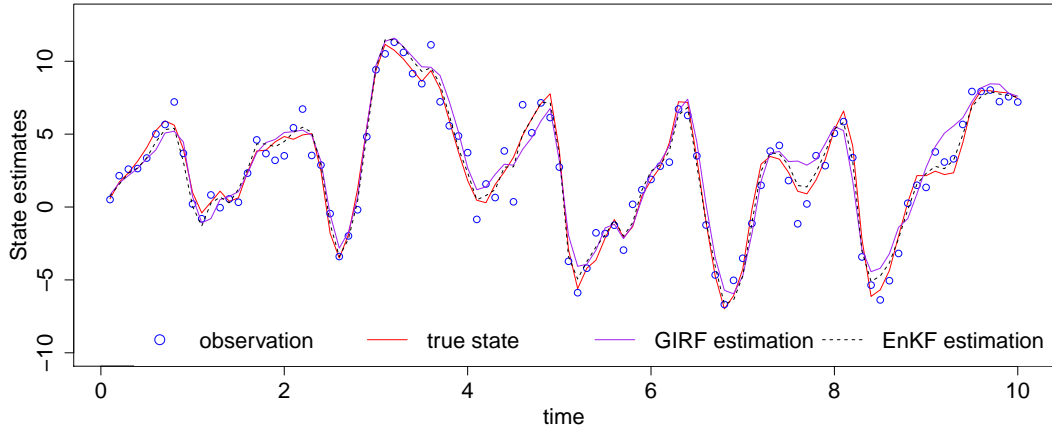
## S6 Additional figures for examples in Section 7

Figure S-7 compare the estimated filter means by GIRF (Algorithm 1) and ensemble Kalman filter (EnKF) for the first component in the one hundred and two hundred dimensional stochastic Lorenz 96 model when the observation interval is 0.1 (only the first one hundred time points are shown for visibility). In the main text, we compared the two algorithms when observations were taken at intervals of 0.5 and saw that the EnKF was not suitable to handle highly nonlinear latent process. In contrast, the latent process transition kernel is close to being linear and Gaussian in the intervals of length 0.1, and the latent process distribution conditional on data is close to being Gaussian. Figure S-7 demonstrates that the EnKF performs well in this situation. The number of particles, the computation time, and the log likelihood estimates for these two algorithms are summarized in Table S-5. The computational time of the two algorithms were comparable, but the likelihood estimates by EnKF were higher than those by GIRF (Algorithm 1). With these results, we can reconfirm that EnKF scales well to high dimensions when the one-step forecast distribution of the latent process is approximately Gaussian.

Figure S-8 shows the estimates of the likelihoods for the fifty dimensional stochastic Lorenz 96 model when  $\sigma_p$  and  $\sigma_m$  were fixed at 1.0 and the observation interval was 0.5. The fact that the slice log likelihood estimates dropped sharply at  $F = 10$  was not shown in Figure 5 in the main text.



(a)



(b)

Figure S-7: The estimated filter means for the first coordinate in stochastic Lorenz 96 model when the observation interval is 0.1, (a)  $d = 100$ , (b)  $d = 200$ .

	$d = 100$		$d = 200$	
	EnKF	GIRF	EnKF	GIRF
No. of particles	6,000	2,000	6,000	2,000
Computation time (min)	60	47	129	118
$\log \hat{\ell}$	-33203	-38183	-68471	-83969

Table S-5: The computational costs and the log likelihood estimates by EnKF and GIRF (Algorithm 1) for one and two hundred dimensional stochastic Lorenz 96 model when the observation interval is 0.1.

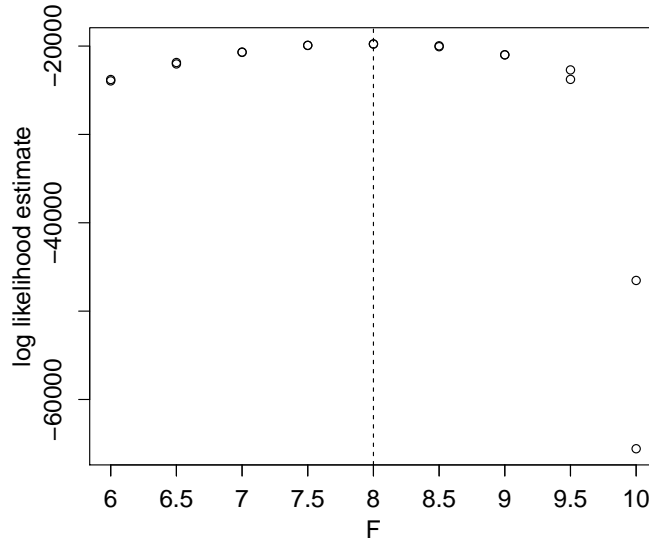


Figure S-8: The slice likelihood estimates at  $\sigma_p = \sigma_m = 1$  for the fifty dimensional Lorenz 96 model in Section 7.2.

## References

- Ades, M. and Van Leeuwen, P. J. (2015) The equivalent-weights particle filter in a high-dimensional system. *Quarterly Journal of the Royal Meteorological Society*, **141**, 484–503.
- Andrieu, C., Doucet, A. and Holenstein, R. (2010) Particle Markov chain Monte Carlo methods. *Journal of the Royal Statistical Society: Series B (Statistical Methodology)*, **72**, 269–342.
- Bakker, K. M., Martinez-Bakker, M. E., Helm, B. and Stevenson, T. J. (2016) Digital epidemiology reveals global childhood disease seasonality and the effects of immunization. *Proceedings of the National Academy of Sciences*, 201523941.
- Bakry, D., Gentil, I. and Ledoux, M. (2013) *Analysis and geometry of Markov diffusion operators*, vol. 348. Springer Science & Business Media.
- Becker, A. D., Birger, R. B., Teillant, A., Gastanaduy, P. A., Wallace, G. S. and Grenfell, B. T. (2016) Estimating enhanced prevaccination measles transmission hotspots in the context of cross-scale dynamics. *Proceedings of the National Academy of Sciences*, **113**, 14595–14600.
- Bengtsson, T., Bickel, P. and Li, B. (2008) Curse-of-dimensionality revisited: Collapse of the particle filter in very large scale systems. In *Probability and Statistics: Essays in Honor of David A. Freedman*, 316–334. Institute of Mathematical Statistics.
- Bérard, J., Del Moral, P. and Doucet, A. (2014) A lognormal central limit theorem for particle approximations of normalizing constants. *Electron. J. Probab*, **19**, 1–28.
- Beskos, A., Crisan, D. and Jasra, A. (2014a) On the stability of sequential Monte Carlo methods in high dimensions. *The Annals of Applied Probability*, **24**, 1396–1445.
- Beskos, A., Crisan, D., Jasra, A., Kamatani, K. and Zhou, Y. (2017) A stable particle filter for a class of high-dimensional state-space models. *Advances in Applied Probability*, **49**, 24–48.
- Beskos, A., Crisan, D. O., Jasra, A. and Whiteley, N. (2014b) Error bounds and normalising constants for sequential Monte Carlo samplers in high dimensions. *Advances in Applied Probability*, **46**, 279–306.
- Bjørnstad, O. N. and Grenfell, B. T. (2001) Noisy clockwork: Time series analysis of population fluctuations in animals. *Science*, **293**, 638–643.

- Blackwood, J. C., Streicker, D. G., Altizer, S. and Rohani, P. (2013) Resolving the roles of immunity, pathogenesis, and immigration for rabies persistence in vampire bats. *Proceedings of the National Academy of Sciences*, **110**, 20837–20842.
- Blake, I. M., Martin, R., Goel, A., Khetsuriani, N., Everts, J., Wolff, C., Wassilak, S., Aylward, R. B. and Grassly, N. C. (2014) The role of older children and adults in wild poliovirus transmission. *Proceedings of the National Academy of Sciences*, **111**, 10604–10609.
- Bretó, C., He, D., Ionides, E. L. and King, A. A. (2009) Time series analysis via mechanistic models. *The Annals of Applied Statistics*, 319–348.
- Bretó, C. and Ionides, E. L. (2011) Compound Markov counting processes and their applications to modeling infinitesimally over-dispersed systems. *Stochastic Processes and their Applications*, **121**, 2571–2591.
- Bunch, P. and Godsill, S. (2016) Approximations of the optimal importance density using Gaussian particle flow importance sampling. *Journal of the American Statistical Association*, **111**, 748–762.
- Cappé, O., Godsill, S. J. and Moulines, E. (2007) An overview of existing methods and recent advances in sequential Monte Carlo. *Proceedings of the IEEE*, **95**, 899–924.
- Chen, R., Wang, X. and Liu, J. S. (2000) Adaptive joint detection and decoding in flat-fading channels via mixture Kalman filtering. *IEEE transactions on Information Theory*, **46**, 2079–2094.
- Chopin, N. (2004) Central limit theorem for sequential Monte Carlo methods and its application to Bayesian inference. *Annals of statistics*, 2385–2411.
- Chopin, N., Jacob, P. E. and Papaspiliopoulos, O. (2013) SMC<sup>2</sup>: An efficient algorithm for sequential analysis of state space models. *Journal of the Royal Statistical Society: Series B (Statistical Methodology)*, **75**, 397–426.
- Chorin, A. J., Morzfeld, M. and Tu, X. (2013) A survey of implicit particle filters for data assimilation. In *State-Space Models* (eds. Y. Zeng and S. Wu), 63–88. Springer.
- Chorin, A. J. and Tu, X. (2009) Implicit sampling for particle filters. *Proceedings of the National Academy of Sciences*, **106**, 17249–17254.
- Clapp, T. and Godsill, S. (1999) Fixed-lag smoothing using sequential importance sampling. *Bayesian statistics 6: Proceeding of the Sixth Valencia International Meeting*, **6**, 743–752.
- Cleveland, W. S., Grosse, E. and Shyu, W. M. (1992) Local regression models. In *Statistical Models in S* (eds. J. Chambers and T. Hastie), 309–376. Chapman and Hall.
- Dalziel, B. D., Bjørnstad, O. N., van Panhuis, W. G., Burke, D. S., Metcalf, C. J. E. and Grenfell, B. T. (2016) Persistent chaos of measles epidemics in the prevaccination United States caused by a small change in seasonal transmission patterns. *PLoS Computational Biology*, **12**, e1004655.
- Del Moral, P. (2004) *Feynman-Kac Formulae: Genealogical and Interacting Particle Systems with Applications*. New York: Springer.
- Del Moral, P. and Guionnet, A. (2001) On the stability of interacting processes with applications to filtering and genetic algorithms. *Annales de l’Institut Henri Poincaré (B) Probability and Statistics*, **37**, 155–194.
- Del Moral, P. and Jacod, J. (2001) Interacting particle filtering with discrete observations. In *Sequential Monte Carlo methods in practice*, 43–75. Springer.
- Del Moral, P. and Murray, L. M. (2015) Sequential Monte Carlo with highly informative observations. *SIAM/ASA Journal on Uncertainty Quantification*, **3**, 969–997.
- Diggle, P. J. and Gratton, R. J. (1984) Monte Carlo methods of inference for implicit statistical models. *Journal of the Royal Statistical Society. Series B (Methodological)*, 193–227.



- Douc, R., Cappé, O. and Moulines, E. (2005) Comparison of resampling schemes for particle filtering. In *Proceedings of the 4th International Symposium on Image and Signal Processing and Analysis, 2005*, 64–69. IEEE.
- Doucet, A., Briers, M. and Sénécal, S. (2006) Efficient block sampling strategies for sequential Monte Carlo methods. *Journal of Computational and Graphical Statistics*, **15**, 693–711.
- Doucet, A., De Freitas, N. and Gordon, N. (2001) *Sequential Monte Carlo Methods in Practice*. Springer.
- Doucet, A., Godsill, S. and Andrieu, C. (2000) On sequential Monte Carlo sampling methods for Bayesian filtering. *Statistics and Computing*, **10**, 197–208.
- Doucet, A. and Johansen, A. M. (2011) A tutorial on particle filtering and smoothing: Fifteen years later. In *Oxford Handbook of Nonlinear Filtering* (eds. D. Crisan and B. Rozovskii). Oxford University Press.
- Doucet, A., Pitt, M., Deligiannidis, G. and Kohn, R. (2015) Efficient implementation of Markov chain Monte Carlo when using an unbiased likelihood estimator. *Biometrika*, **102**, 295–313.
- Eggo, R. M., Cauchemez, S. and Ferguson, N. M. (2010) Spatial dynamics of the 1918 influenza pandemic in England, Wales and the United States. *Journal of The Royal Society Interface*, rsif20100216.
- Evensen, G. (1994) Sequential data assimilation with a nonlinear quasi-geostrophic model using Monte Carlo methods to forecast error statistics. *Journal of Geophysical Research: Oceans*, **99**, 10143–10162.
- Fasiolo, M., Pya, N. and Wood, S. N. (2016) A comparison of inferential methods for highly nonlinear state space models in ecology and epidemiology. *Statistical Science*, **31**, 96–118.
- Giraud, F. and Del Moral, P. (2017) Nonasymptotic analysis of adaptive and annealed Feynman–Kac particle models. *Bernoulli*, **23**, 670–709.
- Gordon, N. J., Salmond, D. J. and Smith, A. F. (1993) Novel approach to nonlinear/non-Gaussian Bayesian state estimation. *IEE Proceedings F (Radar and Signal Processing)*, **140**, 107–113.
- He, D., Ionides, E. L. and King, A. A. (2009) Plug-and-play inference for disease dynamics: Measles in large and small populations as a case study. *Journal of the Royal Society Interface*.
- Houtekamer, P. L. and Mitchell, H. L. (2001) A sequential ensemble Kalman filter for atmospheric data assimilation. *Monthly Weather Review*, **129**, 123–137.
- Ionides, E. L., Breto, C., Park, J., Smith, R. A. and King, A. A. (2017) Monte Carlo profile confidence intervals for dynamic systems. *Journal of The Royal Society Interface*, **14**, 20170126.
- Ionides, E. L., Nguyen, D., Atchadé, Y., Stoev, S. and King, A. A. (2015) Inference for dynamic and latent variable models via iterated, perturbed Bayes maps. *Proceedings of the National Academy of Sciences*, **112**, 719–724.
- Johansen, A. M. (2015) On blocks, tempering and particle MCMC for systems identification. In *Proceedings of 17th IFAC Symposium on System Identification*, 969–974.
- Karlin, S. and Taylor, H. M. (1981) *A Second Course in Stochastic Processes*. Academic Press, New York.
- Kitano, H. (2002) Computational systems biology. *Nature*, **420**, 206.
- Le Gland, F. and Oudjane, N. (2004) Stability and uniform approximation of nonlinear filters using the Hilbert metric and application to particle filters. *The Annals of Applied Probability*, **14**, 144–187.
- Lei, J., Bickel, P. and Snyder, C. (2010) Comparison of ensemble Kalman filters under non-Gaussianity. *Monthly Weather Review*, **138**, 1293–1306.
- Lin, M., Chen, R. and Liu, J. S. (2013) Lookahead strategies for sequential Monte Carlo. *Statistical Science*, **28**, 69–94.

- Lorenz, E. N. (1996) Predictability: A problem partly solved. *Proceedings of the Seminar on Predictability*, **1**, 1–18.
- Miller, R. N., Carter, E. F. and Blue, S. T. (1999) Data assimilation into nonlinear stochastic models. *Tellus A: Dynamic Meteorology and Oceanography*, **51**, 167–194.
- Neal, R. M. (2001) Annealed importance sampling. *Statistics and Computing*, **11**, 125–139.
- Owen, J., Wilkinson, D. J. and Gillespie, C. S. (2015) Scalable inference for Markov processes with intractable likelihoods. *Statistics and Computing*, **25**, 145–156.
- Palmer, T. N. (2012) Towards the probabilistic Earth-system simulator: a vision for the future of climate and weather prediction. *Quarterly Journal of the Royal Meteorological Society*, **138**, 841–861.
- Papadakis, N., Mémmin, É., Cuzol, A. and Gengembre, N. (2010) Data assimilation with the weighted ensemble Kalman filter. *Tellus A: Dynamic Meteorology and Oceanography*, **62**, 673–697.
- Pitt, M. K. and Shephard, N. (1999) Filtering via simulation: Auxiliary particle filters. *Journal of the American Statistical Association*, **94**, 590–599.
- Pons-Salort, M. and Grassly, N. C. (2018) Serotype-specific immunity explains the incidence of diseases caused by human enteroviruses. *Science*, **361**, 800–803.
- Ranjeva, S. L., Baskerville, E. B., Dukic, V., Villa, L. L., Lazcano-Ponce, E., Giuliano, A. R., Dwyer, G. and Cobey, S. (2017) Recurring infection with ecologically distinct HPV types can explain high prevalence and diversity. *Proceedings of the National Academy of Sciences*, 201714712.
- Rebeschini, P. and Van Handel, R. (2015) Can local particle filters beat the curse of dimensionality? *The Annals of Applied Probability*, **25**, 2809–2866.
- Rogers, L. C. G. and Williams, D. (1994) *Diffusions, Markov processes and martingales: Volume 2, Itô calculus*, vol. 2. Cambridge university press.
- Snyder, C., Bengtsson, T., Bickel, P. and Anderson, J. (2008) Obstacles to high-dimensional particle filtering. *Monthly Weather Review*, **136**, 4629–4640.
- Snyder, C., Bengtsson, T. and Morzfeld, M. (2015) Performance bounds for particle filters using the optimal proposal. *Monthly Weather Review*, **143**, 4750–4761.
- Van Leeuwen, P. J. (2010) Nonlinear data assimilation in geosciences: an extremely efficient particle filter. *Quarterly Journal of the Royal Meteorological Society*, **136**, 1991–1999.
- Vergé, C., Dubarry, C., Del Moral, P. and Moulines, E. (2015) On parallel implementation of sequential Monte Carlo methods: the island particle model. *Statistics and Computing*, **25**, 243–260.
- Whiteley, N. (2013) Stability properties of some particle filters. *The Annals of Applied Probability*, **23**, 2500–2537.
- Wilks, D. S. (2005) Effects of stochastic parametrizations in the Lorenz 96 system. *Quarterly Journal of the Royal Meteorological Society*, **131**, 389–407.
- Xia, Y., Bjørnstad, O. N. and Grenfell, B. T. (2004) Measles metapopulation dynamics: A gravity model for epidemiological coupling and dynamics. *The American Naturalist*, **164**, 267–281.